nagra

Arbeitsbericht NAB 21-22

TBO Bözberg-2-1: Data Report

Dossier VII Hydraulic Packer Testing

April 2022

National Cooperative
for the Disposal of
Radioactive Waste

Hardstrasse 73
P.O. Box 280
5430 Wettingen
Switzerland
Tel. +41 56 437 11 11

www.nagra.ch

nagra.

Arbeitsbericht NAB 21-22

TBO Bözberg-2-1: Data Report

Dossier VII Hydraulic Packer Testing

April 2022

R. Schwarz[1], M.Willmann[2], S. Reinhardt[3], S.M.L. Hardie[4], M. Voß[1] & A. Pechstein[5]

[1] CSD Ingenieure AG
[2] Solexperts AG
[3] AFRY Switzerland Ltd
[4] Schwarz Hara Consult
[5] Nagra

Keywords:
BOZ2-1, Jura Ost, TBO, deep drilling campaign, hydrogeology, hydraulic packer tests, hydraulic conductivity, hydraulic head, gas threshold pressure test equipment

National Cooperative for the Disposal of Radioactive Waste

Hardstrasse 73
P.O. Box 280
5430 Wettingen
Switzerland
Tel. +41 56 437 11 11

www.nagra.ch

Nagra Arbeitsberichte ("Working Reports") present the results of work in progress that have not necessarily been subject to a comprehensive review. They are intended to provide rapid dissemination of current information.

This NAB aims at reporting drilling results at an early stage. Additional borehole-specific data will be published elsewhere.

In the event of inconsistencies between dossiers of this NAB, the dossier addressing the specific topic takes priority. In the event of discrepancies between Nagra reports, the chronologically later report is generally considered to be correct. Data sets and interpretations laid out in this NAB may be revised in subsequent reports. The reasoning leading to these revisions will be detailed there.

This Dossier was prepared by a project team consisting of:
R. Schwarz (QC of test analyses, QC of test reports and writing)
M. Willmann (performance/analysis of the hydraulic packer tests)
S. Reinhardt (analysis of the hydraulic packer tests)
S.M.L. Hardie (writing)
M. Voß (writing)
A. Pechstein (project management, conceptualisation and review)

The present report is based on the mobilisation report for the test equipment and on the detailed reports for the performance and analysis of the hydraulic packer tests. These reports were written by the testing companies Solexperts AG (U. Rösli, M. Willmann) and AFRY Switzerland Ltd (R. Brauchler, H. Fisch, A. Maqueda, S. Reinhardt, P. Schulte).

Editorial work: P. Blaser and M. Unger

The Dossier has greatly benefitted from technical discussions with, and reviews by, external and internal experts. Their input and work are very much appreciated.

"Copyright © 2022 by Nagra, Wettingen (Switzerland) / All rights reserved.
All parts of this work are protected by copyright. Any utilisation outwith the remit of the copyright law is unlawful and liable to prosecution. This applies in particular to translations, storage and processing in electronic systems and programs, microfilms, reproductions, etc."

Table of Contents

Table of Contents I

List of Tables III

List of Figures V

1 Introduction 1
1.1 Context 1
1.2 Location and specifications of the borehole 2
1.3 Documentation structure for the BOZ2-1 borehole 6
1.4 Structure and objectives of this dossier 7

2 Strategy for the hydrogeological investigations 9
2.1 Hydrogeological objectives of the TBO boreholes 9
2.2 Hydrogeological investigation concept for BOZ2-1 9

3 Hydraulic packer tests 11
3.1 Test strategy 11
3.2 Test equipment 13
3.2.1 Downhole equipment 13
3.2.1.1 Heavy-duty double packer system 16
3.2.1.2 Packers 18
3.2.1.3 Downhole sensors in the quadruple sub-surface probe 19
3.2.1.4 Autonomous data logger in test interval 20
3.2.1.5 Zero-displacement shut-in tool 20
3.2.1.6 Test tubing 21
3.2.1.7 Slim tubing 22
3.2.1.8 Submersible pumps 23
3.2.1.9 Progressive cavity pump 24
3.2.2 Surface equipment 25
3.2.2.1 Flow board 25
3.2.2.2 Packer pressure control unit 26
3.2.2.3 Additionally recorded measurements at surface 27
3.2.2.4 Data acquisition system 28
3.2.3 GTPT equipment 29
3.2.3.1 Packers for the GTPT 32
3.2.3.2 Stainless steel lines for the GTPT 33
3.2.3.3 Zero-displacement shut-in tool for GTPT 33
3.2.3.4 Flow control board for GTPT 34

3.3 Test analyses 35
3.3.1 Workflow 35
3.3.2 Special effects 38
3.3.2.1 Borehole history 39
3.3.2.2 Interval temperature changes during testing 40
3.3.2.3 Mechanical effects 40
3.4 Test activities 41
3.5 Details of selected tests 50
3.5.1 Hydraulic packer test BOZ2-1-OPA4 50
3.5.1.1 Interval characterisation 50
3.5.1.2 Test execution 51
3.5.1.3 Analysis 53
3.5.2 Hydraulic packer test BOZ2-1-MUK1 58
3.5.2.1 Interval characterisation 58
3.5.2.2 Test execution 59
3.5.2.3 Analysis 61
3.6 Summary and discussion of hydraulic tests 66
3.6.1 Summary tables and plots 66
3.6.2 Discussion of data and test results 75

4 Summary 77

5 References 79

Appendix A: Abbreviations, nomenclature and definitions A-1

Appendix B: Analysis plots of the hydraulic packer tests BOZ2-1-OPA4 and BOZ2-1-MUK1 ..... B-1

List of Tables

Tab. 1-1: General information about the BOZ2-1 borehole 2
Tab. 1-2: Core and log depth for the main lithostratigraphic boundaries in the BOZ2-1 borehole 5
Tab. 1-3: List of dossiers included in NAB 21-22 6
Tab. 3-1: Preferred test sequence for formations with medium to high transmissivity 12
Tab. 3-2: Preferred test sequence for formations with low to very low transmissivity 12
Tab. 3-3: Specifications for the HDDP 16
Tab. 3-4: Specifications for the HDDP components 17
Tab. 3-5: Specifications for the HDDP packers 18
Tab. 3-6: Specifications for the pressure transmitters mounted in the QSSP 19
Tab. 3-7: Specifications for the data logger 20
Tab. 3-8: Specifications for the zero-displacement shut-in tool 21
Tab. 3-9: Specifications for the test tubing 21
Tab. 3-10: Specifications for the slim tubing 22
Tab. 3-11: Specifications for the submersible pumps 23
Tab. 3-12: Specifications for the PCP 24
Tab. 3-13: Specifications for the flowmeters 25
Tab. 3-14: Specifications for the pressure controller 27
Tab. 3-15: Specifications for the atmospheric pressure sensor 28
Tab. 3-16: Specifications for the physico-chemical sensors 28
Tab. 3-17: Specifications for the 146 mm packers for the GTPT 32
Tab. 3-18: Specifications for the zero-displacement shut-in tool (SIT1) for the GTPT 34
Tab. 3-19: Specifications for the gas flow controller / meters for the GTPT 34
Tab. 3-20: Summary of analytical analysis methods / techniques 36
Tab. 3-21: Specific periods of the pre-test borehole pressure history 40
Tab. 3-22: Hydraulic packer testing in borehole BOZ2-1: test interval and test specifications 43
Tab. 3-23: Hydraulic test BOZ2-1-OPA4: Information on the test interval 50
Tab. 3-24: Hydraulic test BOZ2-1-OPA4: Borehole pressure history 53
Tab. 3-25: Hydraulic test BOZ2-1-OPA4: Formation parameter estimation based on the parameter optimisation of the SW-SWS phase using a radial composite (skin) flow model considering both the borehole pressure history and temperature changes inside the test interval 54

Tab. 3-26: Hydraulic test BOZ2-1-OPA4: Formation parameter estimation based on the parameter optimisation of the SW-SWS phase using a homogeneous flow model considering the borehole pressure history and temperature changes inside the test interval 55

Tab. 3-27: Hydraulic test BOZ2-1-OPA4: 95% uncertainty range associated with the result of the parameter optimisation using a radial composite flow model for the SW-SWS sequence 55

Tab. 3-28: Hydraulic test BOZ2-1-OPA4: Uncertainty ranges and best estimates for the formation parameters estimated by the perturbation analysis 56

Tab. 3-29: Hydraulic test BOZ2-1-OPA4: Uncertainty ranges and best estimates for the formation parameters as a result of the sampling analysis for the test zone compressibility 57

Tab. 3-30: Hydraulic test BOZ2-1-OPA4: Formation parameter estimates based on the parameter optimisation of the SW-SWS-PI sequence using a radial composite flow model considering both the borehole pressure history and the temperature changes inside the test interval 57

Tab. 3-31: Hydraulic test BOZ2-1-OPA4: Best estimates for the formation parameters and associated uncertainty ranges 58

Tab. 3-32: Hydraulic test BOZ2-1-MUK1: Test interval information 59

Tab. 3-33: Hydraulic test BOZ2-1-MUK1: Borehole pressure history 61

Tab. 3-34: Hydraulic test BOZ2-1-MUK1: Formation parameter estimates based on the parameter optimisation for MRW3-MRWS sequence using a radial composite flow model allowing the flow dimension of the inner zone to vary 62

Tab. 3-35: Hydraulic test BOZ2-1-MUK1: 95% uncertainty range associated with the result of the parameter optimisation using a radial composite flow model for the sequence MRW3-MRWS 63

Tab. 3-36: Hydraulic test BOZ2-1-MUK1: Formation parameter ranges associated with the result of the parameter optimisation using a radial composite flow model for the sequence MRW3-MRWS and skin values of between 0 and 16 for the borehole history period (incl. the INF and COM phases) 64

Tab. 3-37: Hydraulic test BOZ2-1-MUK1: Uncertainty ranges and best estimates for the formation parameters yielded by the perturbation analysis 64

Tab. 3-38: Hydraulic test BOZ2-1-MUK1: Best estimates and uncertainty ranges for the formation parameters yielded by the sampling analysis of the formation specific storage 65

Tab. 3-39: Hydraulic test BOZ2-1-MUK1: Formation parameter estimates based on the parameter optimisation for the MRW3-MRWS-SW3-SWS3 sequence 65

Tab. 3-40: Hydraulic test BOZ2-1-MUK1: Best estimates and associated uncertainty ranges for the formation parameters 66

Tab. 3-41: Summary of the hydraulic packer testing in borehole BOZ2-1: Transmissivity and hydraulic conductivity 67

Tab. 3-42: Summary of the hydraulic packer testing in borehole BOZ2-1: Hydraulic head estimates 68

Tab. 3-43: Summary of the hydraulic packer testing in borehole BOZ2-1: Permeability 69

Tab. A-1: Lithostratigraphy abbreviations for test names in BOZ2-1 ..... A-1

Tab. A-2: Test name definitions for hydraulic packer testing A-1

Tab. A-3: Test event abbreviations for hydraulic packer testing A-1

Tab. A-4: Parameter definitions A-2

Tab. A-5: Non-parameter abbreviations A-3

List of Figures

Fig. 1-1: Tectonic overview map with the three siting regions under investigation 1

Fig. 1-2: Overview map of the investigation area in the Jura Ost siting region with the location of the BOZ2-1 borehole in relation to the boreholes Riniken and BOZ1-1 3

Fig. 1-3: Lithostratigraphic profile and casing scheme for the BOZ2-1 borehole 4

Fig. 3-1: General configuration and specifications of the HDDP in double packer configuration 14

Fig. 3-2: General configuration and specifications of the HDDP in single packer configuration 15

Fig. 3-3: Schematic layout of the flow control unit 26

Fig. 3-4: Schematic layout of the packer control unit 27

Fig. 3-5: Schematic layout of the modified HDDP system with the four major phases of the GTPT 31

Fig. 3-6: Schematic layout of the flow control unit for the GTPT 35

Fig. 3-7: Flowcharts for the on-site hydraulic packer test analysis (left) and Quick Look Analysis (QLA) (right) 37

Fig. 3-8: Flowchart for the off-site Detailed Analysis (DA) of a hydraulic packer test 38

Fig. 3-9: Hydraulic packer test BOZ2-1-HRO1: Overview plot of pressure and flow rate vs. time and date 45

Fig. 3-10: Hydraulic packer test BOZ2-1-PWF1: Overview plot of pressure vs. time and date 45

Fig. 3-11: Hydraulic packer test BOZ2-1-PWF2: Overview plot of pressure vs. time and date 46

Fig. 3-12: Hydraulic packer test BOZ2-1-OPA1: Overview plot of pressure vs. time and date 46

Fig. 3-13: Hydraulic packer test BOZ2-1-OPA2: Overview plot of pressure vs. time and date 47

Fig. 3-14: Hydraulic packer test BOZ2-1-OPA3: Overview plot of pressure vs. time and date 47

Fig. 3-15: Hydraulic packer test BOZ2-1-OPA4: Overview plot of pressure vs. time 48

Fig. 3-16: Hydraulic packer test BOZ2-1-LIA1: Overview plot of pressure vs. time 48

Fig. 3-17: Hydraulic packer test BOZ2-1-KEU1: Overview plot of pressure and flow rate vs. time 49

Fig. 3-18: Hydraulic packer test BOZ2-1-MUK1: Overview plot of pressure and flow rate vs. time and date 49

Fig. 3-19: Hydraulic test BOZ2-1-OPA4: Downhole equipment installation record with system layout as used in the field test 52

Fig. 3-20: Hydraulic test BOZ2-1-MUK1: Downhole equipment installation record with system layout as used in the field test 60

Fig. 3-21: Summary of the hydraulic testing in borehole BOZ2-1: Formation transmissivity profile 70

Fig. 3-22: Summary of the hydraulic testing in borehole BOZ2-1: Formation hydraulic conductivity profile 71

Fig. 3-23: Summary of the hydraulic testing in borehole BOZ2-1: Static formation pressure profile 72

Fig. 3-24: Summary of the hydraulic testing in borehole BOZ2-1: Formation hydraulic head profile (m bgl) 73

Fig. 3-25: Summary of the hydraulic testing in borehole BOZ2-1: Formation hydraulic head profile (m asl) 74

Fig. B-1: Hydraulic test BOZ2-1-OPA4: Entire record of the borehole pressure history used in the analysis B-1

Fig. B-2: Hydraulic test BOZ2-1-OPA4: Log-log diagnostic plot of the PSR phase B-1

Fig. B-3: Hydraulic test BOZ2-1-OPA4: Log-log diagnostic plot of the SWS phase using Agarwal time B-2

Fig. B-4: Hydraulic test BOZ2-1-OPA4: Deconvolution diagnostic plot of the SW phase B-2

Fig. B-5: Hydraulic test BOZ2-1-OPA4: Measurement of the temperature and pressure by the QSSP and memory gauge respectively B-3

Fig. B-6: Hydraulic test BOZ2-1-OPA4: Cartesian pressure measurement with numerical cartesian fits using a radial-composite (skin) model (reference case – RC) and a radial-homogeneous flow model (Case 0) B-3

Fig. B-7: Hydraulic test BOZ2-1-OPA4: Probability distribution function of the pressure residuals of the SW-SWS sequence simulation using a radial-composite (skin) model (left) and a radial-homogeneous flow model (right) B-4

Fig. B-8: Hydraulic test BOZ2-1-OPA4: Optimised parameter sets for the perturbation analysis plotted versus the sorted SSE run numbers (bottom plot, SSE value against sorted run number) B-4

Fig. B-9: Hydraulic test BOZ2-1-OPA4: Comparison of the simulations based on the initial parameter optimisation and the simulation using the parameter sets associated with the lowest SSE (run#0) from the perturbation results B-5

Fig. B-10: Hydraulic test BOZ2-1-OPA4: Scatter plots and associated SSE values for the optimised formation parameters given by the perturbation analysis showing K_{out} versus S_{Sout} (top), K_{out} versus P_f (middle) and S_{Sout} versus P_f (bottom) B-6

Fig. B-11: Hydraulic test BOZ2-1-OPA4: Parameter sets for the sampling analysis of test zone compressibility B-7

Fig. B-12: Hydraulic test BOZ2-1-OPA4: Cartesian pressure measurement with numerical cartesian fits of the SW-SWS-PI sequence (Case 1) using a radial-composite (skin) B-8

Fig. B-13: Hydraulic test BOZ2-1-MUK1: Entire record of the borehole pressure history used in the analysis B-8

Fig. B-14: Hydraulic test BOZ2-1-MUK1: Log-log diagnostic plot of the SWS1 phase using Agarwal time B-9

Fig. B-15: Hydraulic test BOZ2-1-MUK1: Log-log diagnostic plot of the SWS2 phase using Agarwal time B-9

Fig. B-16: Hydraulic test BOZ2-1-MUK1: Log-log diagnostic plot of the SWS3 phase using Agarwal time B-10

Fig. B-17: Hydraulic test BOZ2-1-MUK1: Log-log diagnostic plot of the MRWS phase using Agarwal time B-10

Fig. B-18: Hydraulic test BOZ2-1-MUK1: Cartesian plot of measured and simulated rates and pressure values for the simulation based on a parameter optimisation of MRW3-MRWS B-11

Fig. B-19: Hydraulic test BOZ2-1-MUK1: Detailed view of the simulations based on a parameter optimisation of MRW3-MRWS shown in a log-log plot of the MRWS phase (no superposition plot) using Agarwal time B-12

Fig. B-20: Hydraulic test BOZ2-1-MUK1: Optimised parameter sets of the perturbation analysis plotted versus sorted SSE run numbers (in the lowest plot, the SSE values are plotted against sorted run number) B-13

Fig. B-21: Hydraulic test BOZ2-1-MUK1: Scatter plots and associated SSE values of the optimised formation parameters from the perturbation analysis showing r_d versus K_{out} (top), K_{out} versus P_f (middle) and r_d versus P_f (bottom plot) B-14

Fig. B-22: Hydraulic test BOZ2-1-MUK1: Scatter plots and associated SSE values of the optimised formation parameters from the perturbation analysis showing flow dimension of the inner zone versus K_{in} (top), flow dimension of the inner zone versus K_{out} (bottom plot) B-15

Fig. B-23: Hydraulic test BOZ2-1-MUK1: Parameter sets of the sampling analysis of the formation specific storage B-16

Fig. B-24: Hydraulic test BOZ2-1-MUK1: Cartesian plot of measured and simulated rates and pressure values for the simulation based on a parameter optimisation of MRW3-MRWS-SW3-SWS3 ..... B-17

1 Introduction

1.1 Context

To provide input for site selection and the safety case for deep geological repositories for radioactive waste, Nagra has drilled a series of deep boreholes ("Tiefbohrungen", TBO) in Northern Switzerland. The aim of the drilling campaign is to characterise the deep underground of the three remaining siting regions located at the edge of the Northern Alpine Molasse Basin (Fig. 1-1).

In this report, we present the results from the Bözberg-2-1 borehole.

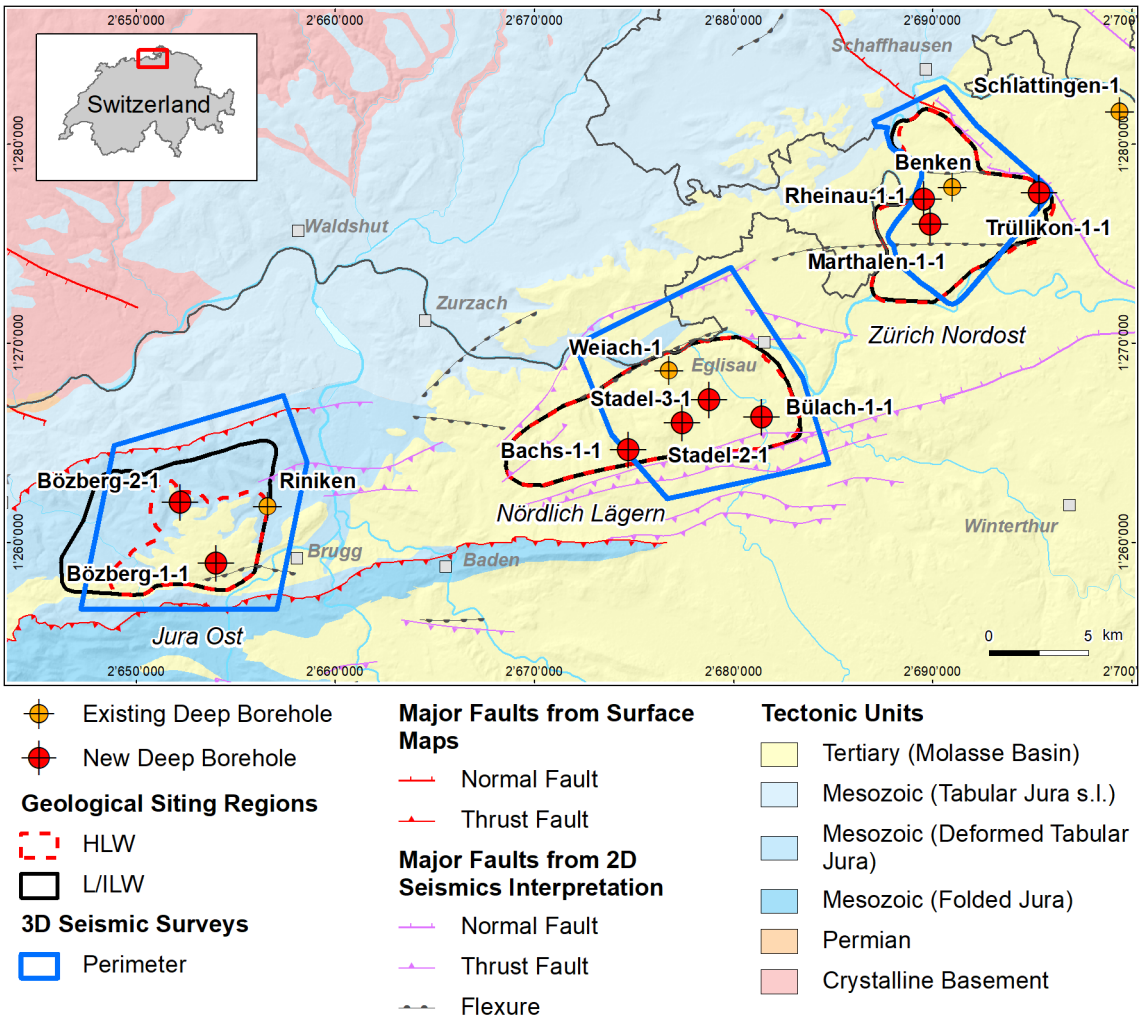

Fig. 1-1: Tectonic overview map with the three siting regions under investigation

1.2 Location and specifications of the borehole

The Bözberg-2-1 (BOZ2-1) exploratory borehole is the fifth borehole drilled within the framework of the TBO project. The drill site is located in the northern part of the Jura Ost siting region (Fig. 1-2). The vertical borehole reached a final depth of 829.11 m (MD)[1]. The borehole specifications are provided in Tab. 1-1.

Tab. 1-1: General information about the BOZ2-1 borehole

Siting region	Jura Ost
Municipality	Bözberg (Canton Aargau / AG), Switzerland
Drill site	Bözberg-2 (BOZ2)
Borehole	Bözberg-2-1 (BOZ2-1)
Coordinates	LV95: 2'652'218.764 / 1'261'985.437
Elevation	Ground level = top of rig cellar: 624.33 m above sea level (asl)
Borehole depth	829.11 m measured depth (MD) below ground level (bgl)
Drilling period	11th August – 14th December 2020 (spud date to end of rig release)
Drilling company	Daldrup & Söhne AG
Drilling rig	Wirth B 152t
Drilling fluid	Water-based mud with various amounts of different components such as[2]: 0 – 370 m: Bentonite & polymers 370 – 615 m: Potassium silicate & polymers 615 – 829.11 m: Pure-Bore®

The lithostratigraphic profile and the casing scheme are shown in Fig. 1-3. The comparison of the core versus log depth[3] of the main lithostratigraphic boundaries in the BOZ2-1 borehole is shown in Tab. 1-2.

[1] Measured depth (MD) refers to the position along the borehole trajectory, starting at ground level, which for this borehole is the top of the rig cellar. For a perfectly vertical borehole, MD below ground level (bgl) and true vertical depth (TVD) are the same. In all Dossiers depth refers to MD unless stated otherwise.

[2] For detailed information see Dossier I.

[3] Core depth refers to the depth marked on the drill cores. Log depth results from the depth observed during geophysical wireline logging. Note that the petrophysical logs have not been shifted to core depth, hence log depth differs from core depth.

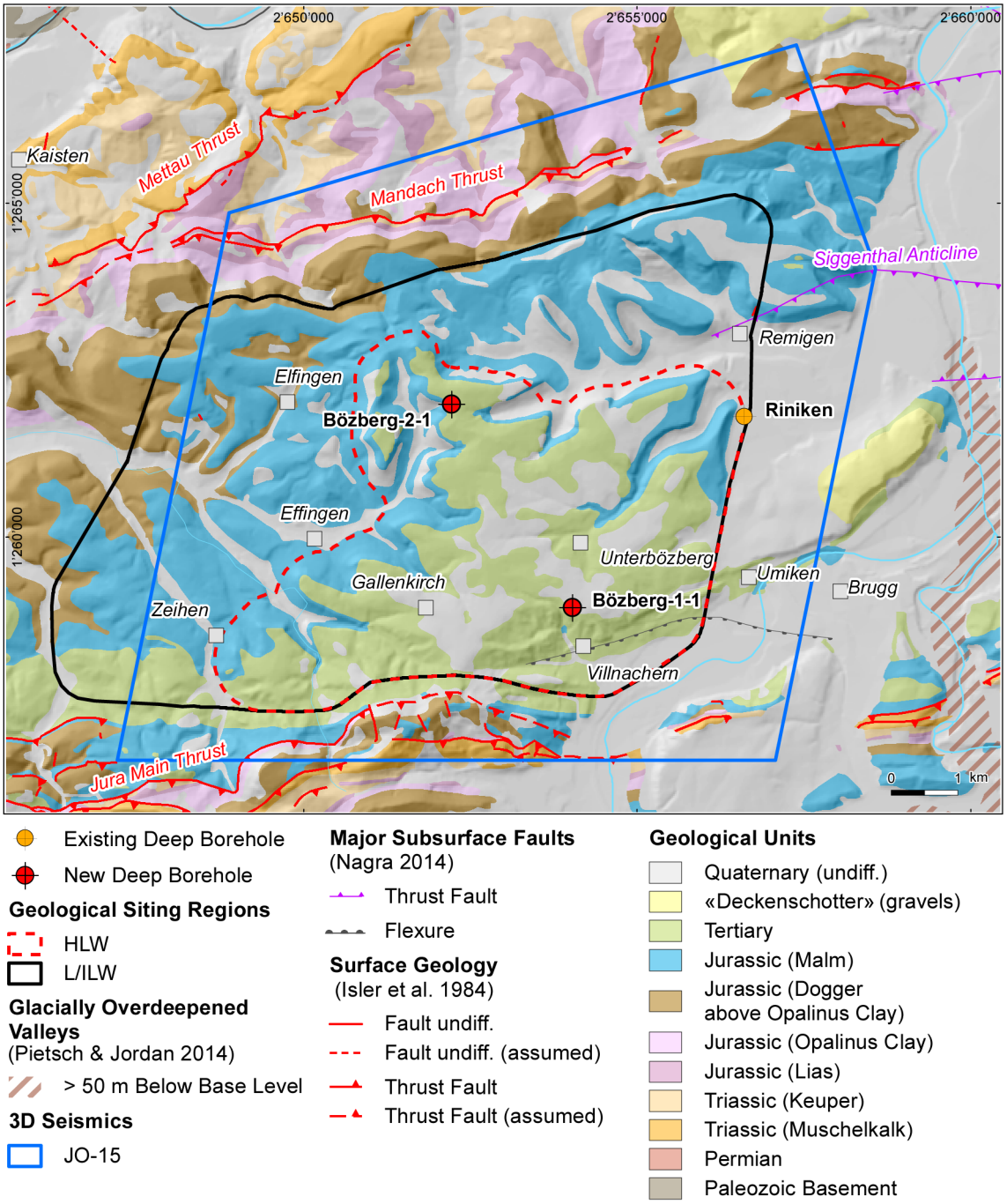

Fig. 1-2: Overview map of the investigation area in the Jura Ost siting region with the location of the BOZ2-1 borehole in relation to the boreholes Riniken and BOZ1-1

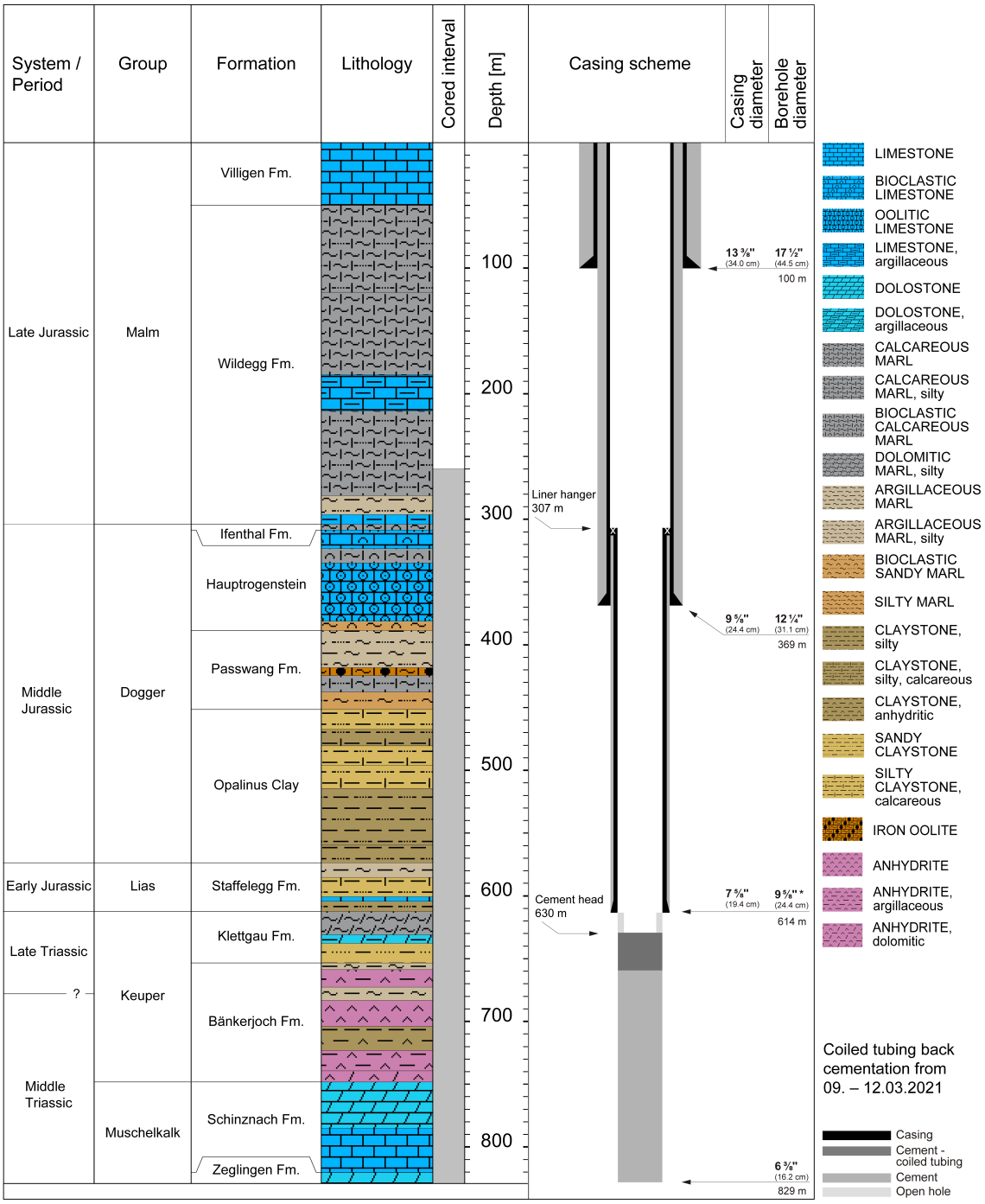

Fig. 1-3: Lithostratigraphic profile and casing scheme for the BOZ2-1 borehole[4]

[4] For detailed information see Dossier I and III.

Tab. 1-2: Core and log depth for the main lithostratigraphic boundaries in the BOZ2-1 borehole[5]

System / Period	Group	Formation	Core depth in m (MD)	Log depth in m (MD)
Jurassic	Malm	Villigen Formation	50.0	—
		Wildegg Formation	303.95	304.38
	Dogger	Ifenthal Formation	308.70	309.07
		Hauptrogenstein	388.54	388.97
		Passwang Formation	451.54	451.90
		Opalinus Clay	573.68	573.89
	Lias	Staffelegg Formation	**612.46**	**612.76**
Triassic	Keuper	Klettgau Formation	653.45	654.70
		Bänkerjoch Formation	748.27	749.52
	Muschelkalk	Schinznach Formation	820.32	821.09
		Zeglingen Formation	829.11	829.88
			final depth	

[5] For details regarding lithostratigraphic boundaries see Dossier III and IV; for details about depth shifts (core goniometry) see Dossier V.

1.3 Documentation structure for the BOZ2-1 borehole

NAB 21-22 documents the majority of the investigations carried out in the BOZ2-1 borehole, including laboratory investigations on core material. The NAB comprises a series of stand-alone dossiers addressing individual topics and a final dossier with a summary composite plot (Tab. 1-3).

This documentation aims at early publication of the data collected in the BOZ2-1 borehole. It includes most of the data available approximately one year after completion of the borehole. Some analyses are still ongoing (e.g. diffusion experiments, analysis of veins, hydrochemical interpretation of water samples) and results will be published in separate reports.

The current borehole report will provide an important basis for the integration of datasets from different boreholes. The integration and interpretation of the results in the wider geological context will be documented later in separate geoscientific reports.

Tab. 1-3: List of dossiers included in NAB 21-22

Black indicates the dossier at hand.

Dossier	Title	Authors
I	TBO Bözberg-2-1: Drilling	P. Hinterholzer-Reisegger
II	TBO Bözberg-2-1: Core Photography	D. Kaehr & M. Gysi
III	TBO Bözberg-2-1: Lithostratigraphy	P. Jordan, P. Schürch, H. Naef, M. Schwarz, R. Felber, T. Ibele & M. Gysi
IV	TBO Bözberg-2-1: Microfacies, Bio- and Chemostratigraphic Analyses	S. Wohlwend, H.R. Bläsi, S. Feist-Burkhardt, B. Hostettler, U. Menkveld-Gfeller, V. Dietze & G. Deplazes
V	TBO Bözberg-2-1: Structural Geology	A. Ebert, L. Gregorczyk, S. Cioldi, E. Hägerstedt & M. Gysi
VI	TBO Bözberg-2-1: Wireline Logging and Microhydraulic Fracturing	J. Gonus, E. Bailey, J. Desroches & R. Garrard
VII	TBO Bözberg-2-1: Hydraulic Packer Testing	R. Schwarz, M. Willmann, S. Reinhardt, S.M.L. Hardie, M. Voß & A. Pechstein
VIII	TBO Bözberg-2-1: Rock Properties, Porewater Characterisation and Natural Tracer Profiles	T. Gimmi, L. Aschwanden, L. Camesi, E. Gaucher, A. Jenni, M. Kiczka, U. Mäder, M. Mazurek, D. Rufer, H.N. Waber, P. Wersin, C. Zwahlen & D. Traber
IX	TBO Bözberg-2-1: Rock-mechanical and Geomechanical Laboratory Testing	E. Crisci, L. Laloui & S. Giger
X	TBO Bözberg-2-1: Petrophysical Log Analysis	S. Marnat & J.K. Becker
	TBO Bözberg-2-1: Summary Plot	Nagra

1.4 Structure and objectives of this dossier

The dossier at hand aims at providing a summary of the conducted hydrogeological investigations (excluding the detailed analysis of the gas threshold pressure test) and acquired hydrogeological data, including assessments of tests and results, but without interpretation.

Borehole BOZ2-1 was the third borehole in the TBO project in which a gas threshold pressure test (GTPT) was conducted. Because the downhole equipment for the GTPT is part of the packer system used for hydraulic packer testing, a description of the equipment is included in this report. The implementation, data collection and analysis of the GTPT will be reported separately.

This report focuses on hydraulic packer testing as no fluid logging was performed in BOZ2-1, and is organised as follows:

- Chapter 2 presents the general strategy for the hydrogeological investigations in the BOZ2-1 borehole.
- Chapter 3 discusses all aspects of the hydraulic packer tests including planning of test strategies, test equipment used, general concerns for the analysis of tests, test activities and hydraulic packer test results in borehole BOZ2-1. Selected tests and analyses are presented in detail. The results are summarised in tables and plots and some assessments are made.
- Chapter 4 summarises and discusses the data and results for the hydraulic packer tests.

Finally, this report includes a set of appendices, which present relevant general project information and further investigation details.

2 Strategy for the hydrogeological investigations

2.1 Hydrogeological objectives of the TBO boreholes

The overall objectives of the hydrogeological investigations are the detailed determination of the hydraulic conductivity and hydraulic head in the aquifers, aquicludes and aquitards on the one hand, and the chemistry and isotopic composition of the deep groundwaters in the aquifers and the porewaters in the aquicludes and aquitards on the other. The results of the hydrogeological investigations in the TBO boreholes form an important dataset for site selection and the safety case. They are mainly needed for the characterisation of:

- Hydraulic and hydrochemical properties of the containment-providing rock zone, which consists of the host rock Opalinus Clay and the confining geological units above and below.
- Hydrogeological conditions in the aquifers providing the hydraulic and hydrochemical boundary conditions for the containment-providing rock zone and providing input for the identification of potential release paths as well as for the planning of the future access structures.

2.2 Hydrogeological investigation concept for BOZ2-1

The hydrogeological investigations for BOZ2-1 comprised only hydraulic packer testing. A fluid logging campaign in the Wildegg Formation (Malm) or the Hauptrogenstein (Dogger) was not required as fluid losses that occurred while coring through the Hauptrogenstein provided enough information to define the test interval.

Hydraulic packer tests were used for the detailed hydraulic characterisation of selected borehole sections to determine: transmissivity (T), hydraulic conductivity (K), hydraulic head (h) and to identify the appropriate flow model. Hydraulic packer tests were performed in scheduled testing phases between drilling phases, and also during drilling phases when potentially highly transmissive features or faults were encountered. Depending on the transmissivity of the test interval, different test methods were applied in BOZ2-1:

- Pumping tests with constant flow rate
- Slug tests
- Pulse tests

These test methods usually are combined, i.e. executed one after the other as a test sequence in test-specific order.

A gas threshold pressure test (GTPT) was conducted in the BOZ2-1 borehole. As an extension to the TBO testing strategy (Section 3.1), exchanges of the drilling mud by synthetic porewater (PEARSON water) were performed in two of the test intervals.

The detailed groundwater sampling, subsequent hydrochemical and isotope analyses (including results) are documented in Lorenz et al. (2022). Further porewater investigations are the subject of Dossier VIII. The laboratory permeability measurements on drill-core sections are discussed in Dossier IX.

3 Hydraulic packer tests

3.1 Test strategy

The geological formations examined in the TBO boreholes exhibit a wide range of transmissivities. The host rock, Opalinus Clay, and its confining units are expected to have very low transmissivities, whilst the regional aquifers like the Malm and the Muschelkalk formations are expected to have relatively high transmissivities.

Nagra has long established hydraulic testing strategies (e.g. Nagra 1997) to extract the maximum information in relation to the hydraulic characteristics of the various geological formations. Two testing strategies are preferred (Tabs. 3-1 and 3-2) depending on the transmissivity of the formation (low to very low or medium to high). A typical test sequence is divided into different test phases: test preparation, diagnostic and main phase. The test sequence may be concluded with a pulse test (PW/PI) to check if the total test interval compressibility changed during the test. Modifications to the strategies are made according to the preliminarily available information, the specific test conditions encountered and results obtained while testing. This may lead to the omission of certain test phases, e.g. the diagnostic phase.

The main difference between the two testing strategies is the selection of appropriate test types and phases as well as the duration of the test phases. In a formation with medium to high transmissivity, pressure disturbances due to drilling or temperature effects dissipate relatively quickly. Accordingly, the test preparation phase is short. The main phase delivers results of sufficient accuracy with respect to the hydraulic properties of the formation in a relatively short period.

In the case of formations with low to very low transmissivity, the test types and their duration are different. For the determination of hydraulic head, the borehole pressure history and test duration are important issues. Depending on the pressure difference between the static formation conditions and the pressure induced in the borehole during the pre-test pressure history, the estimates of hydraulic head can be strongly affected due to non-static pressure conditions in the surrounding borehole area.

A further aspect of the testing strategy is the use of drilling fluid as a test fluid (see Tab. 1-1). In contrast to previous exploration boreholes drilled by Nagra (e.g. Benken), no exchange of drilling fluid in the test interval was performed in the BOZ2-1 borehole prior to hydraulic testing. The main reason was borehole stability. An exception was the interval BOZ2-1-HRO1 where traced water was used for the entire test sequence. In the intervals BOZ2-1-OPA3 and BOZ2-1-OPA4 the hydraulic test strategy was extended by a hydraulic test sequence following the exchange of the drilling fluid with PEARSON water. During both extended test sequences, a gas phase remained in the test interval, either as a residue from the procedure of the fluid exchange (BOZ2-1-OPA3), or due to gas backflow from the formation into the interval after completion of the GTPT (BOZ2-1-OPA4). The remaining gas caused problems during data analysis and interpretation that have, as yet, not been resolved satisfactorily. These extended test sequences are therefore not considered in this report.

The water-based mud used for drilling contained bentonite and polymers as additives for interval BOZ2-1-HRO1, Pure-Bore® for intervals BOZ2-1-MUK1 and BOZ2-1-KEU1, and potassium silicate and polymers for all other intervals (*cf.* Dossier I).

The model implementation as a skin in the test analysis is assumed to adequately address the issues linked with drilling fluid properties at the borehole wall.

Tab. 3-1: Preferred test sequence for formations with medium to high transmissivity

Test phase	**Phase** [1]	**Aims**
Test preparation phase	COM	Temperature and pressure equilibration in the test interval
	PSR	Pressure static recovery with closed shut-in tool; create pressure conditions for the initiation of the first test, first estimate of formation pressure; recognition of temperature and pressure trends
Diagnostic phase	PW	First estimates of hydraulic conductivity, which are used to plan the following test sequence
Diagnostic / main phase	SW	Estimation of hydraulic conductivity, which is used to plan the following test sequence, especially the pumping rate and drawdown of the RW phase
	SWS	Estimation of an accurate flow model and hydraulic parameters; hydrostatic pressure for subsequent pumping phase
Main phase	RW	Defined signal with a larger radius of influence; allows a representative groundwater sample of the formation to be taken as well as the detection of boundary conditions
	RWS	Estimation of an accurate flow model and hydraulic parameters as well as boundary conditions
Optional	PW/PI	Estimation of the total test interval compressibility at the end of the test

[1] For an explanation of the abbreviations see Tab. A-3.

Tab. 3-2: Preferred test sequence for formations with low to very low transmissivity

Test phase	**Phase** [1]	**Aims**
Test preparation phase	COM	Temperature and pressure equilibration in the test interval
	PSR	Pressure static recovery with closed shut-in tool; create pressure conditions for the initiation of the first test, first estimate of formation pressure; recognition of temperature and pressure trends
Diagnostic phase	PW	First estimates of hydraulic conductivity, which are used to plan the following test sequence
Main phase Version 1	SW	Estimation of hydraulic formation parameters during a flow phase
	SWS	Estimation of an accurate flow model and hydraulic parameters during shut-in conditions
	PW/PI (optional)	Estimation of the total test interval compressibility at the end of the test
Main phase Version 2	PW/PI	Estimation of hydraulic formation parameters (as an alternative to SW/SWS)

[1] For an explanation of the abbreviations see Tab. A-3.

3.2 Test equipment

The most relevant components of the field test contractor's equipment have been drawn from the associated mobilisation report and are presented below.

3.2.1 Downhole equipment

The packer system referred to as the heavy-duty double packer system (HDDP) was used for all hydraulic packer tests in open borehole sections. It consists of a top and bottom inflatable packer (non-inflated outer diameter 114 mm for borehole BOZ2-1, except for BOZ2-1-HRO1, BOZ2-1-OPA3 and BOZ2-1-OPA4 with a non-inflated outer diameter of 146 mm) in order to confine a test interval section of appropriate length for the intended test (Fig. 3-1). Inflow and outflow occurred through a perforated filter segment covered by a filter screen mounted on a 2⅞" tubing above the bottom packer.

Four pressure transducers, mounted in a probe carrier shell above the top packer and referred to as the quadruple sub-surface probe or quadruple probe (QSSP), measured the pressures below (P1), within (interval pressure P2) and above the test interval (annulus pressure P3) as well as in the test tubing above the downhole shut-in tool (P4). In addition, the pressure in the test interval was recorded with an autonomous memory gauge at the bottom of the filter screen (P2*).

Temperatures were measured at the level of the QSSP by the temperature sensors associated with each pressure transducer (referred to as T1, T2, T3, T4, respectively) and additionally by the sensor associated with the memory gauge mentioned above (named T2*).

A hydraulically controlled non-displacement downhole shut-in tool (SIT) placed above the probe carrier shell was used to isolate the test zone from the test tubing (2⅞" EUE API CT5 L80). A progressive cavity (PC) pump or Moyno® type pump or a pump housing with a 4" submersible pump, integrated in the test tubing, can be used for production pumping tests.

For testing in a single packer configuration (Fig. 3-2), the system was set up without the bottom packer but with a prolongation of the interval string with the filter at the bottom. Inflow and outflow occurred through a perforated filter segment covered by a filter screen mounted on a 2⅞" tubing at the bottom of the prolongation.

The quadruple flat-pack consists of three hydraulic steel tubes of ¼" outer diameter (OD) and one electrical conductor coated in a thermoplastic protective cover. Two steel tubes were used for packer inflation and one for the control of the SIT and the pressure release valve (PRV), which was only used when the packers could not be sufficiently deflated by opening the packer lines at the surface.

Certain parts of the downhole equipment are described below in more detail.

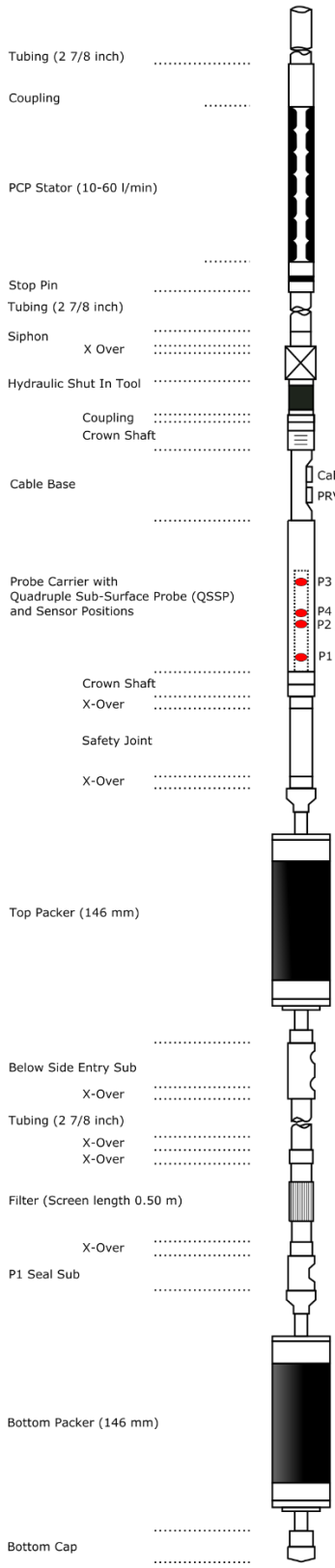

Heavy Duty Double Packer System Buildup

		API 2 7/8 EU	Stub ACME	max. OD [mm]	min. ID [mm]	Length [m]	Tensile Strength [tons]	Weight [kg]
Tubing (2 7/8 inch)		x		93.2 (73.0)	62.0	indiv.	45	
Coupling		x		93.2	62.0	0.15		
PCP Stator (10-60 l/min)				78.6 (93.2)	34.0	2.58	16	53
Stop Pin		x		78.6	62.0	0.40		
Tubing (2 7/8 inch)		x		93.2	62.0	indiv.		
Siphon			x	93.2		0.185		
X Over	0.14		x					
Hydraulic Shut In Tool	0.741		x	106.0	24.0	1.41		69
Coupling	0.667							
Crown Shaft	0.15 / 0.26		x	100.0	40.0	0.378		
Cable Base	0.178		x	105.0	24.0	1.043	16	
Probe Carrier with Quadruple Sub-Surface Probe (QSSP) and Sensor Positions	P3 / P4 / P2 / T2 / P1		x	105.0	3 x Ø19	1.707		132
Crown Shaft	0.27		x	100.0	40.0			
X-Over	0.128 / 0.08							
Safety Joint	0.55		x	93.0	62.0		90	14 (Safety Joint)
X-Over	0.15		x	93.0	50.0			
Top Packer (146 mm)	0.118			146.0	49.0	0.268 / 0.215 / 1.20 / 0.225		120
Below Side Entry Sub			x	100.0	30.0	0.164 / 0.435		
X-Over	0.08	x						
Tubing (2 7/8 inch)		x		93.2 (73.0)	62.0	indiv.	16	
X-Over	0.13							
X-Over	0.08							
Filter (Screen length 0.50 m)	0.95	x		89.0	73.0	1.18		13
X-Over	0.15							
P1 Seal Sub	0.314		x	95.0	...	0.431		
Bottom Packer (146 mm)	0.117		x	146.0	49.0	0.215 / 1.20 / 0.225 / 0.164		98
Bottom Cap				95.0	...	0.16		

Fig. 3-1: General configuration and specifications of the HDDP in double packer configuration

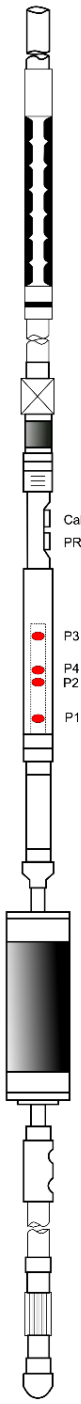

Heavy Duty Single Packer System Buildup

		API 2 7/8 EU	Stub ACME	max. OD [mm]	min. ID [mm]	Length [m]	Tensile Strength [tons]	Weight [kg]
Tubing (2 7/8 inch)		x		93.2 (73.0)	62.0	indiv.	45	
Coupling		x		93.2	62.0	0.15		
PCP Stator (10-60 l/min)				78.6 (93.2)	34.0	2.58	16	53
Stop Pin		x		78.6	62.0	0.40 (0.35)		
Tubing (2 7/8 inch)		x		93.2	62.0	indiv.		
Siphon			x	93.2		0.185		
X Over	0.14		x					
Hydraulic Shut In Tool	0.741 / 0.667		x	106.0	24.0	1.41		69
Coupling	0.15							
Crown Shaft	0.20 / 0.178		x	100.0	40.0	0.378		
Cable Base	Cable Head and Cable Plug / PRV		x	105.0	24.0	1.043	16	
Probe Carrier with Quadruple Sub-Surface Probe (QSSP) and Sensor Positions	P3 / P4 / P2 / T2 / P1		x	105.0	3 x Ø19	0.525 / 0.652 / 0.795 / 0.992 / 1.707		132
Crown Shaft	0.27		x	100.0	40.0			
X-Over	0.126 / 0.06							
Safety Joint	0.25		x	98.55	63.5		(21.14)*	7.5 (Safety Joint)
X-Over	0.15		x	93.0	50.0			
	0.118					0.268		
						0.215		
Top Packer (146 mm)				146.0	49.0	1.20		120
						0.225		
			x			0.164		
Below Side Entry Sub			x	100.0	30.0	0.435		
X-Over	0.08	x						
Tubing (2 7/8 inch)		x		93.2 (73.0)	62.0	indiv.	16	
X-Over	0.13							
X-Over	0.08							
Filter (Screen length 0.50 m)	0.95	x		89.0	73.0	1.18		13
X-Over	0.15							
Bottom Cap	0.314							6

* Shear value with ten shear screws

Fig. 3-2: General configuration and specifications of the HDDP in single packer configuration

3.2.1.1 Heavy-duty double packer system

The technical data of the Heavy-duty double packer system (HDDP) are provided in Tab. 3-3. A summary of the downhole equipment with the most important specifications is given in Tab. 3-4.

Tab. 3-3: Specifications for the HDDP

Tool Description	**HDDP**
Packer configuration	Double packer or single packer
Maximum installation depth	1'400 m (vertical); 1'500 m (inclined) along borehole axis
Maximum fluid pressure	20'000 kPa
Maximum differential pressure	114 mm packer system for 162 mm borehole: ~ 12'200 kPa 146 mm packer system for 216 mm borehole: ~ 8'000 kPa
Maximum downhole temperature	80 °C
Range of interval length	3 – 100 m
Probe	QSSP
Shut-in tool (SIT)	Zero-displacement valve
Control lines	4 core encapsulated flat-pack • Hydraulic line – bottom packer (PA1) • Hydraulic line – top packer (PA2) • Hydraulic line – shut-in tool (SIT) and packer pressure release valve (PRV) • ⅛" (3.175 mm) OD tubing encased single conductor cable

Tab. 3-4: Specifications for the HDDP components

Component	**Specifications**	**Minimum inner diameter (ID)** [mm]	**Weight**
Quadruple flat-pack	3 each ¼" OD × 0.035" WT316L stainless steel welded and cold drawn annealed tubes 153'339 kPa nominal burst pressure 49'139 kPa maximum test pressure Incorporating 1 each ⅛" OD × 0.022" WT316L stainless steel 16 AWG solid CU conductor /P/N 024440) encapsulated to ¼" OD in TT200 thermoplastic Encapsulated as 33 mm × 11 mm in TT210 thermoplastic, suitable for maximum 98.9 °C brine service		0.637 kg/m
Tubing	2⅞" EU API CT5 N80	62	9.68 kg/m
Pup joints	2⅞" EU API CT5 L80/N80	62	9.68 kg/m
Shut-in tool (SIT)	Duplex 1.4462	24	69 kg
Pressure release valve (PRV)	Duplex 1.4462	24	132 kg
Cable base	Duplex 1.4462		
Quadruple sub-surface probe (QSSP)	Duplex 1.4462 4 pressure sensors P1, P2, P3 and P4	3 × Ø19	
Coarse thread safety joint	3 21/32" OD, with 2 7/16" bore with 2⅞" EUE box × pin connections	62	26 kg
Packers for large borehole diameter	IPI 5¾" (146 mm), steel wire reinforced, duplex, natural rubber Packer 1 Packer 2	 49 49	 98 kg 106 kg
Packers for normal borehole diameter	IPI 4½" (114 mm), steel wire reinforced, duplex, Nitrile Butadiene Rubber (NBR) Packer 1 Packer 2	 49 49	 78 kg 67 kg
Filter	HP well screen: sand free filter screen mounted on 2⅞" tubing L80 Length: 0.50 m Length: 1.00 m	 73 73	 13 kg 19 kg
Total system weight	At 1'400 m depth including PCP, quadruple flat-pack cable and centralisers		approx. 15.2 t
Maximum applicable tensile force for entire system	Actual system weight at the corresponding depth, plus 16 tonnes (weakest point)		

3.2.1.2 Packers

Two types of packers were available for use, a 114 mm packer for 162 mm diameter boreholes and a 146 mm packer for 216 mm diameter boreholes (Tab. 3-5). The packers were individually inflated with water through the packer inflation line. The inflation lines were integrated in the quadruple flat-pack and operated using a booster pump. Anti-freeze was added to the water. Both packer pressure lines were connected to the packer control board at the winch and equipped with pressure sensors (pressure range 0 – 60'000 kPa) for packer pressure monitoring. The packer pressure sensors were connected to the data acquisition system (DAS) for continuous recording. To keep packer pressures constant, the packers were connected to a pressure-maintenance system (see Section 3.2.2.2).

Tab. 3-5: Specifications for the HDDP packers

Manufacturer	Inflatable Packers International, Perth, Australia	
Packer types	IPI 4½" (114 mm)	IPI 5¾" (146 mm)
Material and type	Duplex, NBR, sliding end (+ 4 natural rubber packer sleeves)	Duplex, natural rubber, sliding end
Reinforcement type	Steel wire reinforced	Steel wire reinforced
Borehole diameter	162 mm	216 mm
Packer diameters	125 – 230 mm (pressure dependent)	162 – 280 mm (pressure dependent)
Outer diameter, not inflated	114 mm max.	146 mm max.
Inner diameter	49 mm min.	49 mm min.
Overall length: Bottom packer Top packer	 1.93 m 2.08 m	 1.92 m 1.92 m
Rubber sleeve length	1.20 m	1.20 m
Thread connections	2⅞" EUE pin × 2⅞" EUE box	2⅞" EUE pin × 2⅞" EUE box
Max. working temperature for a period > 100 h	+80 °C	+80 °C
Packer inflation lines	Quadruple flat-pack, see Tab. 3-4	Quadruple flat-pack, see Tab. 3-4
Inflation method	Surface controlled	Surface controlled
Inflation fluid	Water and anti-freeze (if necessary)	Water and anti-freeze (if necessary)

3.2.1.3 Downhole sensors in the quadruple sub-surface probe

Four Keller PA-27XW transducers (for transducer types and specifications see Tab. 3-6) were used to monitor fluid pressures in the interval below the bottom packer (P1), within the testing interval (P2), in the annulus between the tubing and borehole wall above the top packer (P3) and in the test string (P4) above the downhole SIT. These four transducers were mounted in the QSSP probe, which was integrated in the probe carrier (see Fig. 3-1). The pressure sensors measured absolute pressure and corrected it to atmospheric pressure; the sensor showed ± 3 kPa at atmospheric pressure conditions.

Each pressure transducer had an associated temperature sensor (referred to as T1, T2, T3 and T4) for full thermal compensation of the pressure measurement (Tab. 3-6). The temperature sensor was mounted inside the pressure transducer housing. Because the temperature measurements were taken at the positions of the pressure transducers, they may not represent the effective temperature of the test interval fluid.

Tab. 3-6: Specifications for the pressure transmitters mounted in the QSSP

Pressure transducer type	Keller PA-27XW, custom-made
Manufacturer	Keller, Winterthur, Switzerland
Year of commissioning	2018
Pressure range (full scale)	0 – 20'000 kPa (absolute)
Accuracy	-0.004…0.005% FS [1]
Resolution	< 0.0007% FS
Minimum recording rate	1 Hz
Temperature range (FS)	-10 °C – 80 °C
Accuracy (temperature)	1 °C
Resolution (temperature)	0.01 °C
Output signal	RS485 (digital)

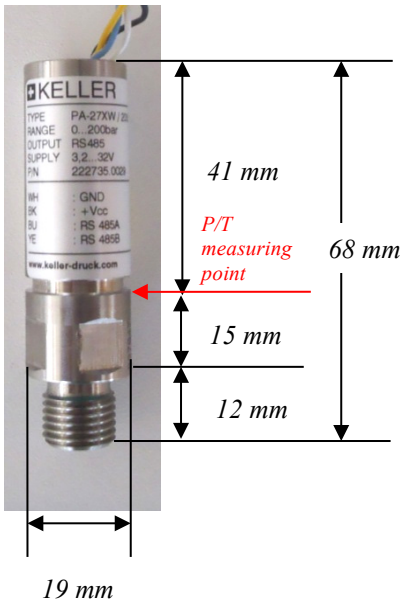

Pressure sensor

[1] FS = full scale

3.2.1.4 Autonomous data logger in test interval

Pressures and temperatures were recorded as redundant measurements in the interval at the lower end of the filter screen (referred to as P2* and T2*, respectively) with an autonomous data logger of the type DataCan Memory Pressure Gauges. The specifications are given in Tab. 3-7. The recorded pressure measurement is an absolute measurement.

Tab. 3-7: Specifications for the data logger

Data logger type	DataCan Memory Pressure Gauge 1.25" Welded Piezo III
Manufacturer	Data Can, Red Deer, Canada
Pressure range (FS [1])	0 – 20'684 kPa (absolute)
Pressure accuracy	0.03% FS
Resolution	0.0003% FS
Temperature range	0 – 150 °C
Temperature accuracy	0.5 °C
Resolution	0.005 °C
Memory capacity	1'000'000 data sets
Minimum recording rate	10 Hz
Year of commissioning	2018

[1] FS = full scale

3.2.1.5 Zero-displacement shut-in tool

The downhole SIT controls the fluid connection between the interior of the test tubing and the test interval. The SIT is a zero-displacement valve that is hydraulically operated via a hydraulic line integrated in the quadruple flat-pack using a booster pump. An axially moveable valve piston opens and closes the valve. The valve piston is moved via the hydraulic (closure) line by applying pressure to close the valve. Releasing the pressure with a pre-stressed spring resets the valve piston and opens the valve (pressure-disturbance free opening).

With a pressure compensation element, the pressure at interval depth (annulus pressure) is used to support the spring and to keep the opening/closing pressure constant for the entire borehole depth. The spring force is high enough to ensure a proper functioning of the valve also at low groundwater levels. The specifications are given in Tab. 3-8.

Tab. 3-8: Specifications for the zero-displacement shut-in tool

Zero displacement shut-in tool (SIT)	Manufactured by Solexperts
Maximum water flow rate	Below 40 l/min without friction loss, max. 350 l/min
Pressure loss caused by SIT at a flow rate of 1 l/min and 10 l/min	± 0 kPa
Closing pressure	9'000 – 10'500 kPa

3.2.1.6 Test tubing

API Spec. 5 CT-05 2⅞" tubing was used as test rods. The detailed specifications of the test tubing are summarised in Tab. 3-9.

Tab. 3-9: Specifications for the test tubing

Test tubing type	Seamless steel tubing pipes: API 5CT-05 (PSL1), 8th edition Pup joints: EUE, Tubing&Coupling; API 5CT-05 (PSL1), 8th edition
Manufacturer	Normec, Celle, Germany
Steel grade	N80 (tubing), N80/L80 (pup joints)
Inner diameter	62.00 mm
Outer diameter	73.02 mm
Coupling outer diameter	93.20 mm
Thread	API 2⅞" EUE
Weight per metre	9.68 kg
Volume per metre	3.02 l
Individual tubing length	Range 2, approx. 9.5 m
Number of individual tubing lengths	124 (certified)
Total length of test tubing	Approx. 1'070 m
Lengths of pup joints	Length, quantity 1.00 m, 2 1.03 m, 1 1.50 m, 2 1.55 m, 1 1.75 m, 1 1.83 m, 1 3.00 m, 3

3.2.1.7 Slim tubing

The rate of pressure increase during the flow phase of a slug test depends on the formation transmissivity and the diameter of the test tubing, which mainly defines the wellbore storage of the test system during the slug. To improve the resolution of the pressure change, a slim tubing was used to reduce the diameter of the test tubing for slug tests in formations with low transmissivity. However, the use of a slim tubing in formations with low transmissivity reduces the dominance of the wellbore storage term that is defined by the diameter. In this case, the wellbore storage term that is determined by the compressibility of the test fluid as well as the equipment (defined by determining the test zone compressibility during a shut-in phase) must be taken into account (Black et al. 1987).

The slim tubing consists of a stiff tube, which is installed into the test tubing. A packer at the bottom of the slim tubing with an outer diameter of 56 mm sealed the annulus between the 2⅞" tubing and the slim tubing. The water level in the slim tubing was measured with the P4 sensor from the QSSP and additionally with a backup pressure sensor installed at the top of the slim tubing packer, referred to as P4-slim. P4-slim has a smaller pressure range and thus a higher precision compared to P4. The technical specifications of the slim tubing are summarised in Tab. 3-10.

After lowering the water level in the 2⅞" test tubing for a slug withdrawal test to the specified depth, the slim tubing was installed in the tubing below the water level. Afterwards, the slim tubing packer was inflated, and the test was started by opening the SIT valve. The water level only increased in the tubing. The use of a stiff tube ensured a constant inner diameter independent of the pressure (fluid level). It should be noted, however, that in the numerical analysis an effective diameter of the slim tubing must be used when using a simulator based on Pickens et al. (1987).

Tab. 3-10: Specifications for the slim tubing

Slim tubing	Manufactured by Solexperts	
Types	Polyethylene tube	Polyamide tube
Inner diameter	12 mm	6 mm
Outer diameter	16 mm	8 mm
Length	300 m	300 m
Packer specifications	Diameter 56 mm, sealing length 1'000 mm, working pressure 1 – 13.5 MPa	
Packer pressure line	Polyamide OD: 6 mm; ID: 3 mm	
Packer pressure sensor	Keller PAA-33X, 0 – 5'000 kPa, accuracy 0.1% FS	
Pressure sensor (P-slim)	Keller DCX-22, 0 – 5'000 kPa, accuracy 0.05% FS, resolution 0.0025% FS	
Installation procedure	Wireline system of the drill rig	

3.2.1.8 Submersible pumps

Frequency driven 3" and 4" Grundfos submersible pumps can be used for pumping tests and during open-hole pumping. The specifications are included in Tab. 3-11. The flow rate can be arbitrarily adjusted because of the frequency control of the pump.

Tab. 3-11: Specifications for the submersible pumps

Submersible pump types	4" down-hole pump	3" down-hole pump
Manufacturer	Grundfos, Fällanden, Switzerland	
Type	SP14-27E	SQE1-110
Regulation	Frequency-controlled	Frequency-controlled
Dimensions	101 × 3'040 mm	74 × 852 mm
Pumping rate at 150 m	100 l/min	10 l/min
Range of pumping rates	Max. 300 l/min	Max. 28 l/min
Maximum installation depth	160 m	160 m
Maximum temperature	40 °C	35 °C
Weight	57 kg (pump) 31 kg (motor)	6 kg
Pump housing	Yes	No
Specifications of pump housing	Length: 4.22 m OD max: 180 mm Weight: 130.3 kg	
Purpose	Pumping tests	Pumping tests

3.2.1.9 Progressive cavity pump

For constant rate withdrawal tests (pumping tests) a progressive cavity pump (PCP), a so-called Moyno® type pump, was used. The PCP consists of a helical rotor and a twin helix in a rubber stator. The stator is integrated into the test tubing string and allows for pumping, if necessary, but does not preclude any other test methods. For pumping, a suitable rotor had to be installed by means of the so-called sucker rods until the rotor had fully penetrated the stator. The specifications are listed in Tab. 3-12.

Tab. 3-12: Specifications for the PCP

Progressive cavity pump type	PCP
Manufacturer	Netzsch
Dimensions	Drive head: L × W × H: 1'375 × 767 × 1'263 mm
Pumping rates	1.7 – 60 l/min Pumping rates of < 1.7 l/min can be reached by closing the valve installed in-line at the wellhead
Maximum installation depth	300 m
Temperature	10 °C to 70 °C
Sucker rods, type	¾" × 7.62 m
Sucker rods, quantity	45
Total length	Approx. 300 m
Available stators	1 for pump rates 10.4 – 60 l/min, Temp. 10 °C to 70 °C 1 for pump rates 1.7 – 5.5 l/min, Temp. 10 °C to 70 °C
Available rotors	3 for pump rates 10.4 – 60 l/min, Temp. 10 °C to 30 °C, 30 °C to 50 °C, 50 °C to 70 °C 3 for pump rates 1.7 – 5.5 l/min, Temp. 10 °C to 30 °C, 30 °C to 50 °C, 50 °C to 70 °C

3.2.2 Surface equipment

The surface equipment consisted of the following equipment:

- Winch for quadruple flat-pack cable
- Flow control system
- Pressure vessel for packer pressure stabilisation
- Injection and pumping head
- PCP drive head and control unit
- Data acquisition system

Most of the surface equipment parts were installed in a mobile measuring trailer.

3.2.2.1 Flow board

For the control and measuring of pump (and injection) rates, a flow board with three flowmeters of type Yokogawa AXF/ADMAG were available. The flowmeters covered a flow rate range between 0.03 and 100 l/min (Tab. 3-13). The schematic layout of the flow control unit is displayed in Fig. 3-3.

Tab. 3-13: Specifications for the flowmeters

	Measuring range and accuracy			
	Lower limit		**Upper limit**	
	[l/min]	[% FS]	[l/min]	[% FS]
AXF 002	0.03	1	2.945	0.35
AXF 005	0.1	1	11.78	0.35
ADMAG SE202	1.0	1	100	0.35

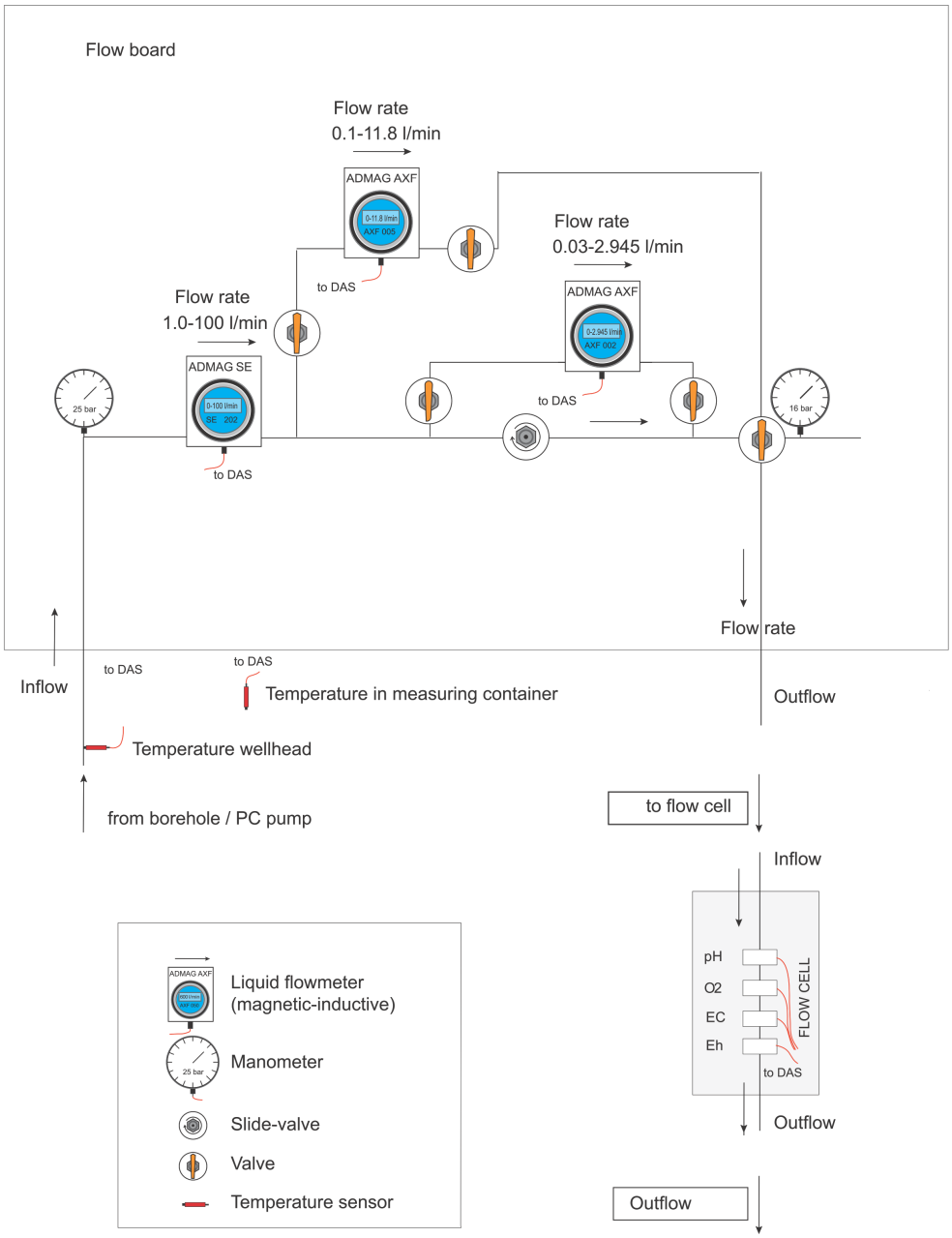

Fig. 3-3: Schematic layout of the flow control unit

3.2.2.2 Packer pressure control unit

Two transducers (type Keller PA-23SY, 60'000 kPa) mounted on the surface inflation control panel were used to monitor the packer inflation pressures (Fig. 3-4). The packer pressure lines are connected to a pressure vessel, which is pressurised by nitrogen. The pressure in the pressure vessel is controlled by a pressure controller for closed volumes. The specifications of the pressure controller are given in Tab. 3-14.

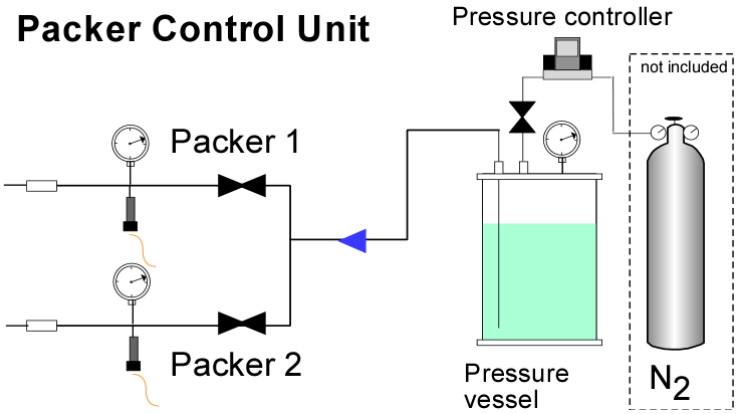

Fig. 3-4: Schematic layout of the packer control unit

Tab. 3-14: Specifications for the pressure controller

Pressure controller type	Dual-valve pressure controller
Manufacturer	Alicat, USA
Pressure range	0 – 20'684 kPa
Accuracy	0.25% FS
Repeatability	0.08% FS

3.2.2.3 Additionally recorded measurements at surface

A single pressure transducer (type Keller PAA-33X, 80 – 120 kPa absolute) was mounted outside the monitoring trailer and used to monitor barometric pressure and air temperature (Tab. 3-15).

During pumping tests, the physico-chemical parameters (e.g. pH, EC, Eh, temperature and oxygen concentration) and the temperature of the extracted fluid were recorded. The specifications of the physico-chemical sensors are given in Tab. 3-16. The specifications of the temperature sensor are also given in Tab. 3-16. The sensors were calibrated on-site before each use.

Tab. 3-15: Specifications for the atmospheric pressure sensor

Temperature sensor type	Keller PAA-33X
Manufacturer	Keller, Winterthur, Switzerland
Pressure range	80 – 120 kPa
Accuracy	0.02% FS
Resolution	0.002% FS

Tab. 3-16: Specifications for the physico-chemical sensors

Sensor type	**EC**	**pH**	**Eh**	**O_2**	**Temp**
Manufacturer	Xylem analytics, Weilheim, Germany				IST AG
Model	WTW TetraCon 325	WTW SensoLyt DW	WTW SensoLyt PtA/Pt	WTW FDO 700 IQ	Pt 1000
Range	1 µS/cm – 2 S/cm	0 – 14	± 2'000 mV	0 – 20 mg/l	-50 – 650 °C
Accuracy	n/a	n/a	n/a	n/a	± 0.15 °C at 0 °C ± 0.35 °C at 100 °C
Resolution	n/a	n/a	n/a	0.01 mg/l (0.01 ppm)	< 0.1 °C
Temperature range	0 – 100 °C	0 – 60 °C	0 – 60 °C	-5 – 50 °C	-50 – 650 °C

3.2.2.4 Data acquisition system

The data acquisition system (DAS) consisted of a Solexperts HDDP interphase for digital and analogue sensors, two industrial PCs, two screens and a keyboard. Data acquisition was performed through the Solexperts GeoMonitor II (GMII) software. The downhole pressures (P1, P2, P3, P4) and temperature measurements (T1, T2, T3, T4) were recorded in real time through the quadruple flat-pack cable assembly. Surface measurements like flowmeter rates, packer pressures, atmospheric pressure and temperature, slim tubing packer pressure and the physico-chemical parameters were recorded either permanently or, if required, with the same scan rate as the downhole pressures from the QSSP.

The scan rates could be adjusted as required between 0.5 s (using a reduced number of sensors) and > 30 s.

The measurements were written to a data file on the PC hard drive in real-time with a continuous data collection and database model. From the PC hard drive, the data were transferred to another network PC continuously for 'online' analysis and data back-up. An uninterruptible power supply was utilised to protect the system from short power interruptions.

3.2.3 GTPT equipment

The test equipment for the GTPT was designed in a modular way to be used together with the HDDP system. Additional equipment parts were provided by Nagra. The individual parts were assembled on-site, together with the HDDP system of the field test contractor.

In addition to performing the GTPT, the GTPT equipment was used to conduct fluid exchanges in specific intervals of the BOZ2-1 borehole. The fluid exchanges were realised after performing a standard hydraulic testing sequence in interval BOZ2-1-OPA3 by exchanging the drilling fluid with PEARSON water and, in interval BOZ2-1-OPA4 by exchanging nitrogen with PEARSON water after the execution of the GTPT.

The additional system parts for the downhole equipment were the following:

- X-over 2⅞" to 4½"
- Second shut-in tool (SIT1) with crown shaft below the bottom packer to control the displacement of the interval fluid to the exchange chamber
- 4½" exchange chamber of variable length (API 4½" tubing NU; N80, OD 114.3 mm, ID 100.5 mm, 12.6 lbs/ft = 18.75 kg/m; coupling OD: 132 mm) below the HDDP system / lower SIT1 for the collection of exchanged interval fluid, e.g., drilling mud, sodium hydroxide (NaOH) solution
- Bottom cap / bull nose 4½"
- Dip tube (OD 21.3 mm, wall thickness 2.6 mm) inside the exchange chamber, stainless steel with threads and couplings of variable length, with swivel connection and installation tools
- 3 (for GTPT) + 1 (for fluid exchange) additional ¼" stainless steel lines (910 m, OD 6.35 mm, inner diameter 4.55 mm) on separate coils (SIT1 line, backflow line from exchange chamber, injection line into the interval, and ventilation line out of the interval, last two equipped with check valves) besides the standard quadruple flat-pack
- 2 pressure sensors Keller PA-23SY to measure the pressure at the injection and backflow lines
- 2 × 146 mm inflatable packers with a double mandrel including five through-going pieces of ¼" stainless steel lines and fittings

The additional surface equipment encompasses the following components:

- Standard hydrotest equipment
- 1 gas flow controller 0 – 5 ln/min (injection line to interval) (ln = litre normal)
- 2 gas flowmeters 0 – 150 ln/min (one connected to back flow line from exchange chamber and one to injection line for NaOH displacement)
- A flow control board for one gas flow controller and two gas flowmeters with valves and manometers
- Closed tanks for NaOH solution and PEARSON water, for injection via the (gas-) injection line
- An additional high-pressure injection pump instead of a booster to obtain a higher injection rate and to save time

The flow controller and flowmeters, as well as all other sensors of the GTPT system, were connected to the DAS.

The most relevant system parts are described in detail in the following sections.

A schematic overview of the GTPT system is shown in Fig. 3-5. The four diagrams show the planned test phases of the GTPT:

1. Repeatedly pressurising the (empty) exchange chamber with nitrogen (N_2) to avoid any damage during installation
2. Injection of NaOH solution through the injection line to push the interval fluid to the exchange chamber and simultaneous extraction of N_2 from the exchange chamber to the surface via the extraction line, SIT1 open
3. Injection of N_2 through the injection line to push the NaOH solution from the interval to the exchange chamber and extraction of N_2 from the exchange chamber to the surface via the extraction line, SIT1 open
4. Start of GTPT: Relatively slow injection of N_2 at constant rate into the interval, SIT1 and SIT2[6] closed

In borehole BOZ2-1, the applicability of using the GTPT equipment to implement fluid exchanges was tested. A fourth ¼" stainless steel line (ventilation line) was installed with entry directly below the upper packer in order to allow the release of any gas phase that entered the interval during test phase 1. Fluid exchanges using the GTPT equipment were performed by execution of GTPT procedure test phases 0 and 1 (Fig. 3-5). Test phase 2 was subsequently conducted by injection of PEARSON water instead of nitrogen (N_2). If PEARSON water was injected after a GTPT was completed, N_2 was released from the interval via the ventilation line and PEARSON water was simultaneously injected through the injection line, directly into the interval.

[6] In this section, the usual SIT from the HDDP, which controls the fluid connection between the interior of the test rods and the test interval, is labelled SIT2; in the test string, it is positioned above SIT1, which controls the fluid connection between the exchange chamber and the test interval during a GTPT.

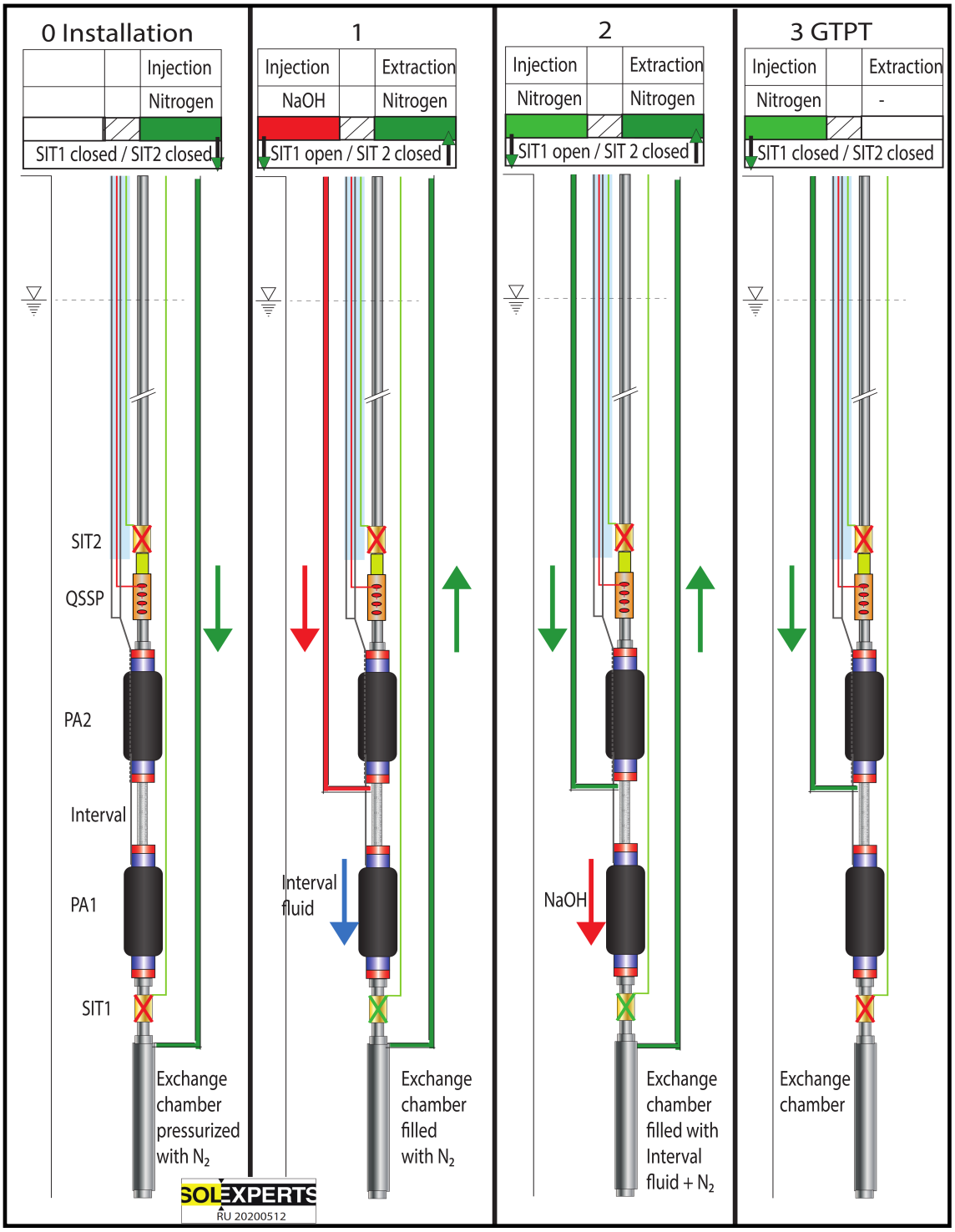

Fig. 3-5: Schematic layout of the modified HDDP system with the four major phases of the GTPT

3.2.3.1 Packers for the GTPT

The system comprises two new packers with a diameter of 146 mm which have a double mandrel including five pieces of ¼" stainless steel lines and the corresponding fittings.

A detailed description of packers and the use of the ¼" stainless steel lines is given in Tab. 3-17. Before installation, the packers with the corresponding lines were saturated with water and anti-freeze (if necessary).

Tab. 3-17: Specifications for the 146 mm packers for the GTPT

Manufacturer	Inflatable Packers International (IPI), Perth, Australia
Packer types	IPI 5¾" (146 mm)
Material and type	Duplex, 316 ss, Nitrile Butadiene Rubber (NBR), sliding end
Mandrel	Double mandrel with 5 through-going pieces of ¼" stainless steel lines
Use of ¼" stainless steel lines	Packer 1 (lower packer): 1. Line to the QSSP sensor P1 2. SIT1 line 3. Not used 4. Backflow line 5. Not used Packer 2 (upper packer) 1. Inflation line packer 1 2. SIT1 line 3. Injection line 4. Backflow line 5. Ventilation line Note: The final allocation of the line ports is defined on-site
Reinforcement type	Steel wire reinforced
Borehole diameter	162 / 216 mm
Packer diameters	162 – 280 mm (pressure dependent)
Outer diameter, not inflated	146 mm max.
Inner diameter	43.7 mm min.
Overall length: Bottom packer Top packer	 2.195 m 2.195 m
Weight	95 kg each
Rubber sleeve length	1.20 m
Thread connections	2⅞" EUE pin × 2⅞" EUE box
Packer inflation lines	Quadruple flat-pack
Inflation method	Surface controlled
Inflation fluid	Water and anti-freeze

3.2.3.2 Stainless steel lines for the GTPT

Four additional ¼" stainless steel lines (OD 6.35 mm, ID 4.55 mm), each with a length of 910 m, were installed together with the downhole equipment and used as follows:

- Activation and de-activation of the SIT1 – SIT1 line; marked with white tape.
- Gas/fluid injection into the interval – injection line; marked with green tape.
- Backflow line from the exchange chamber – backflow line; marked with red tape.
- Ventilation line from the interval – ventilation line; marked with brown tape.

The lines were connected to the corresponding stainless steel feed-through, through the top and, if required, through the bottom packer double mandrel. At the surface, the lines were coiled up on the corresponding coils. Each stainless steel line was connected to a valve and a 250 bar manometer. Two coils (injection and backflow lines) were additionally equipped with pressure sensors of the type Keller PA-23SY, 0 – 300 bar.

The outlet port for the injection line at the lower end of the top packer was equipped with a check valve which enabled flow into the test interval but no backflow from the test interval into the injection line. The check valve opened at 4 bar injection pressure. A second check valve was used at the end of the ventilation line, but in opposite direction, allowing flow from the interval if the pressure in the line was 4 bar below interval pressure.

3.2.3.3 Zero-displacement shut-in tool for GTPT

The new SIT1 is similar to the SIT2 (the HDDP SIT used for hydraulic packer testing) which controls the fluid connection between the interior of the test rods and the test interval. The SIT1 is a zero-displacement valve which controls the fluid connection between the exchange chamber and the test interval. The SIT1 is hydraulically operated over a ¼" stainless steel line using the booster pump. The opening and closing are performed via an axially moveable valve piston. The valve piston is moved via the hydraulic (closure) line by application of pressure and the valve is closed. The valve piston is reset at pressure release through a pre-stressed spring, and the valve is opened (pressure-free open).

With a pressure compensation element, the pressure at interval depth (annulus pressure) is used to support the spring and to keep the opening/closing pressure constant for the entire borehole depth. The spring force is high enough to ensure proper functioning of the valve, also at deep groundwater levels. The specifications are given in Tab. 3-18.

Tab. 3-18: Specifications for the zero-displacement shut-in tool (SIT1) for the GTPT

Manufacturer	Solexperts AG
Maximum water flow rate	Below 40 l/min without friction loss, max. 350 l/min
Pressure loss caused by SIT at a flow rate of 1 to 10 l/min	± 0 kPa
Closing pressure	9'000 – 10'500 kPa

3.2.3.4 Flow control board for GTPT

For the control and measuring of gas injection and extraction rates, the high-pressure gas flow controller and flowmeters were mounted to a flow control board. The flow controller for the control of the injection flow rate has a measuring range of 0.1 – 5 ln/min. The two flowmeters for the flow rate measurements during the displacement of NaOH with gas and during backflow have a measuring range of 3 – 150 ln/min (Tab. 3-19). A schematic drawing of the flow board is included in Fig. 3-6.

In addition to the flow controller and flowmeters, the flow board is equipped with two manometers for 100 bar, two for 160 bar and one for 250 bar maximum pressure. Two needle valves are used to control the flow rates at the injection side and at the backflow side.

Tab. 3-19: Specifications for the gas flow controller / meters for the GTPT

	Gas flow controller (Flow_G_INJ)	**Gas flowmeter (Flow_G_DIS)**	**Gas flowmeter (Flow_G_BCK)**
Manufacturer	Bronkhorst	Bronkhorst	Bronkhorst
Type	IN-FLOW	IN-FLOW	IN-FLOW
Measuring range	0.1 – 5 ln/min	3 – 150 ln/min	3 – 150 ln/min
Accuracy (incl. linearity)	± 0.5% Rd (reading), ± 0.1% FS	± 0.5% Rd (reading), ± 0.1% FS	± 0.5% Rd (reading), ± 0.1% FS
Inlet pressure	50 – 200 bar (calibrated for 125 bar)	70 – 200 bar (calibrated for 135 bar)	50 – 100 bar (calibrated for 75 bar)
Output pressure	1 – 150 bar	–	–
Minimum ΔP	2 bar	–	–
Medium	N_2	N_2	N_2

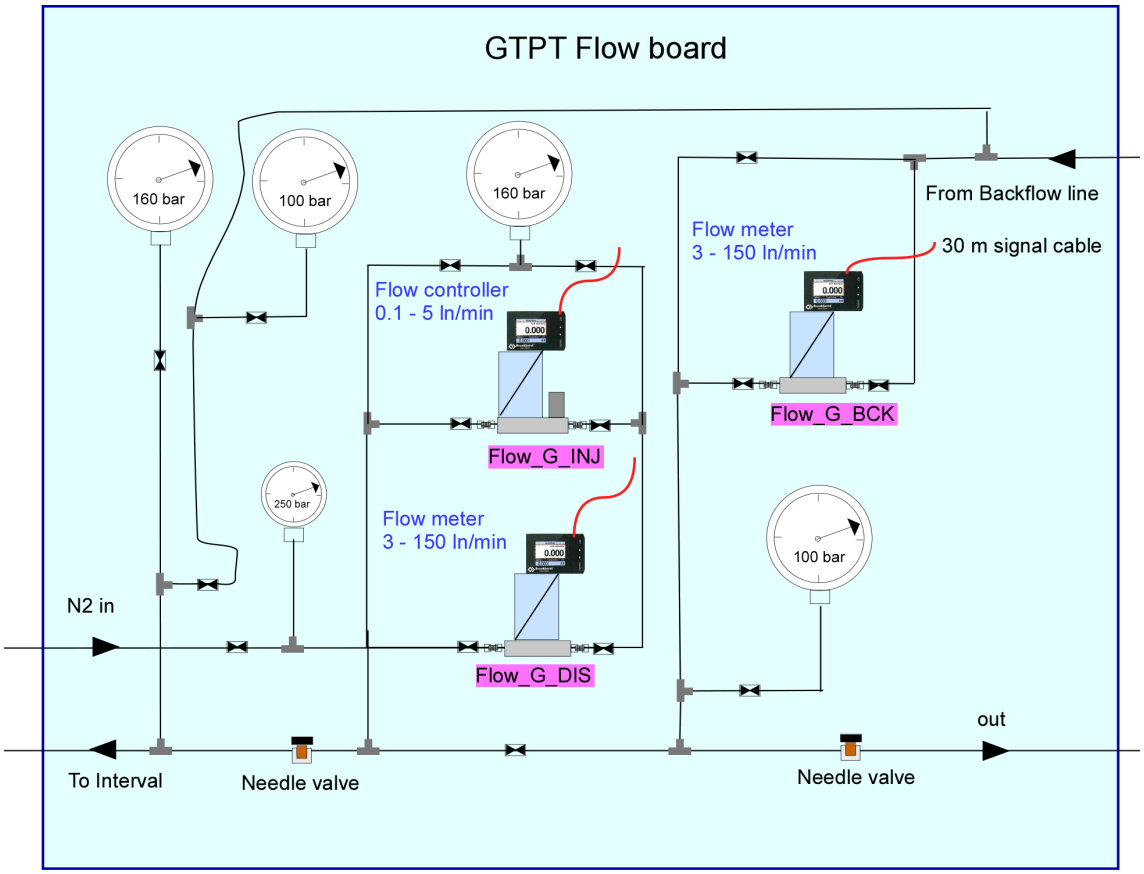

Fig. 3-6: Schematic layout of the flow control unit for the GTPT

3.3 Test analyses

3.3.1 Workflow

For BOZ2-1, the general on-site analysis approach involved mainly numerical techniques considering the entire borehole pressure history. Analytical solutions and graphical diagnostic representations were used to analyse the flow model selected, to present the results and to conduct more detailed consistency checks between measurements and simulations. This ensured a comprehensive evaluation of the recorded data. The numerical solutions were assessed further with a perturbation analysis. Prior to commencement of the hydraulic tests, the starting input parameters and in particular, the representation of the borehole history period, were defined.

The on-site analysis workflow supported the test design to achieve the quality objectives defined by Nagra:

- Identification of the most appropriate flow model, e.g. by log-log diagnostic plots (Agarwal 1980)
- Numerical simulation of individual test sequences in cartesian coordinates

  The suitability of the applied flow model was checked with diagnostic representations of the recorded and simulated pressure data, and a limited perturbation analysis was used to assess the credibility of the numerical solution

- Assessment of the credibility of the numerical solution and associated uncertainties through perturbation and sampling analysis
- Numerical simulation of the entire test sequence in cartesian coordinates using the optimised parameter set obtained from individual phase analysis

  This final step was used to check the consistency of the model with the entire data set
- Consistency check of the test analysis and the estimated parameters by the technical supervisor

The results were used to continuously optimise the test design to achieve the quality objectives within the dedicated time of testing. A general flowchart of the analysis work is provided in Fig. 3-7.

Three programmes were used for the analytical and numerical interpretation: Hugo TM (Solexperts AG), nSIGHTS software (Geofirma Engineering Ltd. & INTERA 2011) and Multisim (AFRY Switzerland Ltd.). The Cooper-Bredehoeft-Papadopulos type-curves were used to analyse both slug and pulse tests (Cooper et al. 1967, Bredehoeft & Papadopulos 1980). Recovery tests were analysed according to Agarwal (1980). A summary of the applied test analysis methods is presented in Tab. 3-20.

Tab. 3-20: Summary of analytical analysis methods / techniques

Test phase	**Analysis method**	**Reference**
Pulse test	Type-curve matching (BP)	Bredehoeft & Papadopulos (1980)
	Diagnostics: log-log plot showing ΔP and derivative using the deconvolution approach of Peres	Peres et al. (1989)
Slug test (flow phase SW)	Type-curve matching (CBP)	Cooper et al. (1967) Ramey & Agarwal (1972)
Slug test recovery (pressure recovery after slug flow phase, SWS)	Diagnostics: log-log plot showing ΔP and derivative versus "equivalent time" (Agarwal)	Agarwal (1980)
	Straight-line analysis on transient pressure data	Agarwal (1980)
Constant rate test	Diagnostics: log-log plot showing ΔP and derivative versus time	Bourdet et al. (1989)
	Straight-line analysis on transient pressure data	Cooper & Jacob (1946)
Pressure recovery after constant rate tests	Diagnostics: log-log plot showing ΔP and derivative versus "superposition time" (Agarwal)	Agarwal (1980) Birsoy & Summers (1980)
	Straight-line analysis on transient pressure data	Agarwal (1980)

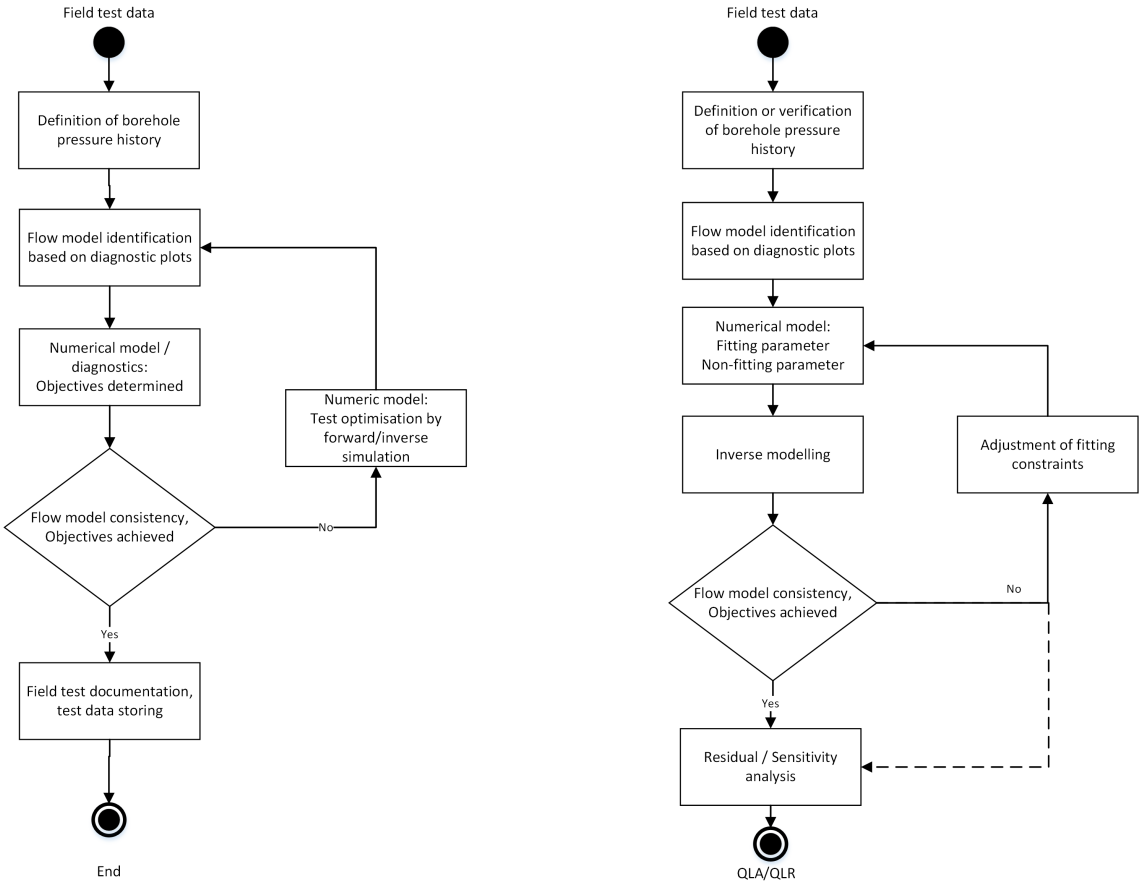

Fig. 3-7: Flowcharts for the on-site hydraulic packer test analysis (left) and Quick Look Analysis (QLA) (right)

The Detailed Analysis (DA) was performed off-site after the test was completed and is based on the Quick Look analysis (QLA) reported in the Quick Look Report (QLR). The QLR was reviewed as part of the Quality Control (QC) programme. During this task, open questions and potential ambiguities of the analysis were defined. Based on the outcome of the QC review, further specifications and, if necessary, further analyses were implemented. Fig. 3-8 provides the general flowchart of the DA, which includes perturbation and non-fitting parameter analysis (of the sampling analysis), to obtain the most reasonable parameter results and ranges of uncertainty. The work is summarised in a Detailed Report (DR), with the QLR included as an Appendix.

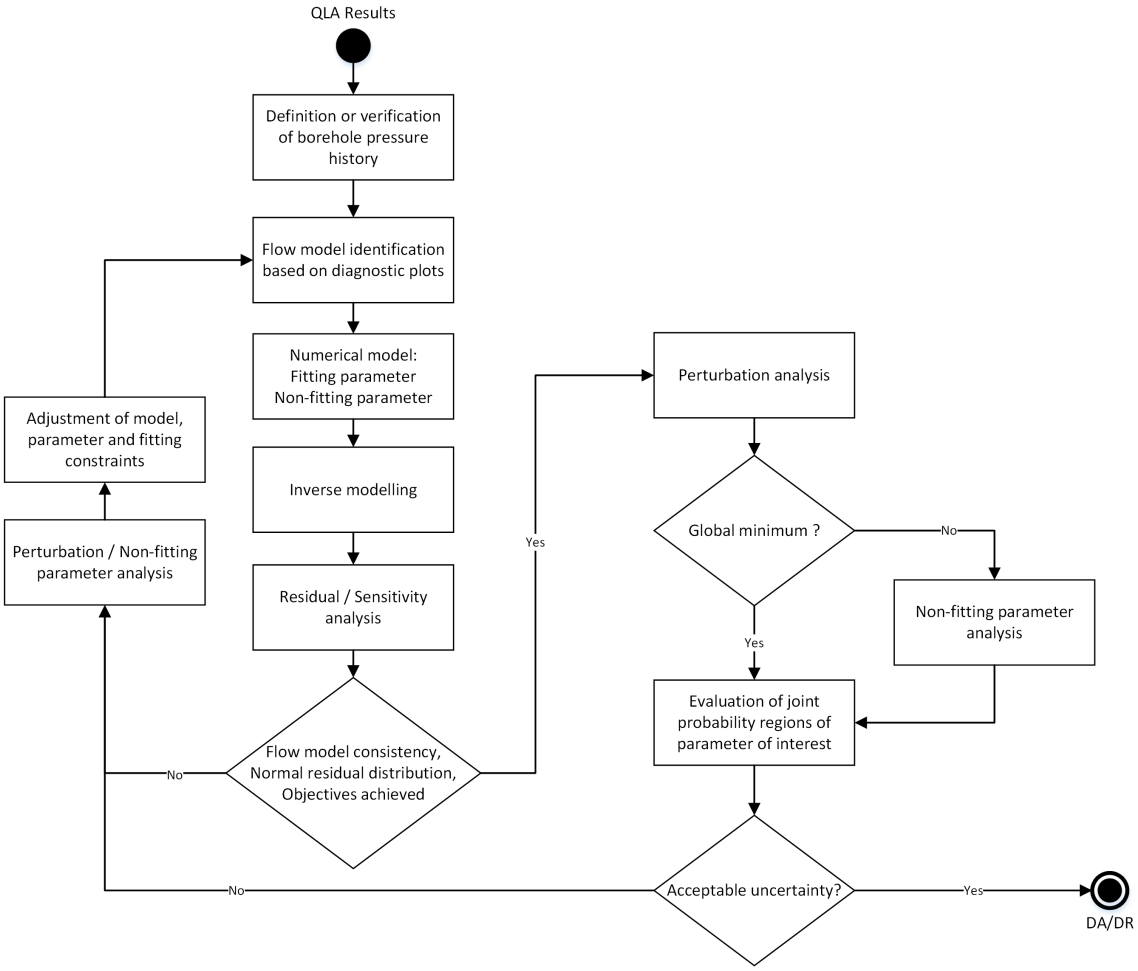

Fig. 3-8: Flowchart for the off-site Detailed Analysis (DA) of a hydraulic packer test

3.3.2 Special effects

The time series measured during hydraulic packer tests are the pressure and temperature inside the test interval. Their development over time was analysed to estimate the hydraulic properties of the formation surrounding the test interval. Various factors affected the recorded time series. All hydraulic tests are affected by factors beyond the test execution and the model used for their analysis (analytical solutions based on assumptions to derive them, numerical models based on the physical processes included in their base equation system). These are referred to as disturbances because they are not considered in the analysis. However, it is possible to describe the development of temperature and pressure signals using the diffusion equation. Disturbances are of short duration in formations with medium to high transmissivity. In formations with low transmissivity, disturbances in the pressure or temperature field can have a significant influence on the pressure signal measured during the test in the test interval (e.g. Nagra 1997, Grauls 1999, Nagra 2001).

Any disturbances of the pressure field during the time before the hydraulic test is started, are summarised under the name 'borehole pressure history'. Disturbances in the pressure and temperature fields can be caused by drilling and other activities before testing. In addition, disturbances

can occur even during testing, e.g. mechanical effects due to changes in the stress field surrounding the interval, or osmosis due to the chemical interaction of the formation and drilling fluid. However, results from the experiment 'Deep Borehole Hydraulic Testing Experiment' in the Mont Terri Rock Laboratory show that osmotic effects have no significant impact on the determination of transmissivity and hydraulic head (Marschall et al. 2003).

As the TBO boreholes are multi-purpose boreholes with many other objectives besides hydraulic packer testing, there is always a trade-off between disciplines regarding optimal test conditions. The hydraulic packer tests were performed without exchange of drilling fluid with testing fluid with the aim of reducing potential pressure or temperature disturbances. In addition to this preventative measure, the numerical analysis tool can estimate the effect of these influences, so that plausibility ranges for the parameter estimations can be defined. In the following, possible individual special effects that have previously been identified, e.g. for the Benken borehole (Nagra 2001), are discussed in more detail.

3.3.2.1 Borehole history

All numerical analyses took into account the borehole pressure history. The borehole pressure history was constructed based on activities that took place prior to hydraulic testing. Drilling through the midpoint of the test interval was used as the starting point of the pressure history. The borehole pressure history data were incorporated into the numerical analyses. The following information was used:

- Date and time of drilling through the interval midpoint, from drilling logs
- Drilling fluid density
- Mud level in the borehole prior to testing
- Pressure records of preceding hydraulic testing

The drilling fluid densities were measured four times per day and documented in the drill mud report by the drill mud engineer from AKROS Oilfield Services GmbH. In addition, continuous recordings were available from the mud logging company GEODATA during periods of coring and mud circulation, and mud level measurements in the borehole were performed from time to time.

Most affected by the borehole pressure history is the determination of the static formation pressure (hydraulic potential), which in turn depends on the transmissivity of the formation. In formations with low transmissivity, like the Opalinus Clay, the determination of the static formation pressure can be impossible to carry out in a reasonable time due to the long duration of the pressure history. This was proven by measurements carried out using the Benken long-term monitoring system, which demonstrated that the static formation pressures of the Opalinus Clay determined by hydraulic tests were much higher than those subsequently determined by long-term measurements (e.g. Jäggi & Vogt 2020).

The specific periods of the borehole pressure history taken into account for the analysis of the hydraulic packer tests in borehole BOZ2-1 are provided in Tab. 3-21.

Tab. 3-21: Specific periods of the pre-test borehole pressure history

Pre-test refers to the period prior to the separation of the test interval from the rest of the borehole through the inflation of the last packer.

Test name	**Drilling through midpoint:** date and time	**Start hydraulic testing:** date and time	**Borehole history duration** [h]
BOZ2-1-HRO1	29.08.2020 20:38	02.09.2020 16:38	92.00
BOZ2-1-OPA1	25.09.2020 02:54	01.10.2020 00:26	141.53
BOZ2-1-OPA2	22.09.2020 04:43	04.10.2020 09:42	292.98
BOZ2-1-PWF1	21.09.2020 13:15	07.10.2020 13:43	384.47
BOZ2-1-PWF2	20.09.2020 19:39	09.10.2020 22:52	459.22
BOZ2-1-LIA1	27.09.2020 17:39	14.10.2020 06:06	396.45
BOZ2-1-OPA3	26.09.2020 00:12	18.10.2020 04:43	532.52
BOZ2-1-OPA4	23.09.2020 14:28	26.10.2020 01:02	778.57
BOZ2-1-KEU1	20.11.2020 22:10	22.11.2020 00:13	26.05
BOZ2-1-MUK1	30.11.2020 19:29	03.12.2020 15:13	67.73

3.3.2.2 Interval temperature changes during testing

All activities inside the open borehole also affect the temperature field in and around the borehole. In formations with low transmissivity, this temperature disturbance affects the pressure field surrounding the borehole due to coupled thermo-hydraulic processes. The analysis of hydraulic tests using the numerical software packages nSIGHTS (pre-version 3), Multisim and WellSi can incorporate temperature changes during the hydraulic test that lead to a change in fluid volume and thus pressure within a confined test interval volume. The fluid volume change in the test interval was calculated using the volumetric thermal expansion coefficient of the fluid (water), which itself is temperature-dependent. The pressure change is linearly dependent on the interval fluid volume change using a proportionality factor, the compressibility of the interval.

3.3.2.3 Mechanical effects

The mechanical deformations caused by drilling- and testing-related stress redistribution in the formation can also influence the pressure response during a hydraulic test. Normally, the conceptual model for the description of the storage coefficient used in the underlying hydraulic models assumes a compressible pore volume and an incompressible grain structure. In this model, changes in pore pressure are considered as movement of the fluid into and out of the pore volume. The coupling between fluid volume change and mechanical deformations results in a time-dependent deformation for an elastic medium (Detournay & Cheng 1988). The Opalinus Clay has shown a time-dependent deformation during tunnel excavation in Mont Terri (see Lisjak et al. 2015 for a summary of the observations and for a numerical interpretation of the data). Opalinus Clay time-dependent behaviour is most likely due to the undrained and drained excavation response, rather than mechanical creep phenomena. In formations with low transmissivity, time-dependent deformations can have an influence on the pressure signal observed in the test interval.

However, there are no data on mechanical deformations available for the tests in borehole BOZ2-1 that would allow the characterisation of mechanical effects on the tests in formations with low transmissivity. Deformations of the borehole wall can be included in the analysis by all the numerical software packages used by the means of an appropriate parameterisation during the analysis in the same way as for temperature changes inside the interval. The resulting pressure change is caused by volume changes, which can be either linear or quadratic. The proportionality factor between the volume change and the pressure change is the interval compressibility.

3.4 Test activities

A total of ten test intervals were investigated within borehole BOZ2-1 using the HDDP in single and double packer configuration. The most important test specifications are summarised in Tab. 3-22. The hydraulic packer tests were performed in the following geological formations (*cf.* Dossier III):

- Dogger Group with a focus on the Hauptrogenstein Formation (BOZ2-1-HRO1) and Passwang Formation including the Rothenfluh Member, the "Humphriesi-Schichten", Waldenburg Member, the Brüggli Member and the "Cond. Equivalents of the Sissach, Hauenstein and Hirnichopf Members" (BOZ2-1-PWF1, BOZ2-1-PWF2)
- Dogger Group with a focus on Opalinus Clay (BOZ2-1-OPA1, BOZ2-1-OPA2, BOZ2-1-OPA3, BOZ2-1-OPA4)
- Lias Group with a focus on the Staffelegg Formation including the Frick, Beggingen and Schambelen Members (BOZ2-1-LIA1)
- Keuper Group with a focus on the Klettgau Formation including the Gansingen and Ergolz Members and the Bänkerjoch Formation (BOZ2-1-KEU1)
- Muschelkalk Group with a focus on the Schinznach Formation including the Asp, Stamberg, Liedertswil, Leutschenberg and Kienberg Members (BOZ2-1-MUK1)

All hydraulic tests were performed in the cored borehole section with a borehole diameter of 6⅜", 114 mm (deflated diameter) packers and without any prior fluid exchange, i.e. with the drilling fluid being used as the interval test fluid. The exceptions to this were for BOZ2-1-HRO1 which was performed in an 8½" diameter borehole after a prior fluid exchange with traced water and extended hydraulic tests in the BOZ2-1-OPA3 and -OPA4 intervals which were performed after a fluid exchange with PEARSON water and used 146 mm (deflated diameter) packers. The density and viscosity of the drilling fluid were recorded by the mud engineer in daily mud reports. The tubing was typically filled with traced tap water. Sodium-Fluorescein at concentrations of approximately 1 ppm was used to trace the drilling mud, sodium-naphthionate or 1.5-naphthalene disulfonate acid – NDSA (for the hydraulic test within the shales) were used as tracers for the testing water in the tubing at concentrations of approximately 10 ppm. The SIT was closed during the entire time the HDDP was lowered to the test depth and also during installation. In test intervals with low transmissivity, the interval fluid density was not affected by traced water in the test tubing as mainly withdrawal tests were performed and either no, or only very little, fluid flow occurred. If a pressure increase of more than 100 kPa was observed in the test interval during inflation of the top packer, the SIT was opened and the COM phase started. Due to the higher density of the mud in the test interval, for formations with low transmissivity, it was assumed that no flow occurred from the test tubing into the test interval during the COM phase. Flow from the formation into the borehole by means of slug and pumping tests was created during all tests.

A swabbing tool was used to create the pressure difference between the test tubing and the test interval. For each of the pumping tests the PCP was used, and the position of the PCP stator in the test string was optimised up to the limit of the allowable pumping head. If two tests were performed sequentially without pulling the HDDP out of the borehole between tests, a stator was already installed for the first test (usually the deeper test).

Drilling stopped shortly before hydraulic testing of the BOZ2-1-HRO1, BOZ2-1-KEU1 and BOZ2-1-MUK1 intervals. The time gap between drilling and the start of hydraulic testing was significantly longer for the other test intervals, where a series of hydraulic tests were performed after drilling a longer borehole section. The measured pressures (measured by the downhole QSSP sensors) and pumping rates (measured by the flow board at the surface) for all tests conducted in borehole BOZ2-1 are provided in Figs. 3-9 to 3-18. The figures are taken directly from the detailed reports (DR) of the field test contractor.

The interval temperature change was included in the analysis of low-permeable formations. Interval temperature variation was not considered for hydraulic tests which included a pumping period due to the higher formation transmissivity. The temperature change in the test interval, from the start of the initial pressure recovery after closing the shut-in valve (PSR) until the end of the test, ranged from a decrease of 0.10 K to an increase of 5.01 K for all tests.

Tab. 3-22: Hydraulic packer testing in borehole BOZ2-1: test interval and test specifications

Test name[1]	**Interval depth** [m MD]	**Interval midpoint** [m MD]	**Packer configuration**	**Test phases**[1]	**Testing period** (duration)	**Geological information** [depth and length values are rounded; groups and formations are usually named from top down; for details see Dossier III]	**Objectives**[2] [secondary aims in brackets ()]
BOZ2-1-HRO1	334.30 – 365.93	350.12	Double	INF, COM, PSR, SW1, SWS1, SW2, SWS2, RW, RWS, PI, PW1, PW2, SW3, SWS3, DEF	02.09. – 08.09.2020 (131.5 h)	Dogger Group: marly limestone and iron-ooids interbedded with calcareous marlstone of the Hauptrogenstein Formation. This test was conducted after mud losses in the Hauptrogenstein Formation.	T, h_s, (FM), WS
BOZ2-1-PWF2	402.00 – 425.02	413.51	Double	INF, COM, PSR, SW, SWS, PW, DEF	09.10 – 12.10.2020 (61.3 h)	Dogger Group: marlstone and limestones interspersed with iron-oolite of the Passwang Formation. This hydraulic test was designed as an overview test for the upper part of the Passwang Formation.	T, h_s, FM
BOZ2-1-PWF1	429.30 – 452.32	440.81	Double	INF, COM, PSR, SW, SWS, PW, DEF	07.10. – 09.10.2020 (52.3 h)	Dogger Group: mainly marls and limestones interspersed with iron-oolite of the Passwang Formation; approximately 0.78 m of Opalinus Clay at the bottom of the interval. This hydraulic test was designed as an overview test for the lower part of the Passwang Formation.	T, h_s, FM
BOZ2-1-OPA2	455.00 – 478.02	466.51	Double	INF, COM, PSR, SW, SWS, PW, DEF	04.10. – 07.10.2020 (71.6 h)	Dogger Group, test interval entirely within Opalinus Clay. This test was designed as an overview test of the upper part of the Opalinus Clay where silty calcareous beds are present.	T, h_s, FM
BOZ2-1-OPA4	507.20 – 513.55	510.38	Double	INF, COM, PSR, SW, SWS, PI	26.10. – 28.10.2020 (64.6 h)	Dogger Group: test interval entirely within Opalinus Clay. The test preceded the realisation of a GTPT in the same interval. This test was designed to test a zone with a fault zone. It preceded a GTPT.	T, h_s, FM
BOZ2-1-OPA1	527.50 – 550.52	539.01	Double	INF, COM, PSR, SW, SWS, PW, DEF	01.10. – 04.10.2020 (76.6 h)	Dogger Group: test interval entirely within Opalinus Clay. This test was designed as an overview test of the clay rich zone of the Opalinus Clay.	T, h_s, FM
BOZ2-1-OPA3	559.18 – 566.16	562.67	Double	INF, COM, PSR, SW, SWS, PW	18.10. – 20.10.2020 (60.0 h)	Dogger Group: test interval entirely within Opalinus Clay. This test was designed to test a zone with fault zone.	T, h_s, FM

Tab. 3-22: continued

Test name[1]	**Interval depth** [m MD]	**Interval midpoint** [m MD]	**Packer configuration**	**Test phases**[1]	**Testing period** (duration)	**Geological information** [depth and length values are rounded; groups and formations are usually named from top down; for details see Dossier III]	**Objectives**[2] [secondary aims in brackets ()]
BOZ2-1-LIA1	598.00 – 615.00	606.50	Single	INF, COM, PSR, SW, SWS, PW, DEF	14.10. – 16.10.2020 (65.2 h)	Lias Group with approx. 14.46 m of the Staffelegg Formation (approx. 2.77 m of Frick Member, 3.5 m of the Beggingen Member and approx. 8.19 m of the Schambelen Member) and the Keuper Group with approx. 2.54 m of the Klettgau Formation, Gruhalde Member. Rocks within the test interval mainly consist of (partly marly) claystones and marly limestones. This overview test was designed to investigate the clay-rich part of the Staffelegg Formation (Schambelen Member) and the carbonate-rich rocks of the Beggingen Member.	T, h_s, FM
BOZ2-1-KEU1	631.40 – 658.00	644.70	Single	INF, COM, PSR, SW, SWS, PW, SW2, SWS2, SW3, SWS3, RW0, RWS0, RW1, MRWS, PI1, PI2, DEF	22.11. – 25.11.2020 (74.2 h)	Keuper Group with approx. 22.05 m of the Klettgau Formation (approx. 6.42 m of the Gansingen Member and approx. 15.63 m of the Ergolz Member) and approx. 4.55 m of the Bänkerjoch Formation. Rocks within the test interval mainly consist of marlstones, claystones and sandstones. The aim of this test was to target possible transmissive zones of the Klettgau Formation.	T, h_s, (FM), WS
BOZ2-1-MUK1	747.50 – 805.50	776.50	Single	INF, COM, PSR, SW1, SWS1, SW2, SWS2, MRW, MRWS, SW3, SWS3, DEF	03.12. – 07.12.2020 (81.3 h)	Approximately 0.77 m of the Bänkerjoch Formation (Keuper Group) at the top of the interval; approx. 57.23 m of the Schinznach Formation in the Muschelkalk Group with approx. 4.37 m of the Asp Member, 32.36 m of the Stamberg Member, 8.79 m of the Liedertswil Member and approx. 11.71 m of the Leutschenberg and Kienberg Members consisting mainly of dolostones as well as claystones, marlstones and limestones. This test was conducted after mud losses in the Schinznach Formation.	T, h_s, (FM), WS

[1] For an explanation of the test names and test phases see Tabs. A-2 and A-3, respectively.

[2] FM = flow model, T = transmissivity, h_s = static hydraulic head, WS = water sample.

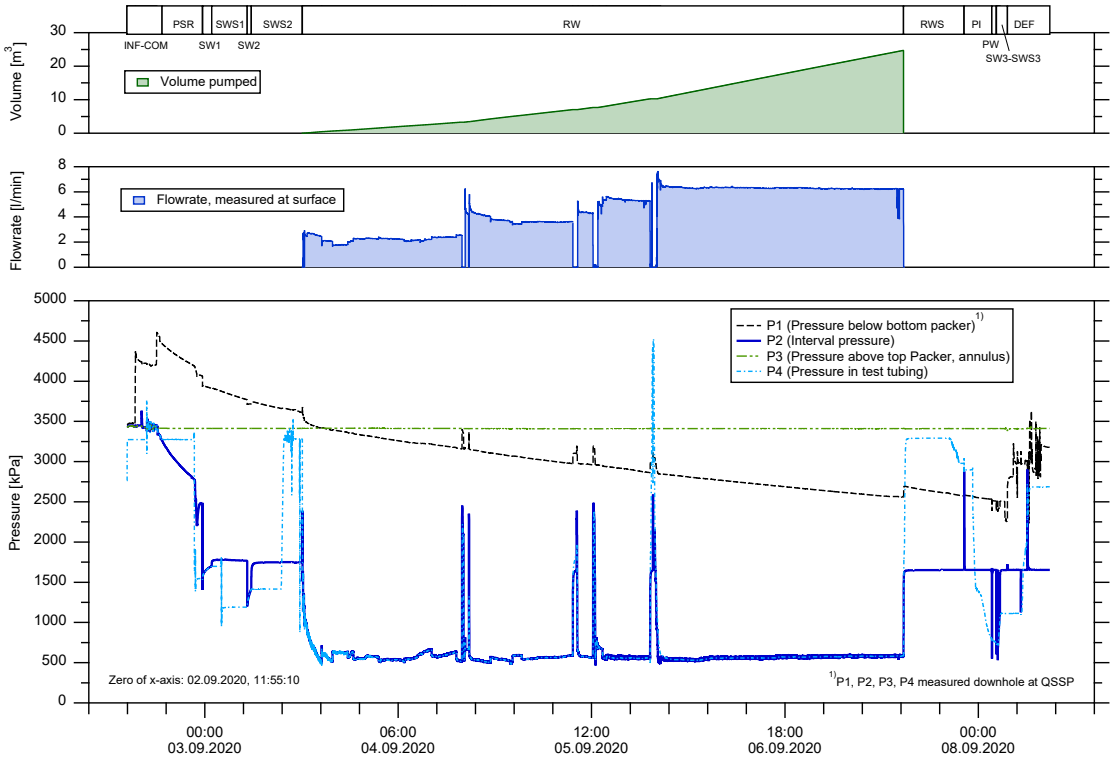

Fig. 3-9: Hydraulic packer test BOZ2-1-HRO1: Overview plot of pressure and flow rate vs. time and date

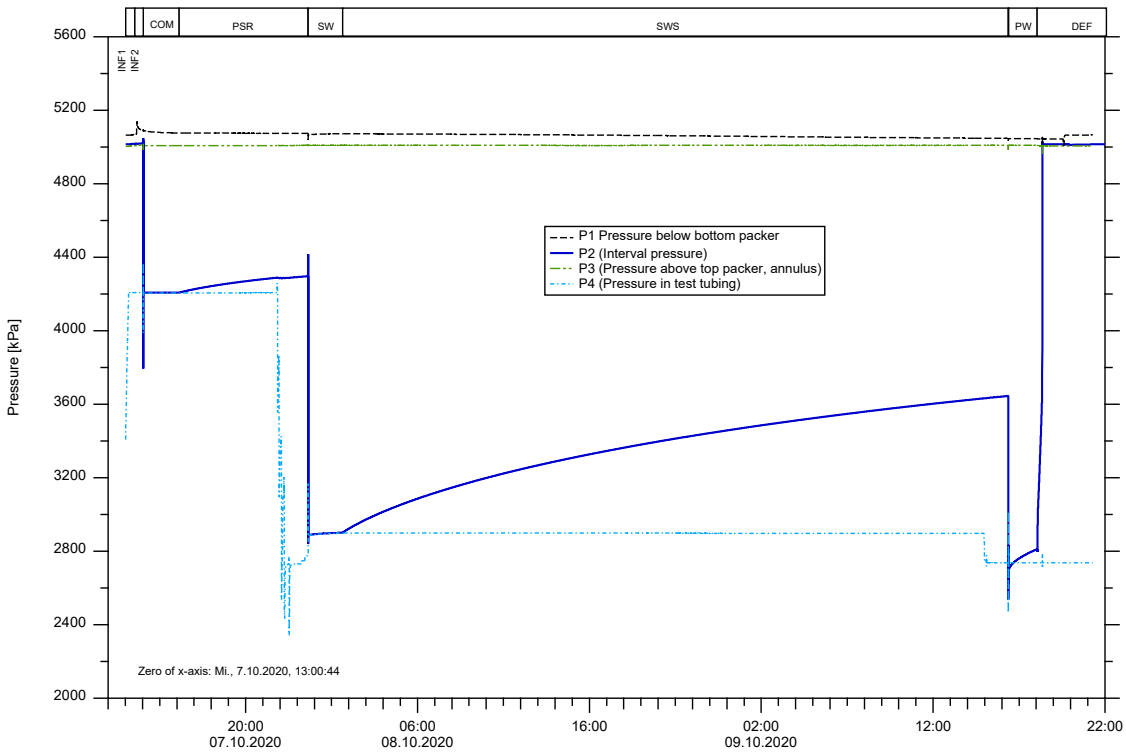

Fig. 3-10: Hydraulic packer test BOZ2-1-PWF1: Overview plot of pressure vs. time and date

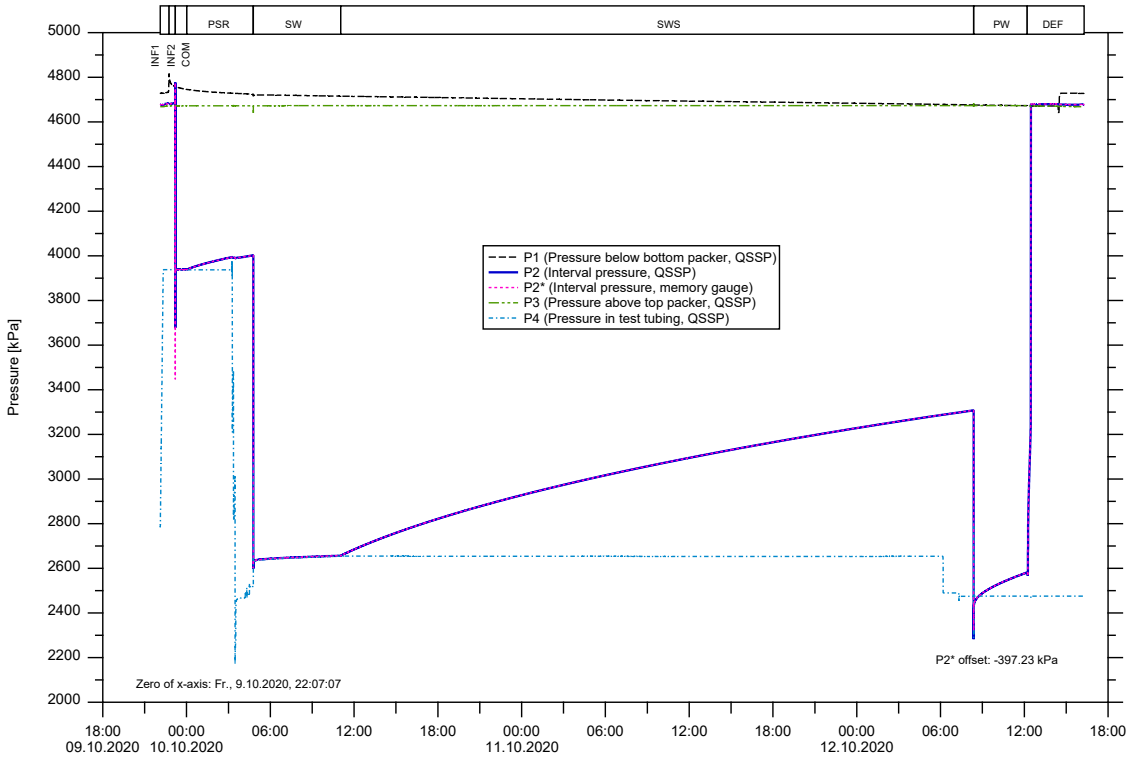

Fig. 3-11: Hydraulic packer test BOZ2-1-PWF2: Overview plot of pressure vs. time and date

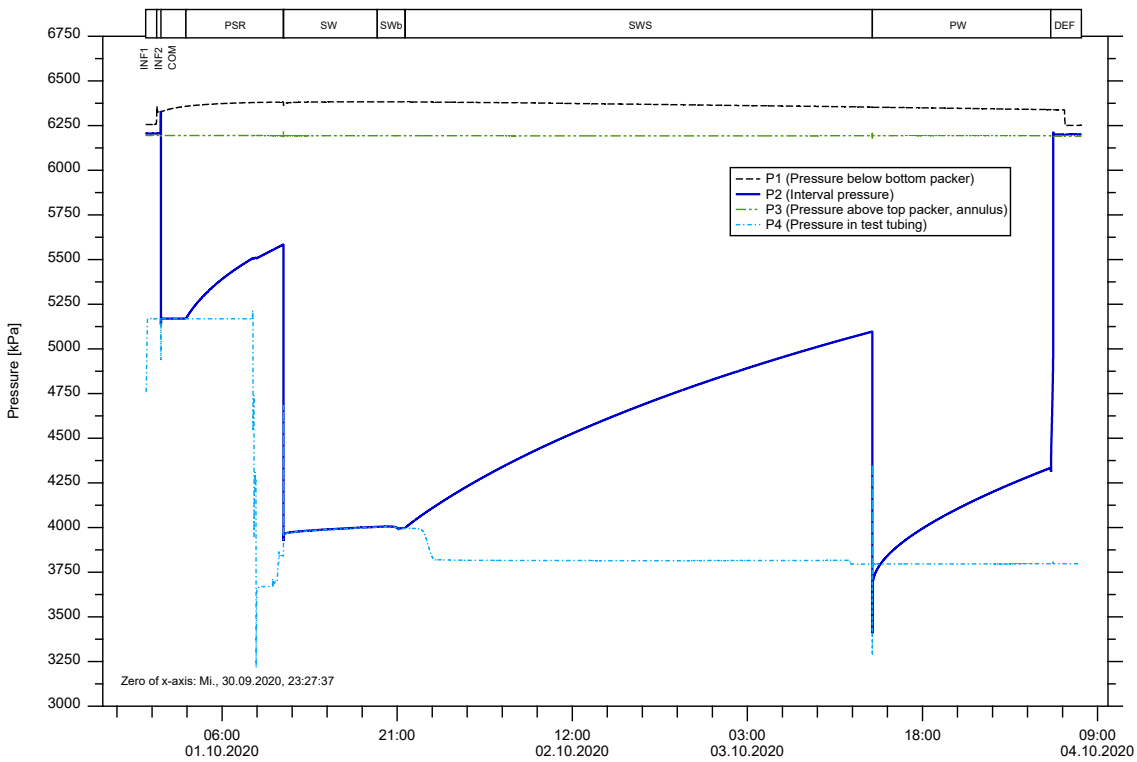

Fig. 3-12: Hydraulic packer test BOZ2-1-OPA1: Overview plot of pressure vs. time and date

SWb as part of SW was excluded from the analysis due to its irregular behaviour.

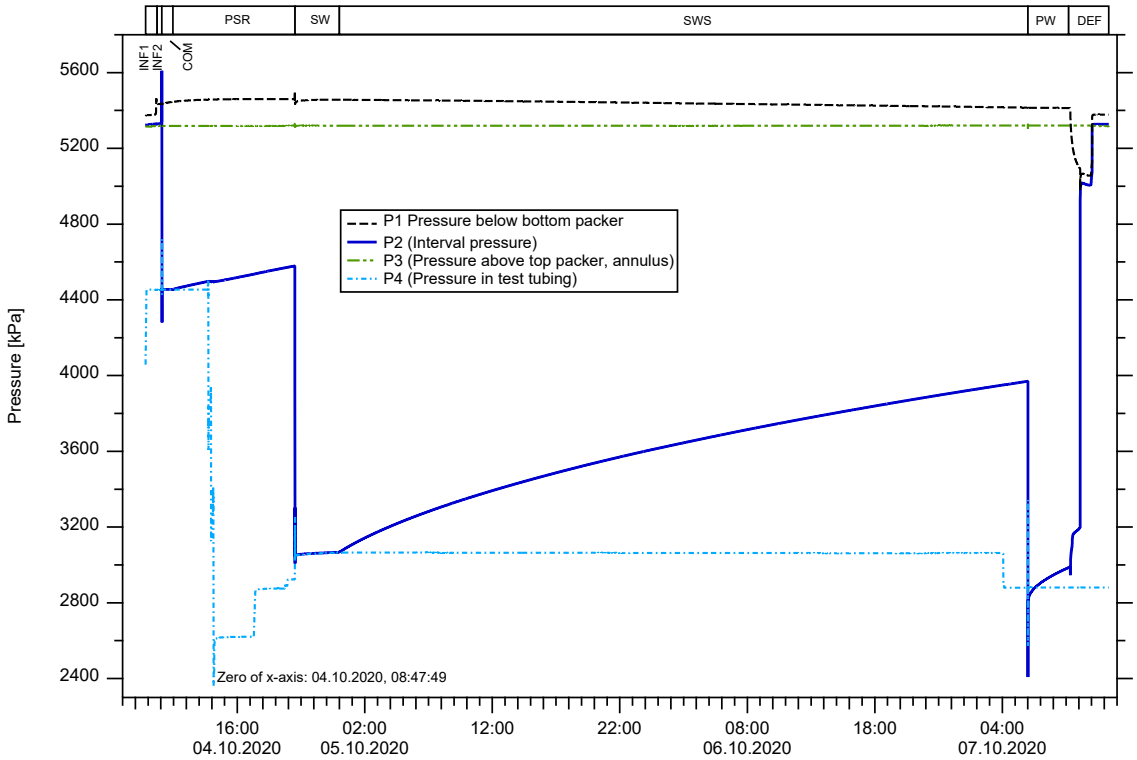

Fig. 3-13: Hydraulic packer test BOZ2-1-OPA2: Overview plot of pressure vs. time and date

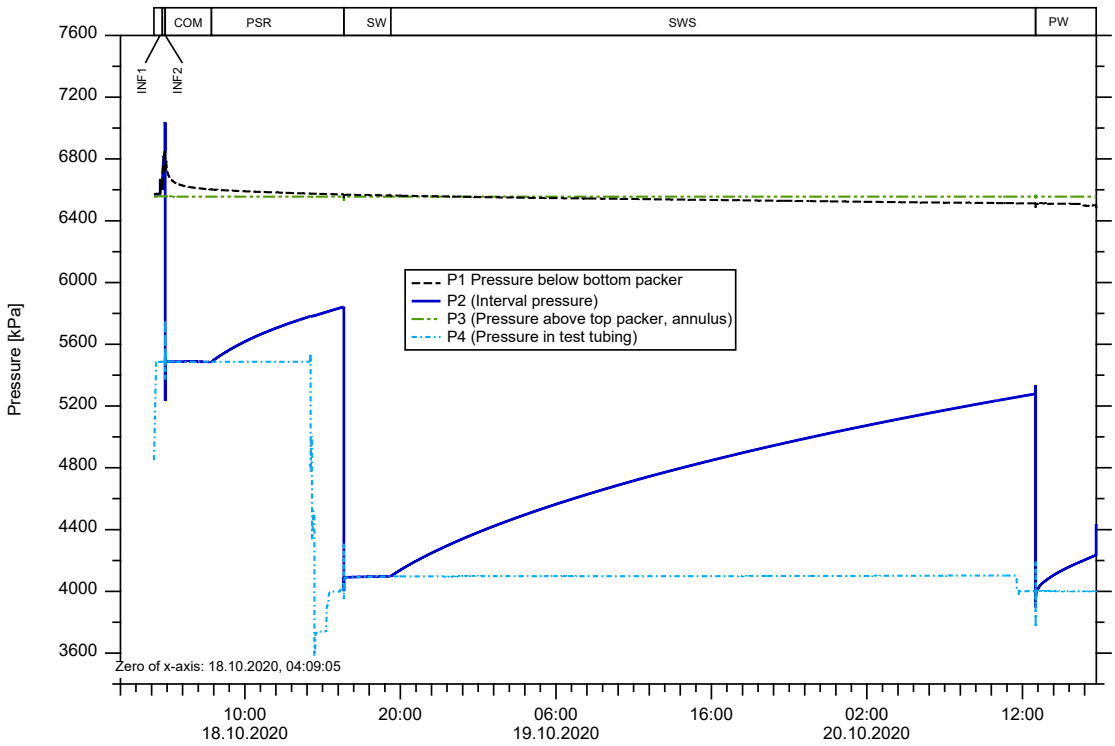

Fig. 3-14: Hydraulic packer test BOZ2-1-OPA3: Overview plot of pressure vs. time and date

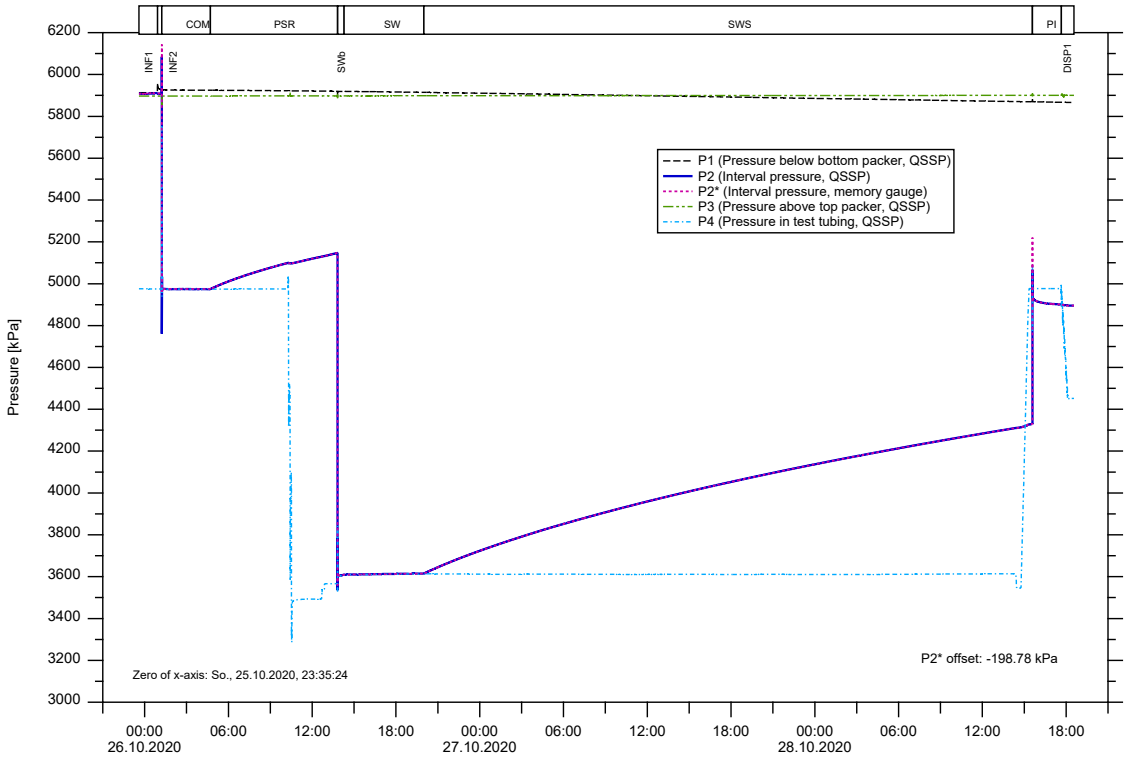

Fig. 3-15: Hydraulic packer test BOZ2-1-OPA4: Overview plot of pressure vs. time
SWb as part of SW was excluded from the analysis due to its irregular behaviour.

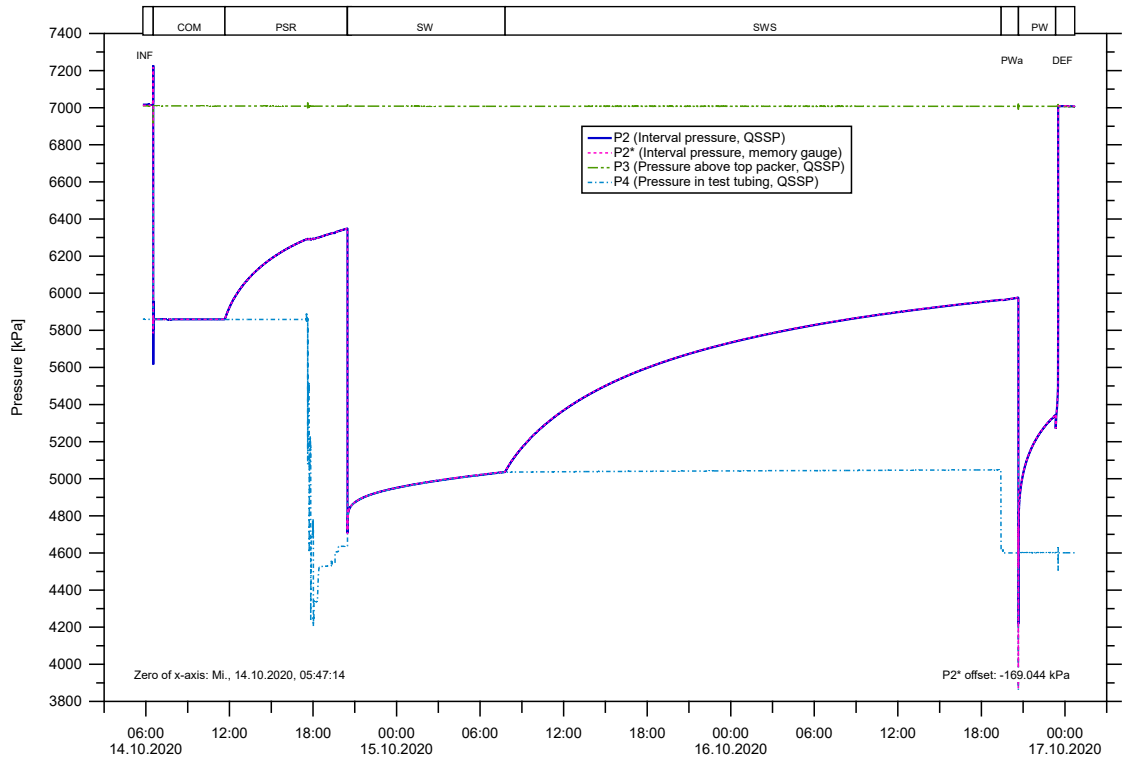

Fig. 3-16: Hydraulic packer test BOZ2-1-LIA1: Overview plot of pressure vs. time

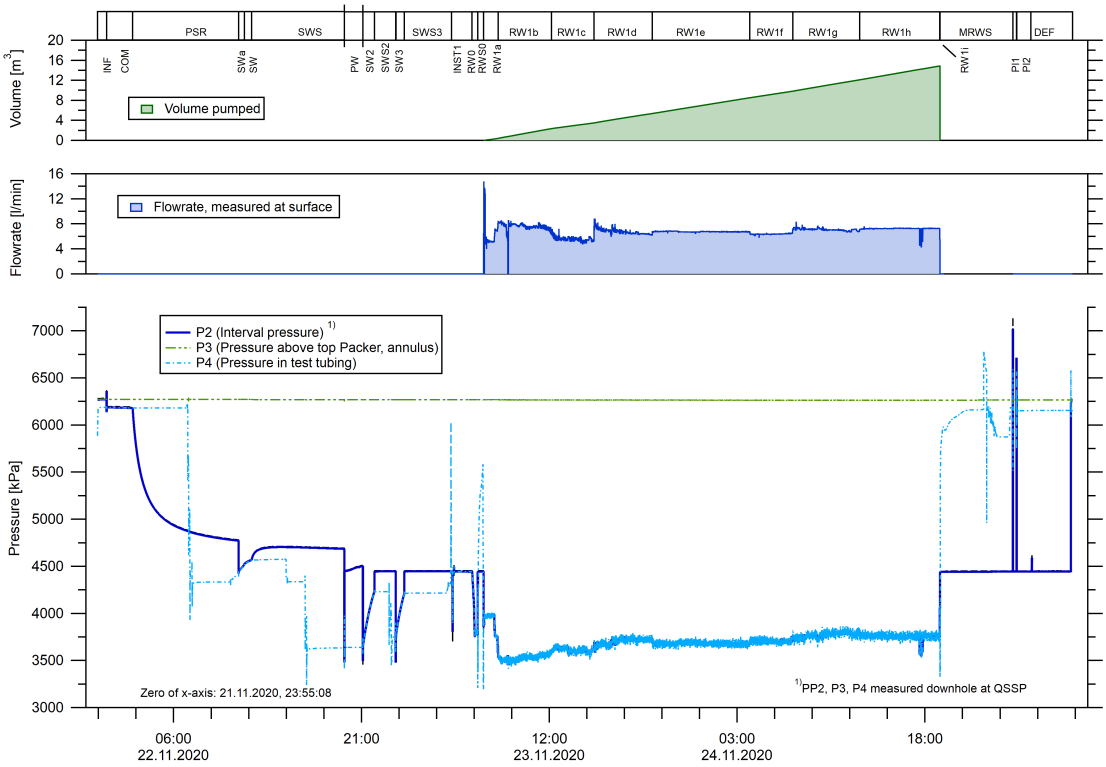

Fig. 3-17: Hydraulic packer test BOZ2-1-KEU1: Overview plot of pressure and flow rate vs. time

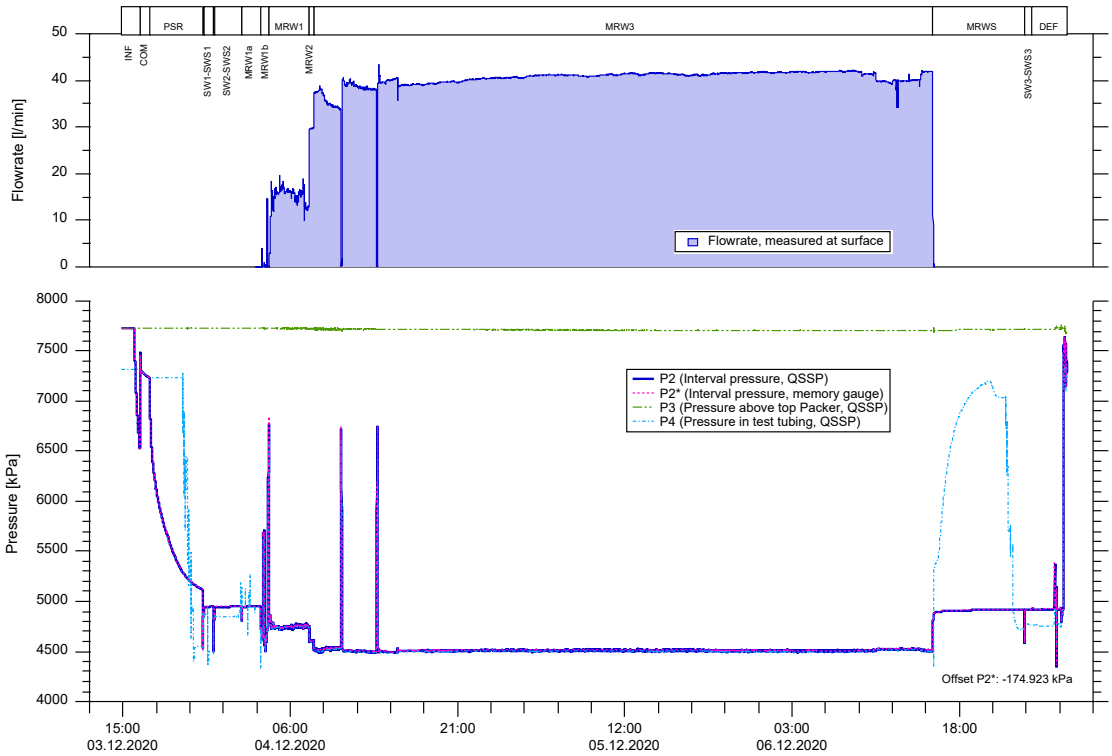

Fig. 3-18: Hydraulic packer test BOZ2-1-MUK1: Overview plot of pressure and flow rate vs. time and date

3.5 Details of selected tests

Two of the hydraulic packer tests are presented below in more detail: BOZ2-1-OPA4 and BOZ2-1-MUK1. The hydraulic test BOZ2-1-OPA4 was performed in a combination of a slug and slug-recovery phase and an additional pulse phase. It represents the test strategy preferred for formations with low to very low transmissivity (*cf.* Tab. 3-2 in Section 3.1). The second hydraulic test BOZ2-1-MUK1 was performed in a sequence of slug and slug-recovery phases and a multi rate pumping phase followed by a pressure recovery phase. It represents the preferred test strategy for formations with low to medium transmissivity (*cf.* Tab. 3-1 in Section 3.1).

The two test examples show the application of the two main approaches, which were used to provide estimates of the formation parameters including the associated ranges of uncertainty. The results of the two test analyses are provided in Section 3.6 together with the results of all other tests performed.

3.5.1 Hydraulic packer test BOZ2-1-OPA4

The hydraulic packer test BOZ2-1-OPA4 represents an example of testing formations with very low transmissivity after a long pressure history duration using a short hydraulic test execution duration. For the analysis, the measurements of the P2 sensor (503.96 m MD) inside the QSSP were used.

3.5.1.1 Interval characterisation

The hydraulic test BOZ2-1-OPA4 was performed in a double packer configuration. The entire interval was located in the Opalinus Clay of the Dogger Group (451.54 – 573.68 m MD). The HDDP used was designed to allow execution of a gas threshold pressure test (GTPT), in order to estimate the gas entry pressure of the formation. The packer test consisted of three parts: the first part was a hydraulic test using drilling fluid (potassium silicate & polymers) as the test fluid. Subsequent to the following gas threshold pressure test (GTPT), an additional hydraulic test was performed with PEARSON water. However, only the results for the first hydraulic test will be presented here. The GTPT is documented and discussed separately. The primary test objectives of the initial hydraulic test were to obtain reliable estimates of T (and K) for the formation, the freshwater hydraulic head and to determine the most appropriate flow model. Details of the tested interval and test duration are provided in Tab. 3-23. The borehole pressure history is presented at the beginning of Section 3.5.1.3.

Tab. 3-23: Hydraulic test BOZ2-1-OPA4: Information on the test interval

[1] Inflation of last packer (upper packer: PA2)

[2] Start of the interval fluid displacement for the subsequent GTPT

Test	**Depth**		**Length**	**Packer configuration**	**Hydraulic testing**		
	from [m MD]	to [m MD]	[m]		Start date [1]	End date [2]	Duration [h]
BOZ2-1-OPA4	507.20	513.55	6.35	Double	26.10.2020	28.10.2020	64.60

3.5.1.2 Test execution

Fig. 3-19 shows the system installation record as provided by the field test contractor. The equipment components are those described above in Section 3.2. The hydraulic test in interval BOZ2-1-OPA4 was performed after the following procedures were completed:

- Period of continued coring up to a depth of 615.00 m MD starting with coring through the midpoint of the test interval
- Petrophysical logging
- Hydraulic test series including BOZ2-1-OPA1, -OPA2, -PWF1, -PWF2, -LIA1 and -OPA3
- Installation of the HDDP

The HDDP was installed in borehole BOZ2-1 for BOZ2-1-OPA4 on 25.10.2020. Due to the execution of a GTPT following the test with drilling fluid, emplacement of the packer began with the installation of the exchange chamber. After the exchange chamber was assembled, the lower shut-in tool (SIT1) was placed on the top of the exchange chamber. The chamber was then filled with a small volume of water and pressurised with nitrogen. The SIT1 was then closed during the following run-in hole (RIH) of the HDDP and was kept closed during the first hydraulic test. During installation of the tubing, the SIT2 was closed, and the tubing was regularly filled up to the top with traced tap water (1.5-NDSA with a concentration of approx. 10 ppm). The QSSP pressure sensors were regularly checked, and the exchange chamber was continuously pressurised during the RIH. The installation was completed 778.57 hours after drilling through the interval midpoint, by inflation of the upper packer (upper packer: PA2). Due to the squeeze effect that occurred in the interval during inflation of the upper packer, the upper shut-in tool (SIT2) was opened to initiate the compliance phase (COM) that lasted 3.5 hours. Next, the SIT2 was closed, and the initial pressure recovery phase (PSR) commenced, lasting around 9.1 hours. After completion of the PSR phase, the slim tubing was installed, and a slug withdrawal test (SW) was performed that lasted for 6.2 hours. The SW test was terminated by the closure of the SIT2 valve. The subsequent pressure recovery (SWS) was recorded for 43.6 hours. Finally, a pulse injection test (PI) was performed and lasted for 2.1 hours. After this time, the first hydraulic test was terminated by the displacement of the interval fluid (potassium silicate & polymers) through SIT1 into the exchange chamber.

Installation Record - Double Packer + Moyno Pump

SOLEXPERTS

Seite 1 / 4

HDDP Packertests				Location	Bözberg	Date	24.10.2020	Engineer	JH
Borehole	BOZ2-1	Direction	vertical	Reference point (= GL)	624.33 m asl	Interval	OPA 4 GTPT	JOB Nr.	2666
Borehole Depth	615.0 m	Casing Depth	369 m bgl	Interval length	6.35 m	Test depth (UPLS)	507.20 m bgl	System	HDDP 146
Borehole Diameter	162 mm	Stickup b. Reference	-1.64 m	Water depth	-2.02 m bgl	Test file	BOZ2_1_GTPT	Quadro Probe	QSSP 3

Note: All depths shown are not correct for borehole deviation

		Qty -	L_{unit} m	L_{total} m	Depth m	OD mm	ID mm	Wgt kg	Str t
Rig floor	-2.82								
Wellhead, Wellhead equipment (not shown)									
Stickup	-4.46 m bgl								
Ground level (GL)		0	0.00		0.00				
Tubing 2"7/8 EU	Tally list 2	55	503.08	503.08		93.2 / 93.2	62.0 / 62.0	4981	45
					498.62	78.6	62.0		
						93.2	62.0	20	
	Siphon + X-Over	1	1.40		498.62	93.2			
SIT2 (2"7/8 DAS)	SIT	1	0.66		499.10	106.0	24.0	69	
	DAP	1	1.17						
Cable Base incl. Coupling + Crown Shaft		1	1.31			105.0	24.0		
Probe Carrier with Quadruple Probe	QSSP P3	1	0.53	8.58	503.69	105	3 x Ø19	132	16.0
	QSSP P4		0.13		503.81				
	QSSP P2		0.14		503.96				
	QSSP P1		0.20		504.15				
			0.63						
Crown Shaft incl. 1 X-Over		1	0.40			100.0	40.0		
Safety Joint		1	0.33			93.7	63.5		90.0
Packer Stick Up			0.27						
Up. Packer Seal	UPUS		0.22		506.00			120	
Upper Packer			1.20			146.0	49.0		
	UPLS		0.27		507.20				
Straddle Length	Packer Stick Down		0.55						
Tubing 2"7/8 EU	Tally list 1	2	3.39	6.35		93.2	62.0	33	
X-Over		1	0.27			93.0	50.0	3	16.0
Filter	Screen	1	0.97			89.0	73.0	19	
X-Over	Including DataCan	P2*	0.41		512.75	93	50.0	3	
Packer Stick Up			0.27						
Lower Packer Seal	LPUS		0.22		513.55				
Lower Packer		1	1.20	2.03		146.0	49.0	105	
	LPLS		0.27		514.75				
Packer Stick Down			0.24						
Crown shaft			0.32		515.57	95.0	--		
SIT1 (2"7/8 DAS)	SIT	1	0.60	2.07		106.0	24.0	69.0	
	DAP	1	0.89						
X-Over		1	0.33						
Connection pressure reservoir		1	0.25		517.64			3.0	
Pressure Reservoir	Tally pressure reservoir	5	43.63	43.73		114.30	100.50	818.1	
Bottom Cap		1	0.10		561.37				

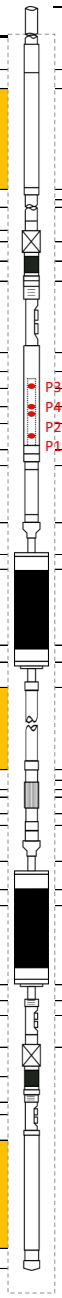

Comments:

Zahlencode:
xx PA2 und PA1
1 Backflow pressure reservoir (rot)
2 SIT1 (weiss)
3 Injection interval (grün)
4 leer evtl. P1-Keller
5 PA1 auf PA2 Spannleitung (blau)

End of Borehole (m bgl): 615.00

Total Weight (kg): 6375

Fig. 3-19: Hydraulic test BOZ2-1-OPA4: Downhole equipment installation record with system layout as used in the field test

3.5.1.3 Analysis

Borehole pressure history

The borehole pressure history used for the analysis of the BOZ2-1-OPA4 test is shown in Fig. B-1 (see Appendix B) and summarised in Tab. 3-24. Calculation of the mean interval fluid density using the P2 pressure measurement (prior to packer inflation) gave a density of 1'201 kg m^{-3}. This value corresponds to the documented density for the drill mud during drilling (1'200 kg m^{-3}; see Dossier I). For periods without a mud level measurement, the mud level was assumed to be at the level of the drain pipe, 1.95 m above ground level. This was due to the fact that for periods with no active mud circulation, the drillers generally kept the borehole filled with mud up to the level of the drain pipe. Therefore, the pressure value of 5'962 kPa was used for the history periods without a measurement and when the borehole was filled with drilling mud. During periods of previous hydraulic testing, the pressure was measured using either the P1 (used for the hydraulic tests above the interval BOZ2-1-OPA4: BOZ2-1-OPA2, -PWF1, -PWF2) or P3 (used for the hydraulic tests below the interval BOZ2-1-OPA4: BOZ2-1-OPA1, -LIA1, -OPA3) QSSP sensors, and were extrapolated to the depth of the P2 transducer at BOZ2-1-OPA4. Once the HDDP was at test depth and data acquisition began, the P2 QSSP sensor measured pressure directly (Fig. 3-15).

Tab. 3-24: Hydraulic test BOZ2-1-OPA4: Borehole pressure history

[1] Interval pressure at the level of the P2 sensor (503.96 m MD) with a pressure offset of 2.58 kPa as calculated from the history information, e.g. fluid level and density.

[2] Drilling through the interval midpoint (510.38 m MD).

[3] Pressure measured when the borehole was filled with mud (e.g. when P2 was at test depth but before packer inflation).

[4] P3 sensor measurement during testing corrected to the P2 sensor level (503.96 m MD).

[5] P1 sensor measurement during testing corrected to the P2 sensor level (503.96 m MD).

[6] Test start refers to the first time recorded on the data acquisition system (DAS) file.

Description	**Start date and time**	**Duration** [h]	**Pressure** [1] [kPa]	
		Total: 777.12	**Start**	**End**
Drilling [2]	23.09.2020 14:28	120.03	5'962	5'962 [3]
Petrophysical logging	28.09.2020 14:30	56.95	5'962 [3]	5'962 [3]
BOZ2-1-OPA1 [4]	30.09.2020 23:27	81.35	5'966	5'962
BOZ2-1-OPA2 [5]	04.10.2020 08:48	76.22	5'995	5'996
BOZ2-1-PWF1 [5]	07.10.2020 13:01	57.10	5'989	5'989
BOZ2-1-PWF2 [5]	09.10.2020 22:07	82.88	5'997	5'997
Check trip	13.10.2020 09:00	20.78	5'997	5'951
BOZ2-1-LIA1 [4]	14.10.2020 05:47	83.37	5'955	5'951
Mud level measurement	17.10.2020 17:09	11.00	5'902	5'951
BOZ2-1-OPA3 [4]	18.10.2020 04:09	154.35	5'954	5'949
Check trip	24.10.2020 14:30	33.08	5'997	5'951
Start testing BOZ2-1-OPA4	25.10.2020 23:35 [6]	-	5'909	-

Flow model evaluation

The hydraulic test sequence was analysed using a 2-zone radial composite flow model. This flow model approach was based on the analysis of the shut-in phase (PSR) and the slug recovery phase (SWS) using Agarwal superposition time as well as the de-convolved slug phase (SW). Figs. B-2, B-3 and B-4 show the diagnostic plots for the PSR, SWS and the SW phases respectively. The diagnostic plot for the PSR phase shows a long-lasting period dominated by wellbore storage and the log-log plot for the SWS phase shows a similar picture. For late times, the pressure curve and derivative begin to separate, indicating the beginning of a transition phase towards the onset of the formation response. A clear formation response as represented by infinite acting radial flow (IARF) conditions cannot be seen in either of these figures. Only in the diagnostic log-log plot of the de-convolved slug phase (SW in Fig. B-4), a flattening of the derivative is seen that might indicate a late time radial flow field, supporting the selection of a radial flow model.

Analysis of the slug – slug recovery (SW-SWS) sequence

In this analysis, temperature changes during the test phases that took place inside the closed test interval were considered. Fig. B-5 shows the development of the downhole temperature and pressure inside the test interval (P2*, T2*), as measured by the memory gauge and the QSSP respectively. The selection of the SW-SWS sequence for the analysis was made due to (i) the long duration of the slug recovery phase, and (ii) the analysis results of the pulse phase that showed difficulties in matching the SW-SWS and PI phases together. This was assumed to be mainly due to the different mud characteristics associated with the changing flow direction and the fact that due to its short duration, the PI phase provided little significant information about the formation parameters. However, the analysis included a validation of the fitting-parameter estimations by inverse optimisation of the SW-SWS-PI sequence. The slug phase was performed using 6 mm diameter (physical) slim tubing. The slim tubing radius was corrected considering the physical slim tubing and the contribution of the system compliance (i.e. the compressibility of the test zone and the compressibility of the water column above the shut-in valve SIT2) according to Black et al. (1987).

The results, derived from the parameter optimisation based on the measured pressure of the SW-SWS sequence, are shown in Tab. 3-25. The derived value for the static formation pressure (P_f) reached the upper limit of the pre-defined range of plausibility (parameter optimisation range). The cartesian fit for the entire sequence pressure measurement is displayed in Fig. B-6 (reference case – RC).

Tab. 3-25: Hydraulic test BOZ2-1-OPA4: Formation parameter estimation based on the parameter optimisation of the SW-SWS phase using a radial composite (skin) flow model considering both the borehole pressure history and temperature changes inside the test interval

[1] Static formation pressure at the depth of the P2 sensor (503.96 m MD).

SW-SWS results (radial composite flow model)	**K** [m s^{-1}]	**S_S** [m^{-1}]	**P_f** [1] [kPa]
Best estimate	8.05×10^{-15}	1.17×10^{-6}	10'129

The resulting discontinuity radius of 0.094 m (thickness of inner zone 13 mm) may indicate that the inner/skin zone is not necessary. However, the results of a parameter optimisation using a homogeneous flow model confirm the existence of an inner/skin zone (*cf.* Fig. B-6, Case 0).

Tab. 3-26 shows the results of the parameter optimisation for the homogeneous flow model. In this case, the formation specific storage reaches the upper limit of the predefined range of plausibility (parameter optimisation range).

Tab. 3-26: Hydraulic test BOZ2-1-OPA4: Formation parameter estimation based on the parameter optimisation of the SW-SWS phase using a homogeneous flow model considering the borehole pressure history and temperature changes inside the test interval

[1] Static formation pressure at the depth of the P2 sensor (503.96 m MD).

SW-SWS results (homogeneous flow model)	**K** [m s^{-1}]	**Ss** [m^{-1}]	**Pf** [1] [kPa]
Best estimate	6.08×10^{-15}	3.60×10^{-6}	7'859

The existence of the inner/skin zone is also supported by the residual analysis. Fig. B-7 provides the probability distribution functions for both simulations. It can be concluded that a normal distribution of the differences between simulated and measured pressure confirms the chosen conceptual model being a radial composite flow model.

Joint parameter regions of the SW-SWS sequence

Based on the results of the parameter optimisation using a radial composite flow model, estimation of the joint parameter regions is possible. Tab. 3-27 provides the 95% uncertainty ranges for the results of the parameter optimisation. The calculated ranges are unrealistically small due to the existence of well-defined and well-constrained minima of the objective function/SSE values. Therefore, further investigations were performed to estimate the uncertainty ranges of the formation parameters.

Tab. 3-27: Hydraulic test BOZ2-1-OPA4: 95% uncertainty range associated with the result of the parameter optimisation using a radial composite flow model for the SW-SWS sequence

[1] Static formation pressure at the midpoint of the test interval (503.96 m MD).

SW-SWS Results (joint parameter region)	**K** [m s^{-1}]	**Ss** [m^{-1}]	**Pf** [1] [kPa]
95% uncertainty range	$8.04 – 8.05 \times 10^{-15}$	$1.16 – 1.17 \times 10^{-6}$	10'126 – 10'132

Estimates of the formation parameter values and uncertainty ranges

An analysis to assess the uncertainty of the results was considered to be necessary. However, this does not apply to the influence of variation of the borehole pressure history, which is always considered as described previously (see Tab. 3-24). In this sense, it should be noted that the main part of the BOZ2-1-OPA4 borehole pressure history was described by the pressure measurements of previous hydraulic tests. Another reason was due to the fact that prior analysis results in the TBO borehole campaign (BUL1-1, MAR1-1) have also shown that there was no significant influence of small variations in mud density during the pressure history period. The analysis for

estimating the uncertainty in the results is thus reduced to a consideration of the uncertainty associated with the parameter optimisation procedure and any inaccuracies in the determination of the wellbore storage. The former can be estimated using a perturbation analysis. In this analysis, the bandwidth of the parameters is determined based on several individual optimisations, which can, for instance, identify whether the result corresponds to a global minimum in the parameter space. The possible influence of uncertainties in the determination of the wellbore storage is assessed by a sampling analysis. In this analysis, the parameters are optimised depending on a representative bandwidth for the wellbore storage.

A perturbation analysis with 500 runs was carried out in which the radius of the discontinuity (skin) was fixed. The results of the single parameter optimisations of the perturbation runs are shown against increasing values of the objective function/sum of squared errors (SSE) in Fig. B-8. The first 153 runs (run#0 to run#152) cover an SSE range between 99'605 and 164'474 (Fig. B-8). Within this range the fits of the SW-SWS sequence are of good to excellent quality and therefore used for the estimation of the parameter uncertainty ranges. Tab. 3-28 shows the resulting formation parameter ranges and best estimates of each parameter associated with the lowest SSE value. The upper limit of the formation specific storage is defined by the range of plausibility (parameter optimisation range) that was estimated based on the bandwidth of the mechanical properties of the Opalinus Clay.

Tab. 3-28: Hydraulic test BOZ2-1-OPA4: Uncertainty ranges and best estimates for the formation parameters estimated by the perturbation analysis

[1] Static formation pressure at the midpoint of the test interval (503.96 m MD).

Perturbation analysis results	**K** [m s^{-1}]	**Ss** [m^{-1}]	**Pf** [1] [kPa]
Best estimate	1.06×10^{-14}	2.59×10^{-6}	9'396
Uncertainty range	$0.54 – 2.55 \times 10^{-14}$	$0.64 – 3.60 \times 10^{-6}$	7'669 – 10'780

Fig. B-9 shows a comparison between the initial parameter optimisation and the simulation associated to the lowest SSE value (run#0) of the perturbation analysis.

Scatter plots of the formation parameters are shown in Fig. B-10. The two upper plots show a clear negative correlation between the formation hydraulic conductivity and both the formation specific storage (outer) and the static formation pressure. Conversely, the plot of the formation specific storage against the static formation pressure are positively correlated.

The sampling analysis for the test zone compressibility was performed for a maximal suitable range of values between 4.3×10^{-10} Pa^{-1} and 1.0×10^{-9} Pa^{-1}. The resulting parameter sets in combination with the resulting objective function value/SSE value as a function of the value of the test zone compressibility are represented in Fig. B-11. Tab. 3-29 shows the resulting formation parameter ranges and best estimates for each parameter associated with the lowest SSE value (test zone compressibility of 7.06×10^{-10} Pa^{-1}). The uncertainty range was defined between the value of 4.47×10^{-10} Pa^{-1} for the test zone compressibility as a lower limit, which is slightly larger than the fluid compressibility, and a corresponding upper value of 7.64×10^{-10} Pa^{-1} associated with an SSE value equal to the objective function value/SSE value of the lower limit. Within this range, the lower estimate of the formation specific storage value reached the range of plausibility (parameter optimisation range).

Tab. 3-29: Hydraulic test BOZ2-1-OPA4: Uncertainty ranges and best estimates for the formation parameters as a result of the sampling analysis for the test zone compressibility

[1] Static formation pressure at the midpoint of the test interval (503.96 m MD).

Sampling analysis results	**K** [m s^{-1}]	**Ss** [m^{-1}]	**Pf** [1] [kPa]
Best estimate	1.30×10^{-14}	0.95×10^{-6}	10'029
Uncertainty range	$1.19 – 2.26 \times 10^{-14}$	$0.63 – 1.90 \times 10^{-6}$	8'292 – 10'162

Parameter optimisation for the SW-SWS-PI sequence

To validate the results of the chosen sequence SW-SWS, the SW-SWS-PI sequence was investigated. The same conceptual model was used to numerically simulate the test data for the SW-SWS-PI sequence, i.e., a radial-composite flow model with a wellbore storage as the inner boundary condition in an infinitely extended reservoir.

The results, derived from the parameter optimisation based on the measured pressure of the SW-SWS-PI sequence, are shown in Tab. 3-30. The cartesian fit for the sequence pressure measurement is displayed in Fig. B-12.

Tab. 3-30: Hydraulic test BOZ2-1-OPA4: Formation parameter estimates based on the parameter optimisation of the SW-SWS-PI sequence using a radial composite flow model considering both the borehole pressure history and the temperature changes inside the test interval

[1] Static formation pressure at the depth of the P2 sensor (503.96 m MD).

SW-SWS-PI results (radial composite flow model)	**K** [m s^{-1}]	**Ss** [m^{-1}]	**Pf** [1] [kPa]
Best estimate	2.40×10^{-14}	1.14×10^{-6}	8'199

Similar to the match on the SW-SWS phases (red line in Fig. B-6), the SW-SWS-PI sequence fit in Fig. B-12 shows, that the conceptual model – the radial composite flow model – can also be applied successfully to the SW-SWS-PI sequence. The variation of parameter estimates and the relatively poor match between the simulated and the measured pressure curve for the PI phase also indicate that the change in flow direction (withdrawal vs. injection test) may have caused a different skin behaviour.

Summary of the analysis

Tab. 3-31 presents the results of the analysis of the formation parameters for interval BOZ2-1-OPA4.The best estimates for the formation parameters were derived from the analysis of the SW-SWS sequence. The best estimates for the formation parameters result from the sampling analysis (with a reliable test zone compressibility of 7.06×10^{-10} Pa^{-1}), relating to the lowest objective function value achieved by this simulation. The uncertainty ranges from the sampling analysis were smaller than the uncertainty ranges derived from the perturbation analysis, with the

exception of the lower limit of formation specific storage. Therefore, the uncertainty ranges for the formation parameters are defined by the results of the perturbation analysis, except for the lower limit of the formation specific storage. The formation parameter estimates derived from the SW-SWS-PI sequence are all within the derived uncertainty ranges.

Nevertheless, the best estimate and the wide uncertainty range of the static formation pressure significantly exceed the expected formation pressure. The derived freshwater heads, based on the estimated formation pressures, are therefore judged as unrealistic and considered to represent "apparent" heads.

Tab. 3-31: Hydraulic test BOZ2-1-OPA4: Best estimates for the formation parameters and associated uncertainty ranges

[1] Static formation pressure at the midpoint of the test interval (510.38 m MD) considering the sensor offset of 2.58 kPa.

BOZ2-1-OPA4	**K** [m s^{-1}]	**Ss** [m^{-1}]	**Ps** [1] [kPa]
Best estimate	1.30×10^{-14}	9.55×10^{-7}	10'101
Uncertainty range	$0.54 – 2.55 \times 10^{-14}$	$0.63 – 3.60 \times 10^{-6}$	7'741 – 10'852

3.5.2 Hydraulic packer test BOZ2-1-MUK1

The hydraulic packer test BOZ2-1-MUK1 represents an example of testing in a formation with medium transmissivity, a moderate pressure history duration and a moderate hydraulic test duration. For this analysis, the QSSP P2 sensor measurements (743.98 m MD) were used.

3.5.2.1 Interval characterisation

The hydraulic test BOZ2-1-MUK1 was performed in a single packer configuration. The main part of the interval (748.27 – 805.50 m MD) is located in the Schinznach Formation of the Muschelkalk Group and the uppermost part (747.50 – 748.27 m MD) belongs to the Bänkerjoch Formation of the Keuper Group. The test interval covers the layers of main interest believed to be potentially conductive in the Schinznach Formation. The primary test objectives were to obtain reliable estimates of T (and K) for the formation and the freshwater hydraulic head as well as collection of a water sample. In addition, an evaluation of the most appropriate flow model for the Schinznach formation of the Muschelkalk Group was also to be carried out. Details of the interval and test duration are provided in Tab. 3-32. During coring in this borehole section, a total of 64 m^3 of mud loss (Pure-Bore®) into the formation was observed, with an approximate flow rate during static losses of 1'300 l/h.

Tab. 3-32: Hydraulic test BOZ2-1-MUK1: Test interval information

Test	**Depth**		**Length**	**Packer configuration**	**Hydraulic testing**		
	from [m MD]	to [m MD]	[m]		Start date	End date	Duration [h]
BOZ2-1-MUK1	747.50	805.50	58.00	Single	03.12.2020	07.12.2020	81.3

3.5.2.2 Test execution

Fig. 3-20 shows the system installation record as provided by the field test contractor. The equipment components are those described above, in Section 3.2. The test in interval BOZ2-1-MUK1 was performed after the following procedures were completed:

- A period of continued coring which started with drilling throughout the midpoint of the test interval
- Wiper trip
- Installation of the HDDP system

The HDDP was installed in borehole BOZ2-1 for the BOZ2-1-MUK1 test on 03.12.2020. After the installation of two pieces of test tubing, the tubing was filled with traced tap water (sodium-naphthionate with a concentration of approx. 10 ppm) and the shut-in tool (SIT) was opened to release the air. During the subsequent placement of the HDDP, the SIT was closed, and the tubing was regularly filled to the top with traced tap water. The QSSP pressure sensors were regularly checked during the RIH of the HDDP. The installation was completed 67.73 hours after drilling through the interval midpoint, by inflation of the packer. The SIT was opened for 0.9 hours after packer inflation (COM), whether no squeeze effect occurred during inflation. The SIT was then closed and the initial pressure recovery phase (PSR) commenced and lasted around 4.8 hours. The following slug withdrawal phase (SW1) lasted for 7.2 minutes, and the subsequent pressure recovery (SWS1) was recorded for 51 minutes. To confirm the previous test phases SW1 and SWS1, second slug and recovery phases were performed. The second slug phase (SW2) lasted for 6 minutes, and the subsequent pressure recovery phase (SWS2) was recorded for 2.4 hours until the SIT was opened to allow installation of the progressive cavity pump (PCP). The pump test phase (MRW) was started with an initial flow rate of about 15 l/min. Due to decreasing pump rates during the MRW phase, the pump was briefly stopped twice for around 3 minutes to unclog the filter. The flow rate finally stabilised at about 40.7 l/min and after 52.4 hours of pumping groundwater sampling was started. The MRW phase was terminated after 59.5 hours, and the corresponding pressure recovery (MRWS) was conducted for a period of 8.2 hours. Finally, a third slug withdrawal sequence (SW3-SWS3) was performed. The final slug phase (SW3) lasted for 1.5 minutes, and the following shut-in phase (SWS3) was recorded for 0.6 hours. After subsequent deflation (DEF) of the packer, the SIT was closed and the entire HDDP system was removed from the borehole.

Installation Record - Single Packer

SOLEXPERTS

Seite 1 / 4

HDDP Packertests				Location	Bötzberg	Date	03.12.2020	Engineer	MC
Borehole	BOZ2-1	Direction	vertical	Reference point (= GL)	624.33 m asl	Interval	MUK1	JOB Nr.	2666
Borehole Depth	805.5 m	Casing Depth	615 m bgl	Interval length	58.00 m	Test depth (UPLS)	747.50 m bgl	System	HDDP 114
Borehole Diameter	161.9 mm	Stickup b. Rig floor	-1.27 m	Water depth	0.80 m bgl	Test file	BOZ2_1_MUK1	Quadro Probe	QSSP 3

Note: All dephts shown are not correct for borehole deviation

		Qty -	L_{unit} m	L_{total} m	Depth m	OD mm	ID mm	Wgt kg	Str t
Rig floor	-2.82								
Wellhead, Wellhead equipment (not shown)									
Stickup	-4.09 m bgl								
Ground level (GL)					0.00				
Tubing 2"7/8 EU	Tally list 3	34	295.32			93.2	62.0	2912	
Moyno-Pump	Tubing extension	0				93.2	62.0		
	Stator	1	3.12	742.93		78.6 (93.2)	0.0	53	45
	Stop pin	0	0.35		294.01	78.6	62.0		
Tubing 2"7/8 EU	Tally list 2	37	444.49			93.2	62.0	4401	
	Pop joint 2"7/8 (without Siphon	1	1.20		738.85	93.2			
SIT 2"7/8 DAS	SIT	1	0.66		739.33	106.0	45.0	69	
	DAP	1	1.22						
Cable Base incl. Coupling + Crown Shaft		1	1.26			96.0	49.5		16.0
Probe Carrier with Quadruple Probe	QSSP P3		0.53		743.71			132	
	QSSP P4		0.13		743.83				
	QSSP P2	1	0.14		743.98	96	34.6		
	QSSP P1		0.20		744.17				
			0.63	8.66					
Crown Shaft		1	0.32			95.0	35.0		
Safety Joint incl. X-Overs			0.61			66.0	32.0		90.0
Packer Stick Up / Above Side Entry Sub			0.37						
Up. Packer Seal – Upper Packer	UPUS	1	0.20		746.30	114.0	32.0	82	
			1.20						
	UPLS		0.20		747.50				
Straddle Length – Packer Stick Down			0.06						
Below Side Entry Sub (BSES)			0.32			66.0	32.0		16.0
X-Over		0	0.00			80.0	60.0	3	
Tubing 2"7/8 EU (Tally list 1)		0	0.00	3.24		93.2	62.0	0	
X-Over		0	0.00						
		0	0.00			93.5	51.2	3	
Filter	Screen)	1	0.26 1.50			72.0	50.0	19	
			0.57						
X-Over		0	0.20		750.36			6	
Bottom Cap		1	0.13		750.74	95.0			

End of Borehole (m bgl): 805.50

Total Weight (kg): 7680

Comments:

Ground level: 0.00

Casing depth: 615.00

Moyno-Pump: 294.01

UPLS: 747.50

End of System: 750.74

Bottom of Borehole: 805.5

Fig. 3-20: Hydraulic test BOZ2-1-MUK1: Downhole equipment installation record with system layout as used in the field test

3.5.2.3 Analysis

Borehole pressure history

The borehole history used for the analysis of the BOZ2-1-MUK1 test is shown in Fig. B-13 and summarised in Tab. 3-33. The mean fluid density for the interval was calculated using the P2 pressure sensor measurement (prior to packer inflation) and resulted in a value of 1'057 kg m^{-3}. This value corresponds to the documented drill mud density recorded during drilling (1'050 kg m^{-3}; see Dossier I). For the numerical simulations, a pressure history was ascribed that assumed a constant drill mud level at the level of the drain pipe (-1.95 m MD) and a drilling fluid density of 1'057 kg m^{-3} was used for the period of drilling through the interval midpoint until drilling termination. These values were used due to the fact that for this period, the drillers generally kept the borehole full to the level of the drain pipe. Once the HDDP system was at test depth, data acquisition began for the BOZ2-1-MUK1 hydraulic test; the QSSP P2 sensor measured pressure directly.

Tab. 3-33: Hydraulic test BOZ2-1-MUK1: Borehole pressure history

[1] Interval pressure at the level of the P2 sensor (743.98 m MD) with a pressure offset of -1.34 kPa as calculated from the history information, e.g. fluid level and density.

[2] Drilling through the interval midpoint (776.50 m MD).

[3] Pressure measured when the borehole was filled with mud (e.g. when P2 was at test depth but before packer inflation).

[4] Test start refers to the first time recorded on the data acquisition system (DAS) file.

Description	**Start date and time**	**Duration** [h]	**Pressure** [1] [kPa]	
		Total: 67.38	**Start**	**End**
Drilling [2]	30.11.2020 19:29	34.27	7'736	7'736 [3]
Wiper trip	02.12.2020 05:45	22.48	7'736	7'736 [3]
Level prior to RIH (measurements)	03.12.2020 04:14	10.63	7'740	7'740
Start testing BOZ2-1-MUK1	03.12.2020 14:52 [4]	-	7'734	-

Flow model evaluation

The evaluation of the flow model approach was based on the pressure recovery phases of the slug phases (SWS1, SWS2, SWS3) and the pumping phase (MRWS). Figs. B-14, B-15 and B-16 show the log-log diagnostic plots for the slug recovery phases, and Fig. B-17 provides the log-log diagnostic plot of the pressure recovery after completion of the pumping phase. The diagnostic plots provide a consistent picture for flow model evaluation. In Fig. B-14 the SWS1 derivative shows a unit slope (wellbore storage) during early times and decreases with half unit slope during middle times with slight fluctuations before it starts to increase until the end of the test phase. This behaviour is very similar to the SWS2 and SWS3 derivatives in Figs. B-15 and B-16. In the SWS3 derivative, a bulge is evident between early and middle time (not well pronounced) that represents a possible skin. This is followed by a decrease in the derivative (with approximately half unit slope) during middle time, indicating possible non-radial / fractional dimension flow (i.e., due to the presence of a vertical flow component in the reservoir flow field). During late time, the derivative flattens towards a more-or-less horizontal progression and is interpreted as infinite acting radial flow behaviour (IARF).

The MRWS phase derivative is illustrated in Fig. B-17. It can be seen that the IARF phase is clearly pronounced without any major disturbances. The observed downward trend of the derivative between -¼- and -½-unit slope during the end of early-middle time indicates a continuously increasing hydraulic conductivity with increasing radial distance from the well, i.e. the presence of a vertical flow component in the flow field of the reservoir. This possible fractional dimension flow / spherical flow behaviour is supported by the cores which showed higher conductivity conduits (*cf.* Dossier II). Based on the flow regime derived by the diagnostic results, a radial composite hydraulic model was chosen for the analysis with the inner zone allowed to deviate from a 2D flow model. In order to simulate the observed cumulative fluid losses during the history period, a positive discrete skin was applied to the borehole history. The presence of the skin reduces the simulated losses during the borehole history and thus enables the simulation of losses at a realistic rate. The existence of the low permeability (skin) zone can be explained by the mud properties of Pure-Bore® and the pressure gradient that was directed from the borehole towards the formation. With continuous pumping, the well was developed during the MRW phase resulting in a significant decrease of the skin factor.

Analysis of the pumping phase and subsequent pressure recovery (MRW3-MRWS)

Due to the observed removal of the borehole skin during the first few hours of pumping, the final 55.56 hours (MRW3) were used for the parameter optimisation by matching the simulated to the measured pressure data. Furthermore, during the parameter optimisation for the MRW3-MRWS sequence, the pressure recovery phase (MRWS) was weighted higher than the pumping phase MRW3. Temperature changes inside the test interval were not considered in the analysis, as the temperature variations are not expected to influence the results due to the high transmissivity of the formation.

The results, derived from the parameter optimisation based on the measured pressure of the MRW3-MRWS sequence, are shown in Tab. 3-34.

The cartesian plot of the simulated and measured pressure data and the associated flow data for the MRW3-MRWS sequence are shown in Fig. B-18. The illustrated simulation uses the results of the parameter optimisation (Tab. 3-34). Fig. B-19 shows a detailed view of the match for the MRWS phase in a log-log plot.

Tab. 3-34: Hydraulic test BOZ2-1-MUK1: Formation parameter estimates based on the parameter optimisation for MRW3-MRWS sequence using a radial composite flow model allowing the flow dimension of the inner zone to vary

A fractional flow dimension of 2.45 was derived for the inner zone flow behaviour.

[1] Fixed to the theoretical value calculated from the best estimates of porosity and rock compressibility for the Schinznach Formation.

[2] Static formation pressure at the depth of the P2 sensor (743.98 m MD).

MRW3-MRWS results	**K** [m s^{-1}]	**Ss** [1] [m^{-1}]	**Pf** [2] [kPa]
Best estimate	1.52×10^{-6}	8.45×10^{-7}	4'930

The positive skin behaviour was not optimised in order to reduce the number of optimisation parameters. The skin value for the borehole pressure history and the INF and COM phases was set to 8. For the PSR phase, both the SW-SWS and SW2-SWS2 phases and the start of the

pumping phase, the skin value was set to 3. After 2.5 hours of pumping (MRW1), the skin was reduced to 0.6, and by the end of MRW3, it was further reduced to 0.1. No skin was assumed for the pressure recovery phase (MRWS). For the inner zone with a radial extension of 39.51 m from the centre of the borehole, a fractional flow dimension (Barker 1988) of 2.45 was matched. This result is in agreement with the flow model derived from flow model diagnostics. The detailed diagnostic view (Fig. B-19) indicates that the composite flow model in combination with the fractional flow dimension applied to the inner zone allowed the reproduction of the pressure measurement, after the initial bulge.

Joint parameter regions for the MRW3-MRS sequence

Based on the results of the parameter optimisation using a radial composite flow model for the MRW3-MRWS sequence with a fractional flow dimension in the inner zone, an estimate of the joint parameter regions was possible. Tab. 3-35 provides the 95% uncertainty ranges for the results. The calculated ranges are unrealistically small due to the existence of well-defined and well constrained minima of the objective function. Therefore, further investigations were performed to better estimate the uncertainty ranges for the formation parameters.

Tab. 3-35: Hydraulic test BOZ2-1-MUK1: 95% uncertainty range associated with the result of the parameter optimisation using a radial composite flow model for the sequence MRW3-MRWS

[1] Static formation pressure at the midpoint of the test interval (743.98 m MD).

MRW3-MRS Results (joint parameter region)	**K** [m s^{-1}]	**P_f** [1] [kPa]
95% uncertainty range	1.51 – 1.53 × 10^{-6}	4'930 – 4'930

Estimates and uncertainty ranges for the formation parameters

An analysis to assess the uncertainty in the formation parameters by varying the pressure history was considered unnecessary due to the fact that prior analysis results in the TBO borehole campaign showed no influence of the borehole history on hydraulic testing in intervals of high hydraulic transmissivity (e.g. in both the BUL1-1 and MAR1-1 boreholes). However, in the current analysis, an additional uncertainty could exist due to the use of a pre-defined positive skin (value of 8) during the borehole pressure history (incl. the INF and COM phases). To assess this potential uncertainty, parameter optimisations on the simulation of the MRW3-MRWS sequence were performed using stepwise decreasing skin values for the borehole history (16, 5, 3 and 0). Tab. 3-36 provides the resulting formation parameter ranges. The uncertainty in the formation specific storage based on the skin variations could not be estimated due to the fact that this value was fixed to the theoretical value of 8.45 × 10^{-7} m^{-1}.

Tab. 3-36: Hydraulic test BOZ2-1-MUK1: Formation parameter ranges associated with the result of the parameter optimisation using a radial composite flow model for the sequence MRW3-MRWS and skin values of between 0 and 16 for the borehole history period (incl. the INF and COM phases)

[1] Static formation pressure at the midpoint of the test interval (743.98 m MD).

MRW3-MRWS Results (skin variation during the borehole pressure history)	**K** [m s^{-1}]	**P_f** [1] [kPa]
Parameter range	1.31 – 1.52 × 10^{-6}	4’924 – 4’931

The uncertainty associated with the parameter optimisation procedure was estimated using a perturbation analysis. In this analysis, the bandwidth of the matched parameters was determined based on several individual optimisations. These individual optimisations can identify whether a result corresponds to a global minimum in the parameter space.

A perturbation analysis with 500 runs was carried out based on the parameter optimisation used for the simulation of the MRW3-MRWS sequence. The results of the single parameter optimisations are plotted against increasing objective function/SSE values in Fig. B-20. 477 perturbation runs (run#0 to run#476) were selected as reliable representations. These fits of the MRW3-MRWS sequence were used to estimate the uncertainty ranges for the formation parameters. Tab. 3-37 shows the best estimates for each formation parameter (associated with the lowest SSE value) and the resulting formation parameter ranges.

Tab. 3-37: Hydraulic test BOZ2-1-MUK1: Uncertainty ranges and best estimates for the formation parameters yielded by the perturbation analysis

[1] Static formation pressure at the midpoint of the test interval (743.98 m MD).

Perturbation analysis results	**K** [m s^{-1}]	**P_f** [1] [kPa]
Best estimate	1.51 × 10^{-6}	4'930
Uncertainty range	0.47 – 2.78 × 10^{-6}	4'919 – 4'948

Scatter plots of the optimised formation parameters are shown in Fig. B-21. The two upper plots show a clear negative correlation between the formation hydraulic conductivity and both the discontinuity radius and the static formation pressure. Conversely, the plot of the radius of discontinuity against the static formation pressure presents a positive correlation. Fig. B-22 shows the scatter plots of the fractional flow dimension of the inner zone versus the inner hydraulic conductivity (top) and the hydraulic conductivity of the formation outer zone (below). A correlation between the flow dimension and the hydraulic conductivity of the inner zone can be clearly recognised. In contrast, no correlation of the outer zone (represented by the hydraulic conductivity) to the flow dimension of the inner zone is evident.

A sampling analysis was performed to assess the possible uncertainty related to the formation specific storage that was fixed to the theoretical value of 8.45 × 10^{-7} m^{-1}. The formation specific storage was calculated in the range of 1.8 × 10^{-7} m^{-1} to 2.4 × 10^{-6} m^{-1}. Tab. 3-38 shows the best estimates for each formation parameter (associated with the lowest SSE value) and resulting formation parameter ranges from the sampling analysis for the formation specific storage.

Tab. 3-38: Hydraulic test BOZ2-1-MUK1: Best estimates and uncertainty ranges for the formation parameters yielded by the sampling analysis of the formation specific storage

[1] Static formation pressure at the midpoint of the test interval (743.98 m MD).

Sampling analysis results	**K** [m s^{-1}]	**P_f** [1] [kPa]
Best estimate	1.39×10^{-6}	4'925
Uncertainty range	$0.92 – 1.4 \times 10^{-6}$	4'925 – 4'931

Fig. B-23 shows the parameter sets resulting from the single parameter optimisation of the sampling analysis based on the MRW3-MRS sequence. The SSE values increase with increasing values for the sampling parameter formation specific storage. In general, the SSE range is quite small in comparison with the perturbation analysis indicating that the influence of the formation specific storage on the fit quality is limited. This could indicate that quasi steady-state conditions were reached during the hydraulic test.

Parameter optimisation for the MRW3-MRWS-SW3-SWS3 sequence

To validate the results of the chosen sequence MRW3-MRWS, the MRW3-MRWS-SW3-SWS3 sequence was investigated. The same conceptual model as for the MRW3-MRWS sequence was used to numerically simulate the test data for the MRW3-MRWS-SW3-SWS3 sequence, i.e., a radial-composite flow model with wellbore storage used as the inner boundary condition in an infinitely extended reservoir and a fractional flow used in the inner zone (near the borehole).

The results derived from parameter optimisation based on the measured pressure of the MRW3-MRWS-SW3-SWS3 sequence are shown in Tab. 3-39. The fit for the pressure measurement sequence is displayed in Fig. B-24.

Tab. 3-39: Hydraulic test BOZ2-1-MUK1: Formation parameter estimates based on the parameter optimisation for the MRW3-MRWS-SW3-SWS3 sequence

[1] Fixed to the theoretical value calculated from the best estimates of porosity and rock compressibility for the Schinznach Formation.

[2] Static formation pressure at the depth of the P2 sensor (743.98 m MD).

MRW3-MRWS-SW3-SWS3 results	**K** [m s^{-1}]	**S_s** [1] [m^{-1}]	**P_f** [2] [kPa]
Best estimate	1.30×10^{-6}	8.45×10^{-7}	4'931

Summary of the analysis

The best estimates for the hydraulic properties are derived from the perturbation analysis, and the results are shown in Tab. 3-40. The uncertainty ranges for the perturbation analysis represent the overall ranges from the entire analysis with respect to the formation parameters. The uncertainty in all formation parameters is small, except for the formation specific storage, which could not be constrained by the analysis due to the small sensitivity in this parameter. The observed fractional flow dimension of the inner zone was confirmed, ranging between 2.35 and 2.74 throughout the analysis.

Tab. 3-40: Hydraulic test BOZ2-1-MUK1: Best estimates and associated uncertainty ranges for the formation parameters

[1] Theoretically defined based on the porosity and rock compressibility for the Schinznach Formation

[2] Static formation pressure at the midpoint of the test interval (743.98 m MD) considering the sensor offset of -1.34 kPa.

BOZ2-1-OPA4	**K** [m s^{-1}]	**S_S** [1] [m^{-1}]	**P_S** [2] [kPa]
Best estimate	1.51×10^{-6}	8.45×10^{-7}	5'252
Uncertainty range	$0.47 – 2.8 \times 10^{-6}$	$0.18 – 2.4 \times 10^{-6}$	5'241 – 5'270

3.6 Summary and discussion of hydraulic tests

3.6.1 Summary tables and plots

The results of the transmissivity and hydraulic conductivity estimates for all tested intervals are summarised in Tab. 3-41, and the estimated freshwater hydraulic heads and static formation pressures are documented in Tab. 3-42. Both tables present the best estimates along with confidence ranges as determined by the field test contractor and documented in the corresponding Detailed Reports.

The permeabilities for all tested intervals are summarised in Tab. 3-43 and were calculated based on the hydraulic conductivities provided in Tab. 3-41. An assumed density of 1'000 kg m^{-3} and a dynamic viscosity of 1×10^{-3} Pa s were used for the calculation of the hydraulic permeabilities.

The hydraulic parameters T, K, P_f and h_S (in terms of m bgl and m asl) are illustrated with respect to both the borehole depth (in m MD) and the geological profile in Figs. 3-21 to 3-25. The best estimates for these parameters are indicated by vertical lines in the corresponding interval position. The associated confidence ranges are shown as dashed rectangles, delimited vertically by the corresponding interval extent and laterally by the minimum and maximum values.

Tab. 3-41: Summary of the hydraulic packer testing in borehole BOZ2-1: Transmissivity and hydraulic conductivity

Test interval details and hydraulic model							**Transmissivity and hydraulic conductivity**					
Test name	**Interval depth**				**Interval length**	**Hydraulic model**	**Best estimate** [1]		**Lowest estimate** [1]		**Highest estimate** [1]	
	From [m MD]	**To** [m MD]	**From** [m asl]	**To** [m asl]	[m]		**T** [m^2 s^{-1}]	**K** [m s^{-1}]	T_{min} [m^2 s^{-1}]	K_{min} [m s^{-1}]	T_{max} [m^2 s^{-1}]	K_{max} [m s^{-1}]
BOZ2-1-HRO1	334.30	365.93	290.03	258.40	31.63	3-zone radial composite	4×10^{-07}	1×10^{-08}	7×10^{-08}	2×10^{-09}	9×10^{-06}	3×10^{-07}
BOZ2-1-PWF2	402.00	425.02	222.33	199.31	23.02	2-zone radial composite	4×10^{-13}	2×10^{-14}	1×10^{-13}	5×10^{-15}	6×10^{-13}	3×10^{-14}
BOZ2-1-PWF1	429.30	452.32	195.03	172.01	23.02	2-zone radial composite	7×10^{-13}	3×10^{-14}	2×10^{-13}	1×10^{-14}	3×10^{-12}	1×10^{-13}
BOZ2-1-OPA2	455.00	478.02	169.33	146.31	23.02	2-zone radial composite	8×10^{-13}	3×10^{-14}	2×10^{-13}	8×10^{-15}	8×10^{-13}	4×10^{-14}
BOZ2-1-OPA4	507.20	513.55	117.13	110.78	6.35	2-zone radial composite	8×10^{-14}	1×10^{-14}	3×10^{-14}	5×10^{-15}	2×10^{-13}	3×10^{-14}
BOZ2-1-OPA1	527.50	550.52	96.83	73.81	23.02	2-zone radial composite	1×10^{-12}	6×10^{-14}	3×10^{-13}	2×10^{-14}	1×10^{-12}	6×10^{-14}
BOZ2-1-OPA3	559.18	566.16	65.15	58.17	6.98	2-zone radial composite	1×10^{-13}	1×10^{-14}	4×10^{-14}	5×10^{-15}	6×10^{-13}	8×10^{-14}
BOZ2-1-LIA1	598.00	615.00	26.33	9.33	17.00	2-zone radial composite	8×10^{-12}	5×10^{-13}	2×10^{-12}	1×10^{-13}	1×10^{-11}	7×10^{-13}
BOZ2-1-KEU1	631.40	658.00	-7.07	-33.67	26.60	2-zone radial composite	1×10^{-04}	6×10^{-06}	5×10^{-05}	2×10^{-06}	9×10^{-04}	3×10^{-05}
BOZ2-1-MUK1	747.50	805.50	-123.17	-181.17	58.00	2-zone radial composite	9×10^{-05}	2×10^{-06}	3×10^{-05}	5×10^{-07}	2×10^{-04}	3×10^{-06}

[1] Based on the results given by the field test contractor in the corresponding DR.

Tab. 3-42: Summary of the hydraulic packer testing in borehole BOZ2-1: Hydraulic head estimates

Test interval details and associated hydraulic model							**Hydraulic head** [m bgl]			**Hydraulic head** [m asl]			**Formation pressure**		
Test name	**Interval depth**				**Interval length**	**Hydraulic model**	**Best** [1] **h**	**Lowest** [1] **h_{min}**	**Highest** [1] **h_{max}**	**Best** [1] **h**	**Lowest** [1] **h_{min}**	**Highest** [1] **h_{max}**	**Best** [1] **P_S**	**Lowest** [1] **$P_{S\,min}$**	**Highest** [1] **$P_{S\,max}$**
	From [m MD]	**To** [m MD]	**From** [m asl]	**To** [m asl]	[m]		[m bgl]	[m bgl]	[m bgl]	[m asl]	[m asl]	[m asl]	[kPa]	[kPa]	[kPa]
BOZ2-1-HRO1	334.30	365.93	290.03	258.40	31.63	3-zone radial composite	162	163	161	463	461	463	1'849	1'833	1'856
BOZ2-1-PWF2	402.00	425.02	222.33	199.31	23.02	2-zone radial composite	-224	-156	-348	849	781	972	6'258	5'591	7'471
BOZ2-1-PWF1	429.30	452.32	195.03	172.01	23.02	2-zone radial composite	-48	-6	-89	672	631	713	4'792	4'386	5'193
BOZ2-1-OPA2	455.00	478.02	169.33	146.31	23.02	2-zone radial composite	-166	-164	-356	790	788	980	6'203	6'187	8'070
BOZ2-1-OPA4	507.20	513.55	117.13	110.78	6.35	2-zone radial composite	-519	-279	-596	1'144	903	1'220	10'101	7'741	10'852
BOZ2-1-OPA1	527.50	550.52	96.83	73.81	23.02	2-zone radial composite	-243	-228	-416	868	853	1'040	7'676	7'529	9'364
BOZ2-1-OPA3	559.18	566.16	65.15	58.17	6.98	2-zone radial composite	-586	-186	-668	1'210	810	1'292	11'269	7'344	12'075
BOZ2-1-LIA1	598.00	615.00	26.33	9.33	17.00	2-zone radial composite	-14	9	-24	638	615	649	6'087	5'858	6'188
BOZ2-1-KEU1	631.40	658.00	-7.07	-33.67	26.60	2-zone radial composite	175	175	174	450	449	450	4'611	4'603	4'618
BOZ2-1-MUK1	747.50	805.50	-123.17	-181.17	58.00	2-zone radial composite	241	242	239	383	382	385	5'252	5'241	5'270

[1] Based on the results given by the field test contractor in the corresponding DR.

Tab. 3-43: Summary of the hydraulic packer testing in borehole BOZ2-1: Permeability

Test interval details						**Permeability estimates** [1]		
Test name	**Interval depth**				**Interval length**	**Best** [2] **k**	**Lowest** [2] **k_{min}**	**Highest** [2] **k_{max}**
	From [m MD]	**To** [m MD]	**From** [m asl]	**To** [m asl]	[m]	[m^2]	[m^2]	[m^2]
BOZ2-1-HRO1	334.30	365.93	290.03	258.40	31.63	1×10^{-15}	2×10^{-16}	3×10^{-14}
BOZ2-1-PWF2	402.00	425.02	222.33	199.31	23.02	2×10^{-21}	5×10^{-22}	3×10^{-21}
BOZ2-1-PWF1	429.30	452.32	195.03	172.01	23.02	3×10^{-21}	1×10^{-21}	1×10^{-20}
BOZ2-1-OPA2	455.00	478.02	169.33	146.31	23.02	4×10^{-21}	8×10^{-22}	4×10^{-21}
BOZ2-1-OPA4	507.20	513.55	117.13	110.78	6.35	1×10^{-21}	6×10^{-22}	3×10^{-21}
BOZ2-1-OPA1	527.50	550.52	96.83	73.81	23.02	6×10^{-21}	2×10^{-21}	7×10^{-21}
BOZ2-1-OPA3	559.18	566.16	65.15	58.17	6.98	2×10^{-21}	6×10^{-22}	8×10^{-21}
BOZ2-1-LIA1	598.00	615.00	26.33	9.33	17.00	5×10^{-20}	1×10^{-20}	7×10^{-20}
BOZ2-1-KEU1	631.40	658.00	-7.07	-33.67	26.60	6×10^{-13}	2×10^{-13}	3×10^{-12}
BOZ2-1-MUK1	747.50	805.50	-123.17	-181.17	58.00	2×10^{-13}	5×10^{-14}	3×10^{-13}

[1] The calculation is based on the hydraulic conductivity provided by the field test contractor in the corresponding DR and standard conditions (density: 1'000 kg m^{-3}, dynamic viscosity: 1×10^{-3} Pa s).

[2] Based on the results given by the field test contractor in the corresponding DR.

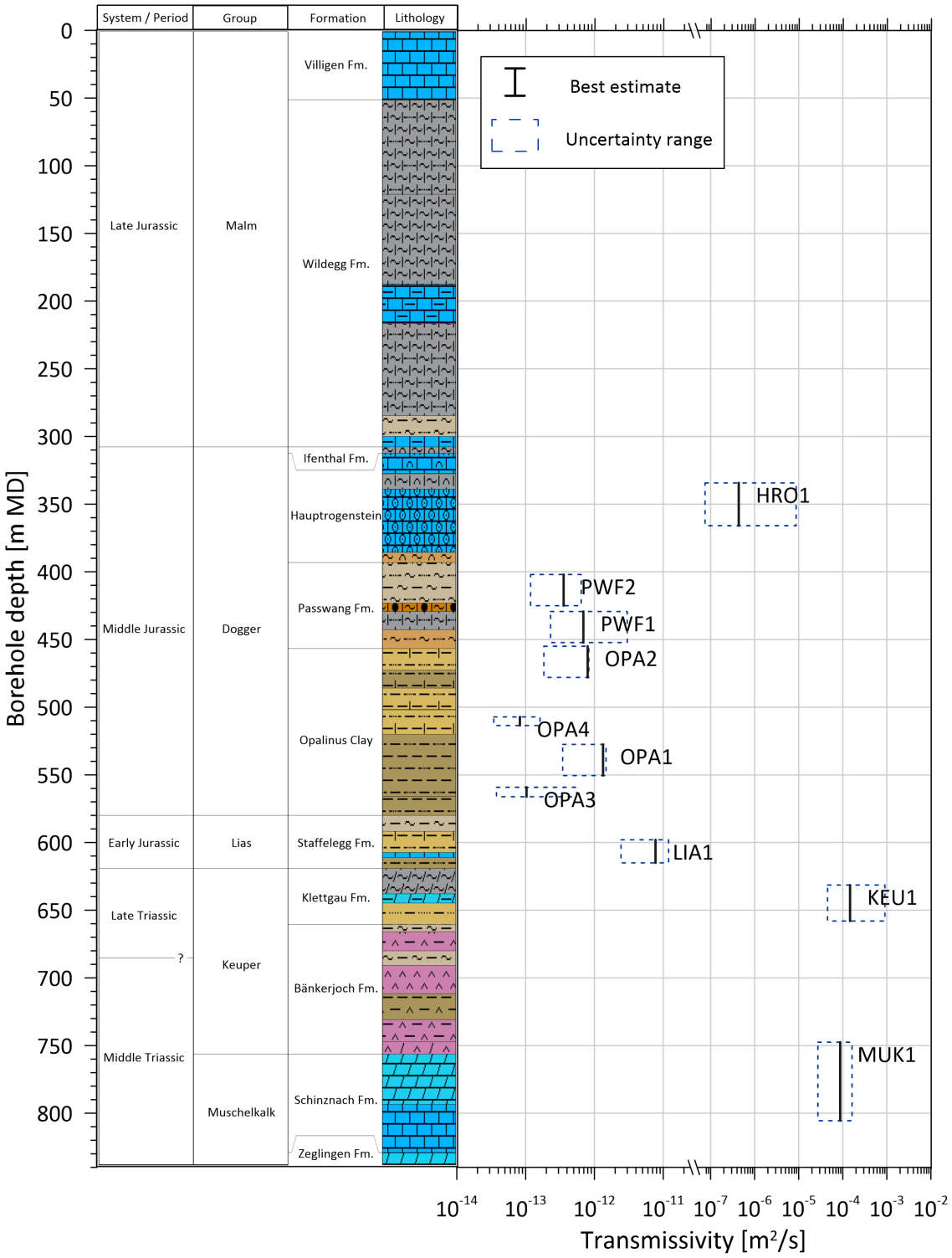

Fig. 3-21: Summary of the hydraulic testing in borehole BOZ2-1: Formation transmissivity profile

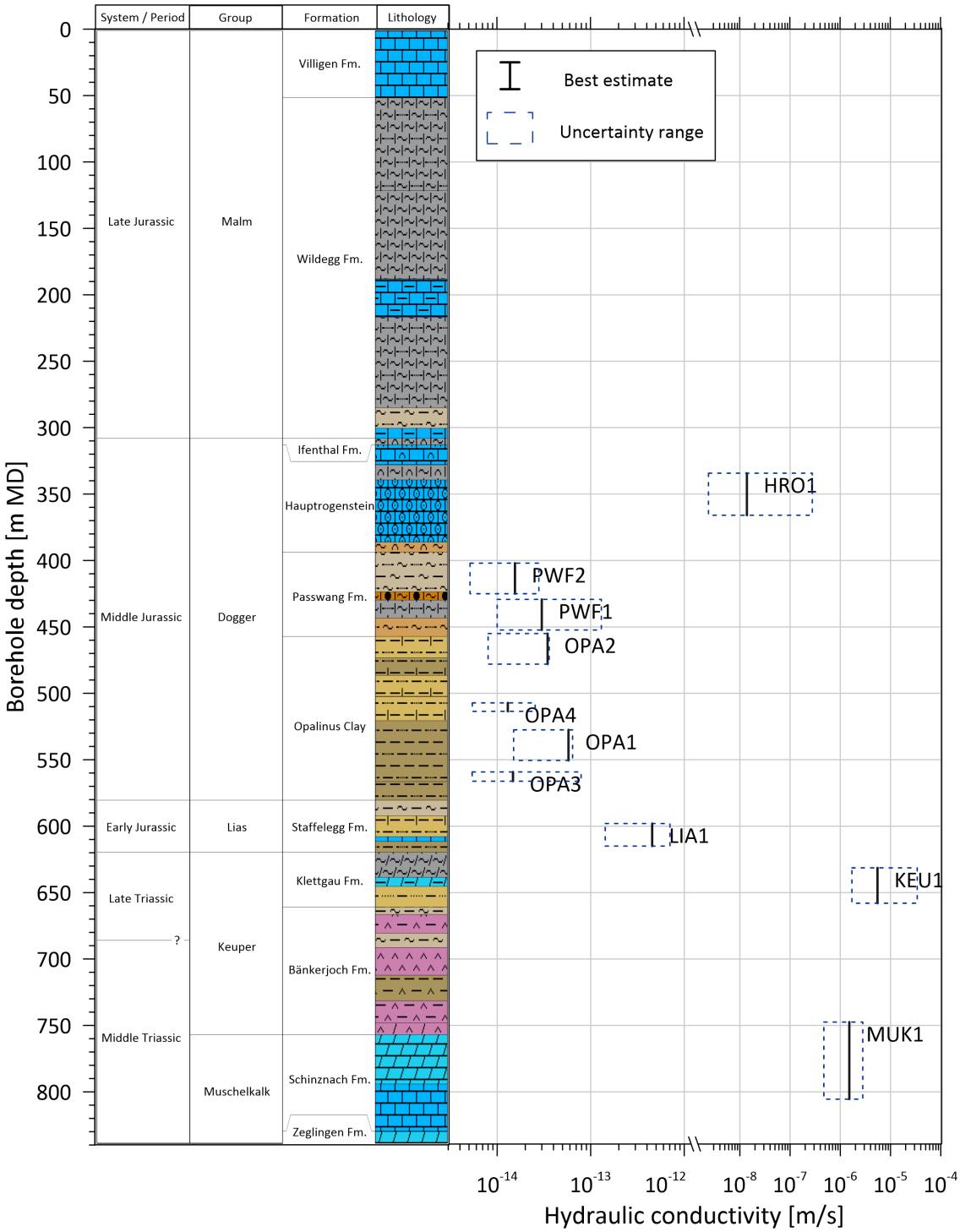

Fig. 3-22: Summary of the hydraulic testing in borehole BOZ2-1: Formation hydraulic conductivity profile

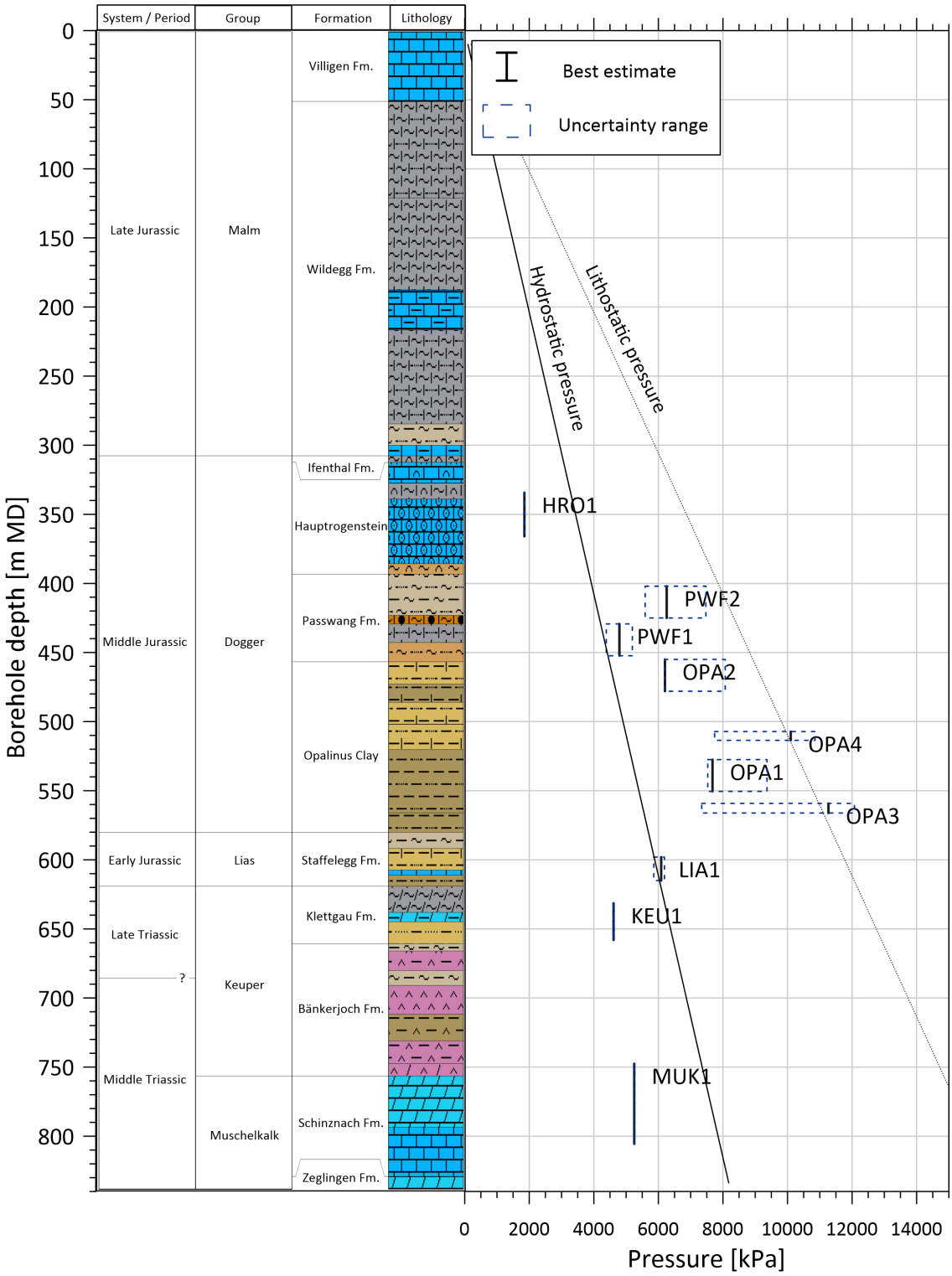

Fig. 3-23: Summary of the hydraulic testing in borehole BOZ2-1: Static formation pressure profile

The lithostatic pressure is based on the assumption of a mean density of 2'000 kg m^{-3}.

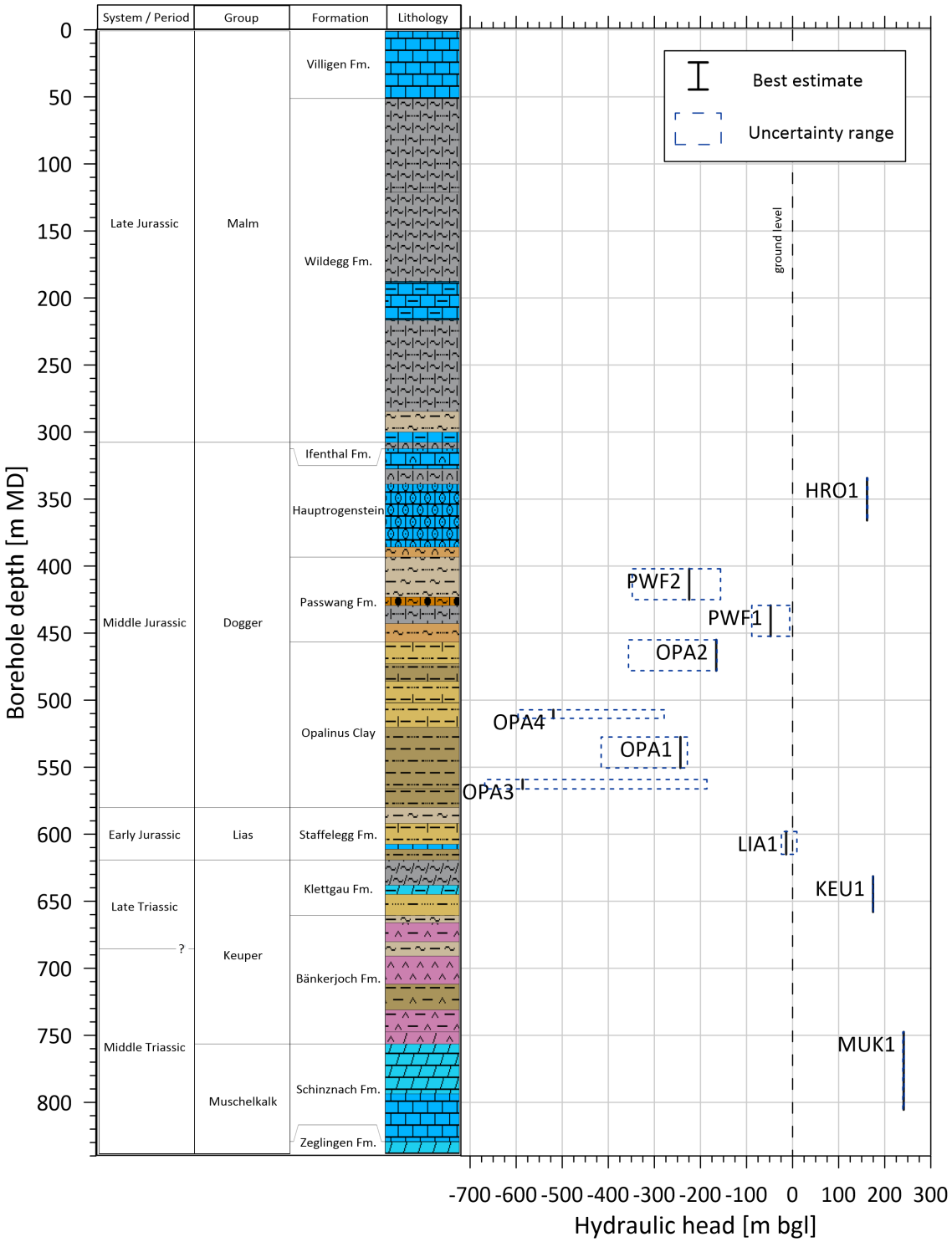

Fig. 3-24: Summary of the hydraulic testing in borehole BOZ2-1: Formation hydraulic head profile (m bgl)

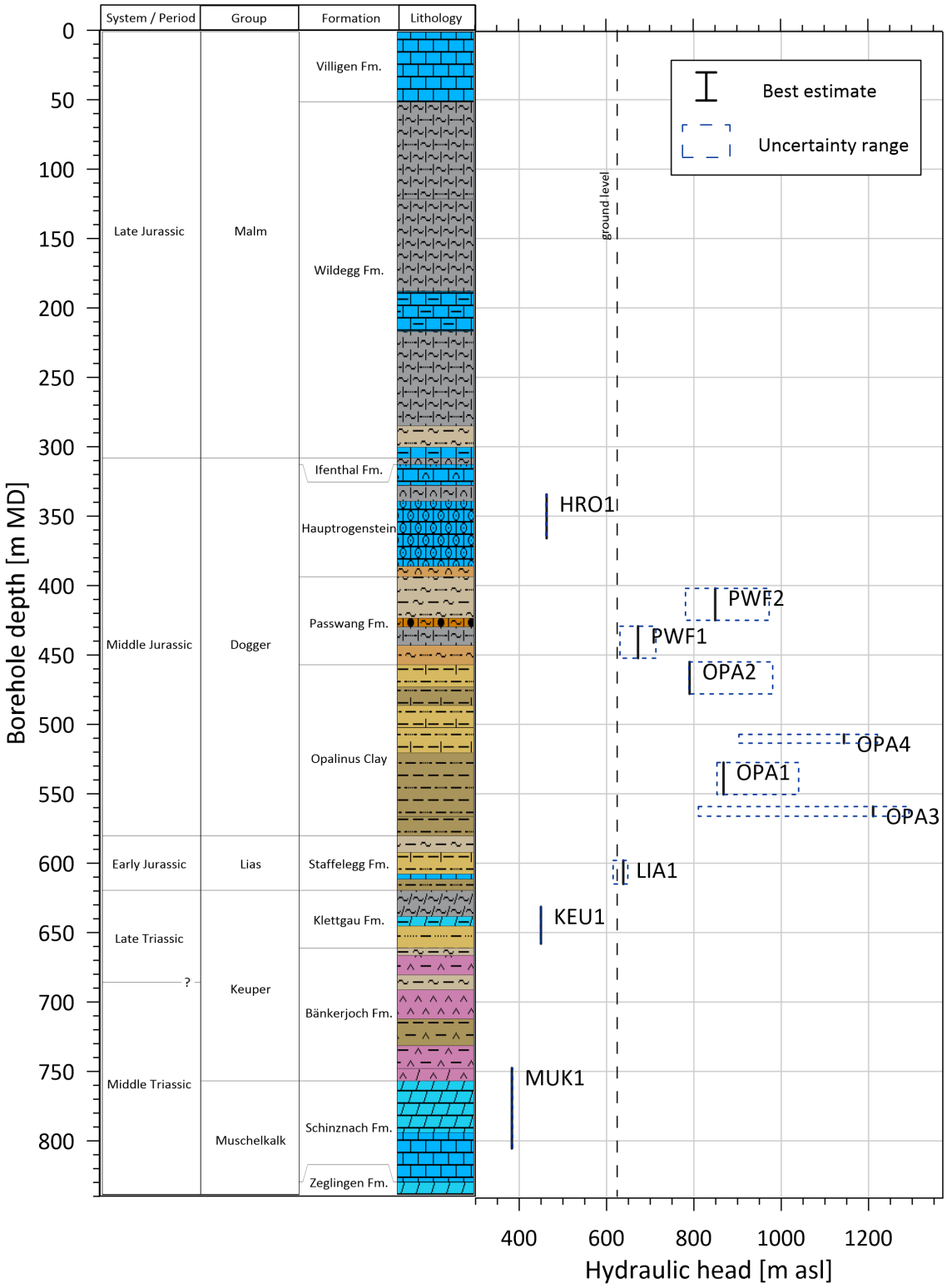

Fig. 3-25: Summary of the hydraulic testing in borehole BOZ2-1: Formation hydraulic head profile (m asl)

3.6.2 Discussion of data and test results

The first hydraulic tests conducted in the BOZ2-1 borehole focused on the Hauptrogenstein as part of the Dogger Group. The BOZ2-1-HRO1 test interval was defined due to steep fractures observed in the cores and mud losses that occurred during drilling (due to which no fluid logging was carried out). The presence of a fracture network was also identified by the flow model diagnostics which indicated a complex flow regime with spherical flow behind a skin zone, up to a distance of 18 m from the borehole. At larger distances (> 18 m), it was possible to simulate the flow in the formation using a cylindrical symmetrical flow model (infinite acting radial flow regime). The best estimate of the hydraulic conductivity (1.4×10^{-8} m s^{-1}) that resulted from hydraulic test BOZ2-1-HRO1 captured the late time hydraulic test response during the infinite radial acting flow. However, the hydraulic conductivity estimate had a large uncertainty associated with it, due to the necessary use of a complex flow model and the rather short period of infinite acting radial flow. The hydraulic head was estimated within a narrow uncertainty range of 2 m.

The Passwang Formation of the Dogger Group was studied by two hydraulic tests carried out within a hydraulic testing series. The BOZ2-1-PWF1 test was performed after the tests BOZ2-1-OPA1 and BOZ2-1-OPA2 and the test BOZ2-1-PWF2 followed test BOZ2-1-PWF1. The main test sequences for both tests consisted of a slug withdrawal and a slug recovery phase followed by a pulse withdrawal test phase. As there were no indications that a more complex model was required, the measurement results from both test intervals in the Passwang Formation were analysed using 2-zone radial composite flow models, representing a skin zone in the vicinity of the borehole (inner zone) followed by the formation (outer zone). The results of both tests were consistent in that estimates of the hydraulic conductivity were low, and additionally, differed only by a factor of 2. The uncertainties were mainly due to the limiting conditions of testing (e.g. duration of history and testing). The estimated hydraulic heads for both tests were unrealistically high and showed large uncertainty.

In borehole BOZ2-1, the Opalinus Clay was investigated using a total of four hydraulic tests. Tests BOZ2-1-OPA1 and -OPA2 were conducted sequentially within test intervals of about 23 m. The hydraulic tests BOZ2-1-OPA3 and -OPA4 were conducted separately as they were performed in shorter test intervals of 6.98 and 6.35 m respectively, in order to test faults zones in situ. Test BOZ2-1-OPA3 was extended by a second hydraulic test sequence using PEARSON water instead of drilling mud. Finally, test BOZ2-1-OPA4 was extended by execution of a GTPT, followed by a second hydraulic test sequence using PEARSON water. As mentioned in Section 3.1, the analyses of both the GTPT and the test sequences using PEARSON water do not form part of this report.

Based on the experience from previous boreholes in the TBO test campaign, the hydraulic tests were started with an initial pressure recovery phase followed directly by a slug withdrawal phase. Subsequently, the slug pressure recovery phase was started by closing the shut-in valve. On completion of the tests, a pulse withdrawal phase was performed. This procedure was used for all hydraulic tests, except BOZ2-1-OPA4 where a pulse injection phase was performed before completion of the test (discussed in more detail in Section 3.5.1). For the four tests in the Opalinus Clay, the borehole pressure history ranged from 142 to 779 hours, whereas the actual test durations ranged between 60.0 and 76.6 hours. The best estimates for the hydraulic conductivity varied by a factor of 4.5, between 1.3×10^{-14} m s^{-1} for BOZ2-1-OPA4 and 5.8×10^{-14} m s^{-1} for test BOZ2-1-OPA1. Hydraulic tests performed within shorter intervals encompassing fault zones in the Opalinus Clay yielded best estimates for hydraulic conductivity which were lower than for longer intervals (but were still within the parameter ranges of these tests). The uncertainty in the

estimates of the hydraulic head were generally high, particularly for tests BOZ2-1-OPA3 and -OPA4 which had the longest borehole histories. Like the results for the hydraulic head in the Passwang Formation, the estimates of the hydraulic head from the tests in the Opalinus Clay were not considered as realistic due to physical processes that cannot be captured by the hydraulic modelling software used, e.g. poroelastic effects.

The Staffelegg Formation of the Lias Group in the BOZ2-1 borehole was studied by a hydraulic packer test in single packer configuration, namely BOZ2-1-LIA1. The analysis of this interval was carried out using a 2-zone radial composite flow model that considered the observed near borehole conditions (skin) as a separate zone. The best estimate derived for the formation hydraulic conductivity was 4.5×10^{-13} m s^{-1}, about one order of magnitude higher than the mean value calculated for the Opalinus Clay. The hydraulic pressure ranged around the hydrostatic pressure with a best estimate for the hydraulic head of 638 m asl (-14 m bgl).

The Klettgau Formation of the Keuper Group was tested via the hydraulic test BOZ2-1-KEU1 using a HDDP system in single packer configuration, and no mud losses (Pure-Bore®) while coring were observed. For the analysis of this test, a 2-zone radial composite flow model was used where the observed positive skin, also obvious in the flow model diagnostics, was modelled as an inner zone. Test BOZ2-1-KEU1 consisted of multiple slug withdrawal and slug recovery tests followed by a rate withdrawal test with subsequent recovery. The numerical analysis of the pumping and recovery phases showed a decreasing trend for the skin factor with continuous pumping, stabilising only during the late production phase. Therefore, the test analyses focussed on the last part of the pumping phase and the subsequent pressure recovery. The late time flow diagnostics also showed signs of the existence of one (or more) far-field no-flow boundary(ies) which could not be finally verified due to signal noise. However, a significant influence of an outer boundary on the estimated formation parameters is not expected. The best estimate for static formation pressure was well defined. The resulting uncertainty range for the hydraulic conductivity was larger, reflecting both the continued development of the well and associated uncertainty in production rates, as well as the uncertainty in the flow model. The hydraulic conductivity was best estimated to be 5.5×10^{-6} m s^{-1} and the best estimate for the hydraulic head was 450 m asl (175 m bgl).

One hydraulic test sequence was performed in the Schinznach Formation of the Muschelkalk Group. The test was performed using a HDDP system in single packer configuration after mud losses (Pure-Bore®) occurred during coring and test preparation. The test BOZ2-1-MUK1 is discussed in more detail in Section 3.5.2. The analysis of test BOZ2-1-MUK1 had to account for a complex flow model identified by flow model diagnostics of the recovery phases (subsequent to the pumping phase and slug phases). The test diagnostics clearly indicated the presence of a non-radial flow section (fractional dimension flow or spherical flow) followed by an infinite acting radial flow regime during late testing times. This behaviour can be analysed by varying either the flow dimension or by implementing time-dependent changes in the hydraulic conductivity or, by changing the hydraulic conductivity as a function of distance from the borehole. For the test analyses, a 2-zone radial composite flow model with a fractional flow dimension in the inner zone and a discrete skin was used. The uncertainty in the flow model was mainly reflected by the uncertainty in the estimated hydraulic conductivity. Considering the complex flow model used, the uncertainty in the estimated hydraulic conductivity was relatively small. Similarly for this test, the hydraulic head estimate had a small associated range of uncertainty. The hydraulic conductivity was best estimated to be 1.5×10^{-6} m s^{-1} and the best estimate for the hydraulic head was 383 m asl (241 m bgl).

4 Summary

Borehole Bözberg-2-1 (BOZ2-1) is the second exploratory borehole drilled in the TBO borehole campaign within the Jura Ost siting region.

A total of 10 hydraulic packer tests were performed in borehole BOZ2-1 between September 2020 and December 2020. All hydraulic packer tests were performed in cored borehole sections using an HDDP packer system in either single or double packer configuration (*cf.* Tab. 3-22). The test activities were performed in the following geological formations (*cf.* Dossier III):

- Dogger Group with a focus on the Hauptrogenstein (BOZ2-1-HRO1) and the Passwang Formation including the Rothenfluh Member and the "Humphriesi-Schichten" (BOZ2-1-PWF2), the Waldenburg Member, the Brüggli Member and the "Cond. Equivalents of the Sissach, Hauenstein and Hirnichopf Members" (BOZ2-1-PWF1)
- Dogger Group with a focus on the Opalinus Clay (BOZ2-1-OPA1, BOZ2-1-OPA2, BOZ2-1-OPA3, BOZ2-1-OPA4)
- Lias Group with a focus on the Staffelegg Formation including the Frick, Beggingen and Schambelen Members (BOZ2-1-LIA1)
- Keuper Group with a focus on the Klettgau Formation including the Gansingen and Ergolz Members and the Bänkerjoch Formation (BOZ2-1-KEU1)
- Muschelkalk Group with a focus on the Schinznach Formation including the Asp, Stamberg, Liedertswil, Leutschenberg and Kienberg Members (BOZ2-1-MUK1)

All hydraulic tests were supported by on-site field analyses to optimise the test procedures. The pressures and flow rates measured during all tests are illustrated in Figs. 3-9 to 3-18. The main results and best estimates of the hydraulic formation parameters are presented in Tabs. 3-41 to 3-43 and Figs. 3-23 to 3-27. The execution of rate withdrawal tests was limited to the hydraulic tests performed in the Dogger Group: Hauptrogenstein (BOZ2-1-HRO1), the Keuper Group: Klettgau Formation (BOZ2-1-KEU1) and the Muschelkalk Group: Schinznach Formation (BOZ2-1-MUK1).

The best estimates and uncertainties for the hydraulic conductivities and transmissivities lie within a reasonable range and are within the expected spectrum of values for the investigated formations (e.g. Nagra 2008, Nagra 2014b). The estimated hydraulic heads for most formations are within a range similar to that of previous investigations (Luo et al. 2014), with the exception of the hydraulic tests performed in both the Passwang Formation and the Opalinus Clay. The tested intervals in the Dogger Group: Hauptrogenstein (BOZ2-1-HRO1), the Keuper Group: Klettgau Formation (BOZ2-1-KEU1) and the Muschelkalk Group: Schinznach Formation (BOZ2-1-MUK1) all show subartesian hydraulic heads. The interval in the Lias Group: Staffelegg Formation (BOZ2-1-LIA1, including the Beggingen Member) shows a hydraulic head at approximately ground level. Due to inevitable, short-term borehole test conditions, the estimated hydraulic heads for the Dogger Group: Passwang Formation (BOZ2-1-PWF1, BOZ2-1-PWF2) and the Opalinus Clay (BOZ2-1-OPA1, BOZ2-1-OPA2, BOZ2-1-OPA3, BOZ2-1-OPA4) appear to be affected by a large overestimation. Therefore, they are considered as 'apparent' hydraulic heads.

General investigations concerning the physical explanation for the overestimation of the hydraulic heads are continuing. The presented analyses consider temperature effects in the test intervals and pressure-induced effects resulting from the high-density drilling mud used after drilling through the interval midpoint. Nagra has installed long-term pressure monitoring systems in BOZ1-1 (close to BOZ2-1) and other selected boreholes to study these effects and other findings in more detail.

5 References

Agarwal, R.G. (1980): A new method to account for producing time effects when drawdown type curves are used to analyze pressure buildup and other test data. Proceedings of the 55th Annual Fall Technical Conference and Exhibition of the Society of Petroleum Engineers. Paper SPE 9289.

Barker, J.A. (1988): A generalized radial flow model for hydraulic tests in fractured rock. Water Resour. Res. 24/10, 1796-1804.

Birsoy, Y.K. & Summers, W.K. (1980): Determination of aquifer parameters from step tests and intermittent pumping data. Ground Water 18, 137-146.

Black, J., Holmes, D., Brightman, M. (1987): Crosshole investigations – Hydrogeological results and interpretations. Nagra Technical Report NTB 87-37.

Bourdet, D., Ayoub, J.A. & Pirard, Y.M. (1989): Use of pressure derivative in well-test interpretation. Society of Petroleum Engineers, SPE Formation Evaluation, 293-302.

Bredehoeft, J.D. & Papadopulos, S.S. (1980): A method for determining the hydraulic properties of tight formations. Water Resour. Res. 16/1, 233-238.

Cooper, H.H. & Jacob, C.E. (1946): A generalized graphical method for evaluating formation constants and summarizing well field history. Am. Geophys. Union Trans. 27, 526-534.

Cooper, H.H., Bredehoeft, J.D. & Papadopulos, S.S. (1967): Response of a finite-diameter well to an instantaneous charge of water. Water Resour. Res. 3/1, 263-269.

Detournay, E. & Cheng, A.H.-D. (1988): Poroelastic response of a borehole in a non-hydrostatic stress field. International Journal of Rock Mechanics and Mining Sciences & Geomechanics Abstracts 25/3, 171-182.

Geofirma Engineering Ltd. & INTERA Inc. (2011): nSIGHTS Version 2.50 User Manual. INTERA Inc., Austin, TX, USA.

Grauls, D. (1999): Overpressures: Causal mechanisms, conventional and hydromechanical approaches. Oil & Gas Science and Technology – Rev. IFP 54, 667-678.

Isler, A., Pasquier, F. & Huber, M. (1984): Geologische Karte der zentralen Nordschweiz 1:100'000. Herausgegeben von der Nagra und der Schweiz. Geol. Komm.

Jäggi, K. & Vogt, T. (2020): OPA: Sondierbohrung Benken, Langzeitbeobachtung 2019, Dokumentation der Messdaten. Nagra Arbeitsbericht NAB 20-05.

Lisjak, A., Garitte, B., Grasselli, G., Müller, H.R. & Vietor, T. (2015): The excavation of a circular tunnel in a bedded argillaceous rock (Opalinus Clay): Short-term rock mass response and FDEM numerical analysis. Tunnelling and Underground Space Technology 45, 227-248.

Lorenz, G.D., Pechstein, A. & Stopelli, E. (2022): Borehole BOZ2-1 (Bözberg-2-1): Fluid sampling and analytical hydrochemical data report. Nagra Arbeitsbericht NAB 22-22.

Luo, J., Monningkoff, B. & Becker, J.K. (2014): Hydrogeological model Jura Ost. Nagra Arbeitsbericht NAB 13-26.

Marschall, P., Croisé, J., Schlickenrieder, L., Boisson, J.Y., Vogel, P. & Yamamoto, S. (2003): Synthesis of hydrogeological investigations at the Mont Terri site (Phases 1 – 5). Mont Terri Technical Report TR 01-02. Mont Terri Project, Switzerland.

Nagra (1997): Hydrological investigations at Wellenberg: Hydraulic packer testing in boreholes SB4a/v and SB4a/s. Methods and field results. Nagra Technischer Bericht NTB 95-02.

Nagra (2001): Sondierbohrung Benken – Untersuchungsbericht. Nagra Technischer Bericht NTB 00-01.

Nagra (2008): Vorschlag geologischer Standortgebiet für das SMA- und das HAA-Lager – Geologische Grundlagen. Nagra Technischer Bericht. NTB 08-04.

Nagra (2014a): SGT Etappe 2: Vorschlag weiter zu untersuchender geologischer Standortgebiete mit zugehörigen Standortarealen für die Oberflächenanlage. Geologische Grundlagen. Dossier II: Sedimentologische und tektonische Verhältnisse. Nagra Technischer Bericht NTB 14-02.

Nagra (2014b): SGT Etappe 2: Vorschlag weiter zu untersuchender geologischer Standortgebiete mit zugehörigen Standortarealen für die Oberflächenanlage. Geologische Grundlagen. Dossier VI: Barriereneigenschaften der Wirt- und Rahmengesteine. Nagra Technischer Bericht NTB 14-02 .

Peres, A.M., Onur, M. & Reynolds, A.C. (1989): A new analysis procedure for determining aquifer properties from slug test data. Water Resour. Res. 25/7, 1591-1602.

Pickens, J.F., Grisak, G.E., Avis, J.D., Belanger, D.W., Thury, M. (1987): Analysis and interpretation of borehole hydraulic tests in deep boreholes: Principles, model development, and application. Water Resour. Res. 23/7, 1341-1375.

Pietsch, J. & Jordan, P. (2014): Digitales Höhenmodell Basis Quartär der Nordschweiz – Version 2013 (SGT E2) und ausgewählte Auswertungen. Nagra Arbeitsbericht NAB 14-02.

Ramey, H.J. & Agarwal, R.G. (1972): Annulus unloading rates as influenced by wellbore storage and skin, Soc. Pet. Engr. J. 12/5, 453.

Appendix A: Abbreviations, nomenclature and definitions

Tab. A-1: Lithostratigraphy abbreviations for test names in BOZ2-1

Lithostratigraphy	**Abbreviation**
Malm Group	MAL
Hauptrogenstein (Dogger)	HRO
Passwang Formation (Dogger)	PWF
Opalinus Clay (Dogger)	OPA
Lias Group	LIA
Keuper Group	KEU
Muschelkalk Group	MUK

Tab. A-2: Test name definitions for hydraulic packer testing

Abbreviation	**Example**
Drill site abbreviation – lithostratigraphy abbreviation[1] + number of test	BOZ2-1-MUK1: First test interval in Muschelkalk aquifer in borehole BOZ2-1

[1] Based on the preliminary information

Tab. A-3: Test event abbreviations for hydraulic packer testing

Test phase	**Abbreviation**
Compliance phase	COM
Packer deflation phase	DEF
Packer inflation phase	INF
Multi-rate pumping test with stepwise constant flow rates	MRW
Pressure recovery after multi-rate pumping test (shut-in)	MRWS
Pulse injection test	PI
Initial pressure recovery 'static pressure recovery' (SIT closed)	PSR
Pulse withdrawal test	PW
Pumping test with constant flow rate ('rate withdrawal test')	RW
Pressure recovery after pumping test with constant flow rate (shut-in)	RWS
Slug withdrawal test (flow phase)	SW
Slug withdrawal test – pressure recovery with closed SIT (shut-in)	SWS

Tab. A-4: Parameter definitions

Abbreviation / symbol	**Description**	**Unit**
c_{tz}	Test zone compressibility	1/Pa
g	Acceleration due to gravity (9.81)	m s^{-2}
h_s	Static hydraulic head (freshwater head) $h_s = z_{ref} - z_{int} + \left[\frac{P_f + \rho_{int}\, g\, (z_{int} - z_2) - P_{atm} - P_{offset}}{\rho_w\, g}\right]$	m asl
k	Intrinsic permeability	m^2
K	Hydraulic conductivity	m s^{-1}
K_{in}	Inner-zone hydraulic conductivity	m s^{-1}
K_{out}	Outer-zone hydraulic conductivity	m s^{-1}
K_s	Hydraulic conductivity of skin zone	m s^{-1}
n	Fractional flow dimension, e.g. Barker (1988)	-
P	Pressure (at QSSP-P2 level, if not otherwise specified)	Pa, kPa
P1	Pressure below bottom packer / interval P1 (downhole probe)	Pa, kPa
P2	Pressure in test interval (downhole probe)	Pa, kPa
P2*	Pressure in test interval (memory gauge)	Pa, kPa
P3	Pressure in annulus (above top packer, downhole probe)	Pa, kPa
P4	Pressure in test tubing above SIT (downhole probe)	Pa, kPa
P_{atm}	Atmospheric pressure	Pa, kPa
P_f	Static formation pressure (fitting parameter, at QSSP-P2 level, respectively P2* level)	Pa, kPa
P_{int}	Pressure at midpoint of test interval	Pa, kPa
P_{offset}	Offset of a pressure probe at atmospheric pressure	Pa, kPa
P_S	Static formation pressure (at midpoint of test interval if not specified otherwise)	Pa, kPa
ΔP_{packer}	Interval packer pressure changes	bar
q	Flow rate	$m^3\ s^{-1}$
Q, Q_{tot}	Cumulative flow volume	m^3
r_d	Radius of discontinuity	m
r_s	Radius of the skin zone extension	m
$r_{w\ int}$	Borehole radius of the test interval	mm
ρ_{int}	Density of interval fluid	kg m^{-3}
ρ_w	Density of formation water (fluid)	kg m^{-3}
S	Storage	-
s	Skin factor	-

Abbreviation / symbol	**Description**	**Unit**
S_s	Specific storage	1/m
$S_{s\ in}$	Inner-zone specific storage	1/m
$S_{s\ out}$	Outer-zone specific storage	1/m
S_{ss}	Specific storage of skin zone	1/m
t_s	Thickness of the skin zone extension	m
T	Transmissivity	$m^2\ s^{-1}$
t, dt	Time, elapsed time	s
T_{int}, T1, T2, T3, T4, T2*	Temperature in test interval, temperature triple probe (sensors 1, 2, 3 or 4 associated with specific transducer; sensor T2* associated with memory gauge)	°C
ΔV_{int}	Interval volume changes	mL
z_2	Depth of pressure sensor of test interval P2	m MD
z_{int}	Depth interval midpoint	m MD
z_{ref}	Reference point elevation	m asl

Tab. A-5: Non-parameter abbreviations

Abbreviation	**Description**	**Unit**
ΔP	Change in pressure	Pa, kPa
ΔV	Change in volume	m^3
1D	One dimensional	
2D	Two dimensional	
3D	Three dimensional	
AG	Aktiengesellschaft (company limited by shares "Ltd.")	
API	American Petroleum Institute	
BHPH	Borehole pressure history	
BOP	Blow out preventer	
BOZ2-1	Bözberg-2 drill site, borehole 1	
BUL1-1	Bülach-1 drill site, borehole 1	
cps	Counts per second	
CU	Copper	
DA	Detailed analysis	
DAS	Data acquisition system	
DR	Detailed report	
EU	External upset coupling	

Abbreviation	**Description**	**Unit**
EUE	External upset end	
FM	Flow model	
FS	Full scale	
GmbH	Gesellschaft mit beschränkter Haftung (company with limited liability)	
GTPT	Gas threshold pressure test	
HDDP	Heavy-duty double packer system	
HLW	High level waste	
IARF	Infinite acting radial flow region	
ID	Inner diameter	
IPI	Inflatable Packers International, Perth, Australia	
IT	Information technology	
L/ILW	Low and intermediate level waste	
ln	Litre normal	ln
MAR1-1	Marthalen-1 drill site, borehole 1	
MD	Measured depth	m
MHF	Micro-hydraulic fracturing	
NBR	Nitrile butadiene rubber	
NDSA	Naphthalene disulfonate acid	
OD	Outer diameter	
PA1	Bottom packer of the hydraulic line of the HDDP	
PA2	Top packer of the hydraulic line of the HDDP	
PCP	Progressive cavity pump	
POOH	Pull out of hole	
PPG	Piston pulse generator	
PRV	Pressure release valve	
QC	Quality control	
QLA	Quick look analysis	
QLR	Quick look report	
QSSP	Quadruple sub-surface probe	
Rd	Reading	
RIH	Run in hole	
SIT	Shut-in tool	
SSE	Sum of squared errors	
TBO	Tiefbohrung(en) (German for deep borehole(s))	

Abbreviation	**Description**	**Unit**
TVD	True vertical depth	m
WS	Water sample	
WT	Water table	
WTW	Wissenschaftlich-technische Werkstätten GmbH	

Appendix B: Analysis plots of the hydraulic packer tests BOZ2-1-OPA4 and BOZ2-1-MUK1

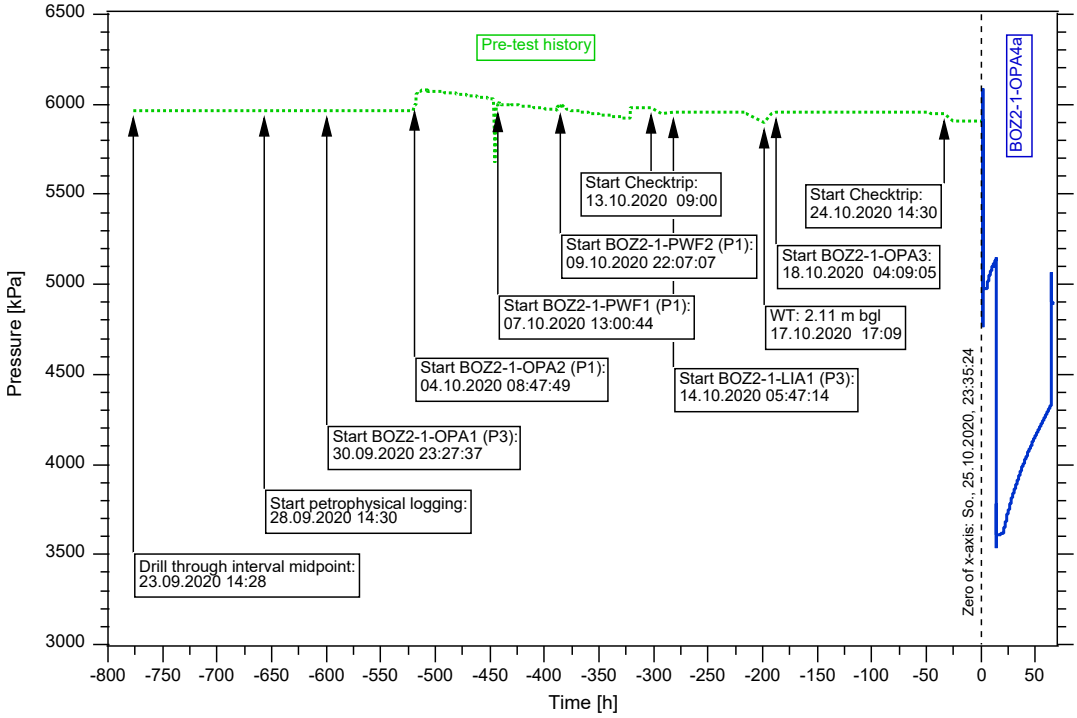

Fig. B-1: Hydraulic test BOZ2-1-OPA4: Entire record of the borehole pressure history used in the analysis

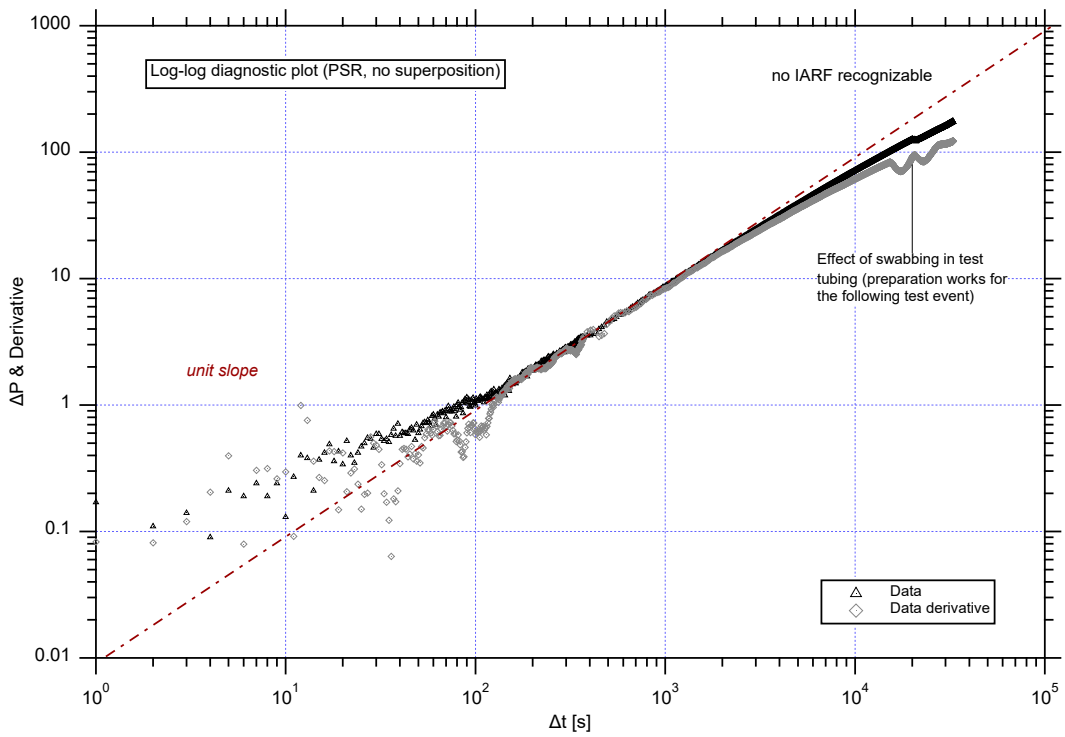

Fig. B-2: Hydraulic test BOZ2-1-OPA4: Log-log diagnostic plot of the PSR phase

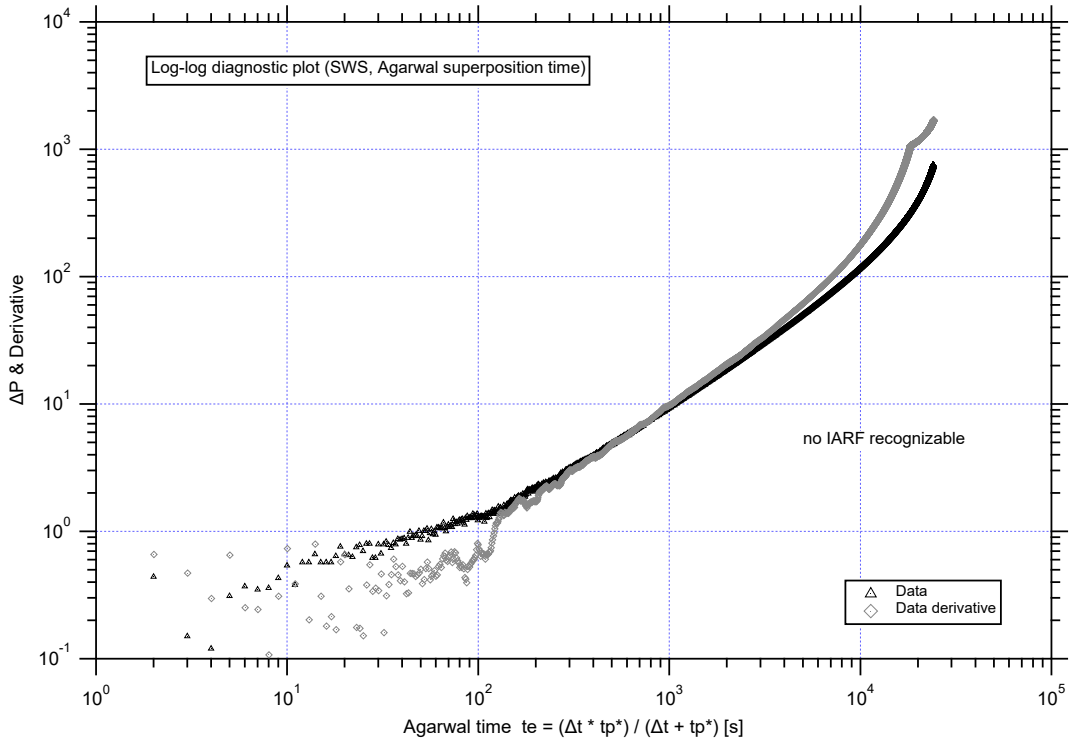

Fig. B-3: Hydraulic test BOZ2-1-OPA4: Log-log diagnostic plot of the SWS phase using Agarwal time

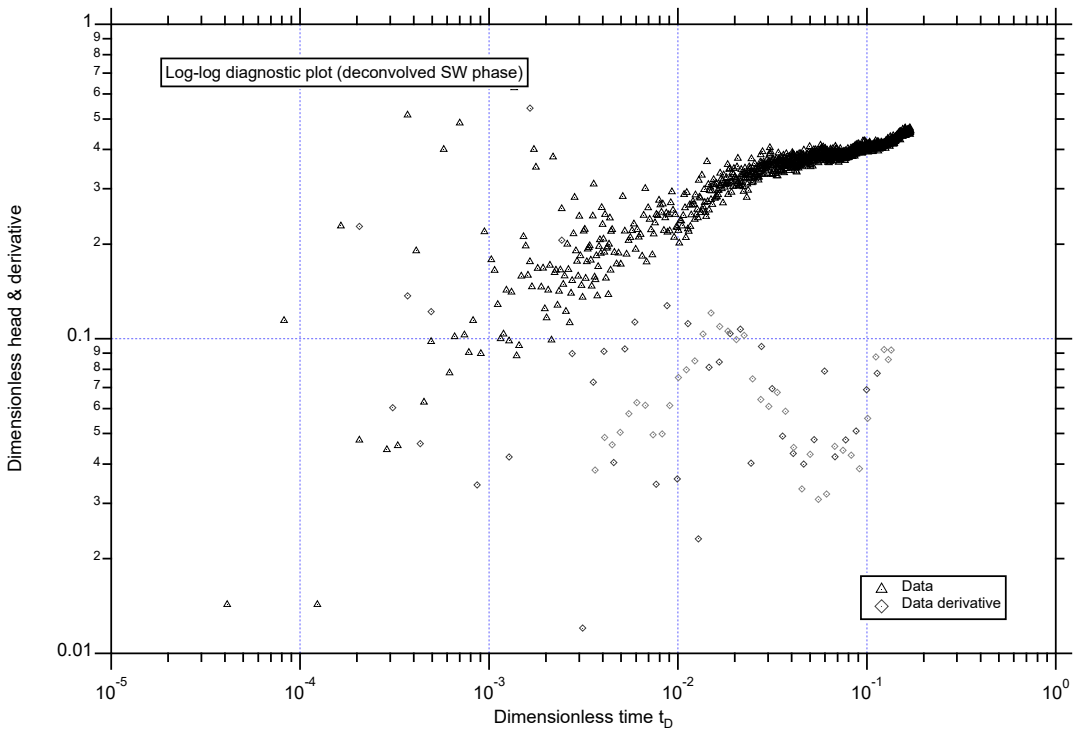

Fig. B-4: Hydraulic test BOZ2-1-OPA4: Deconvolution diagnostic plot of the SW phase

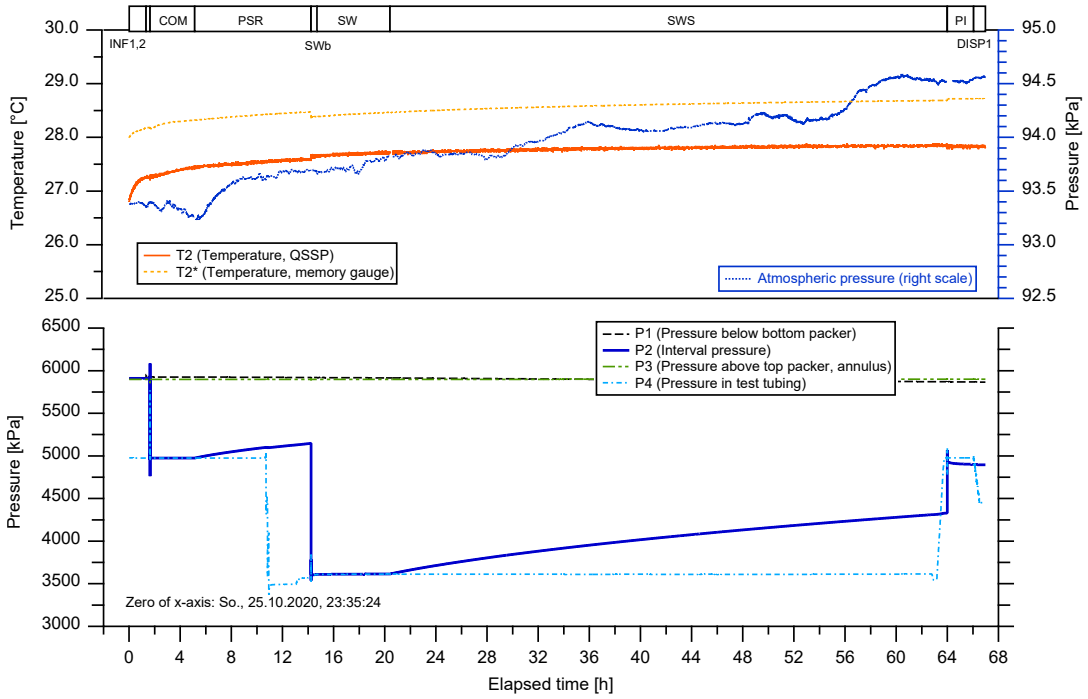

Fig. B-5: Hydraulic test BOZ2-1-OPA4: Measurement of the temperature and pressure by the QSSP and memory gauge respectively

SWb as part of SW was excluded from the analysis due to its irregular behaviour.

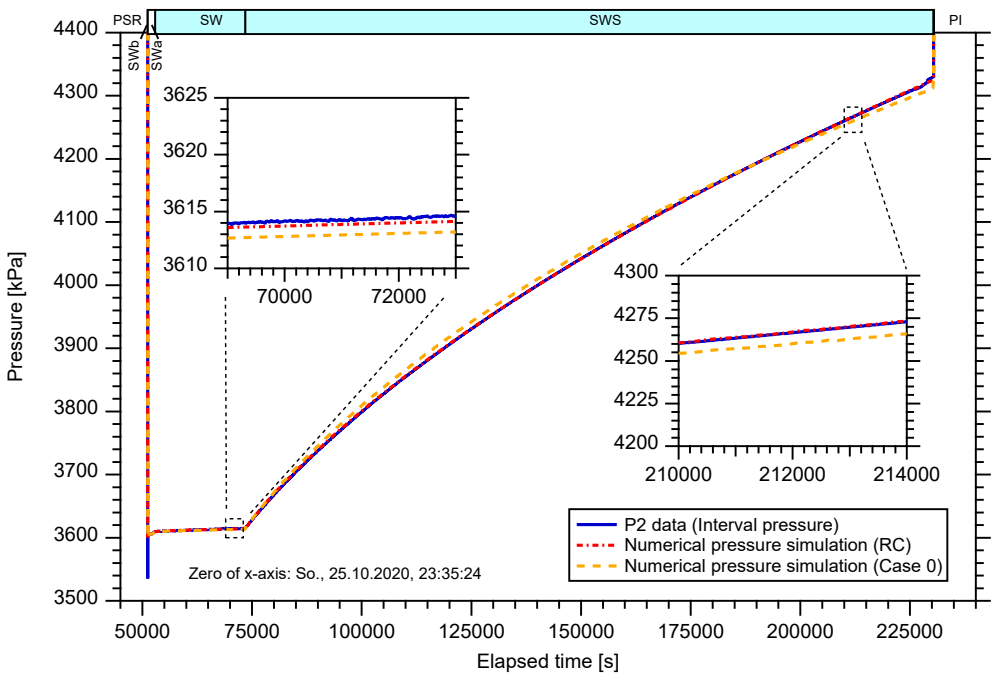

Fig. B-6: Hydraulic test BOZ2-1-OPA4: Cartesian pressure measurement with numerical cartesian fits using a radial-composite (skin) model (reference case – RC) and a radial-homogeneous flow model (Case 0)

SWa and SWb as part of SW was excluded from the analysis due to its irregular behaviour.

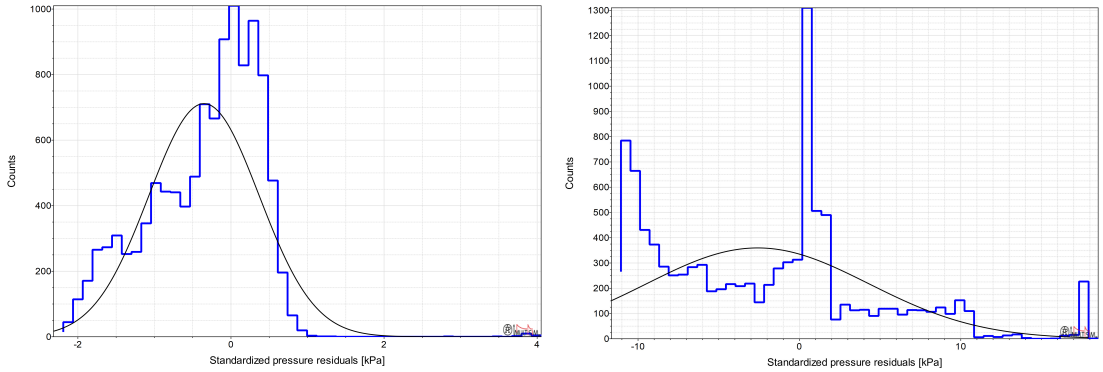

Fig. B-7: Hydraulic test BOZ2-1-OPA4: Probability distribution function of the pressure residuals of the SW-SWS sequence simulation using a radial-composite (skin) model (left) and a radial-homogeneous flow model (right)

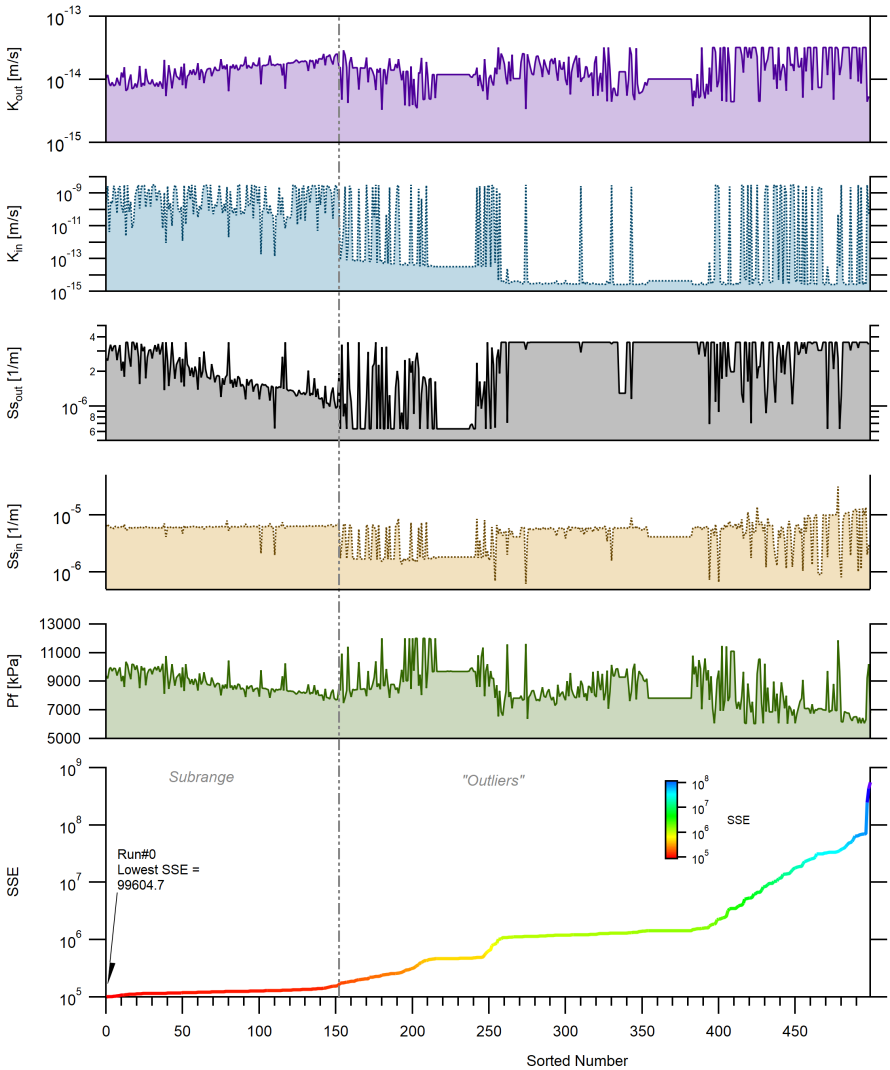

Fig. B-8: Hydraulic test BOZ2-1-OPA4: Optimised parameter sets for the perturbation analysis plotted versus the sorted SSE run numbers (bottom plot, SSE value against sorted run number)

The grey dot-dashed line indicates the selection of the subrange used for the estimation of the uncertainty ranges.

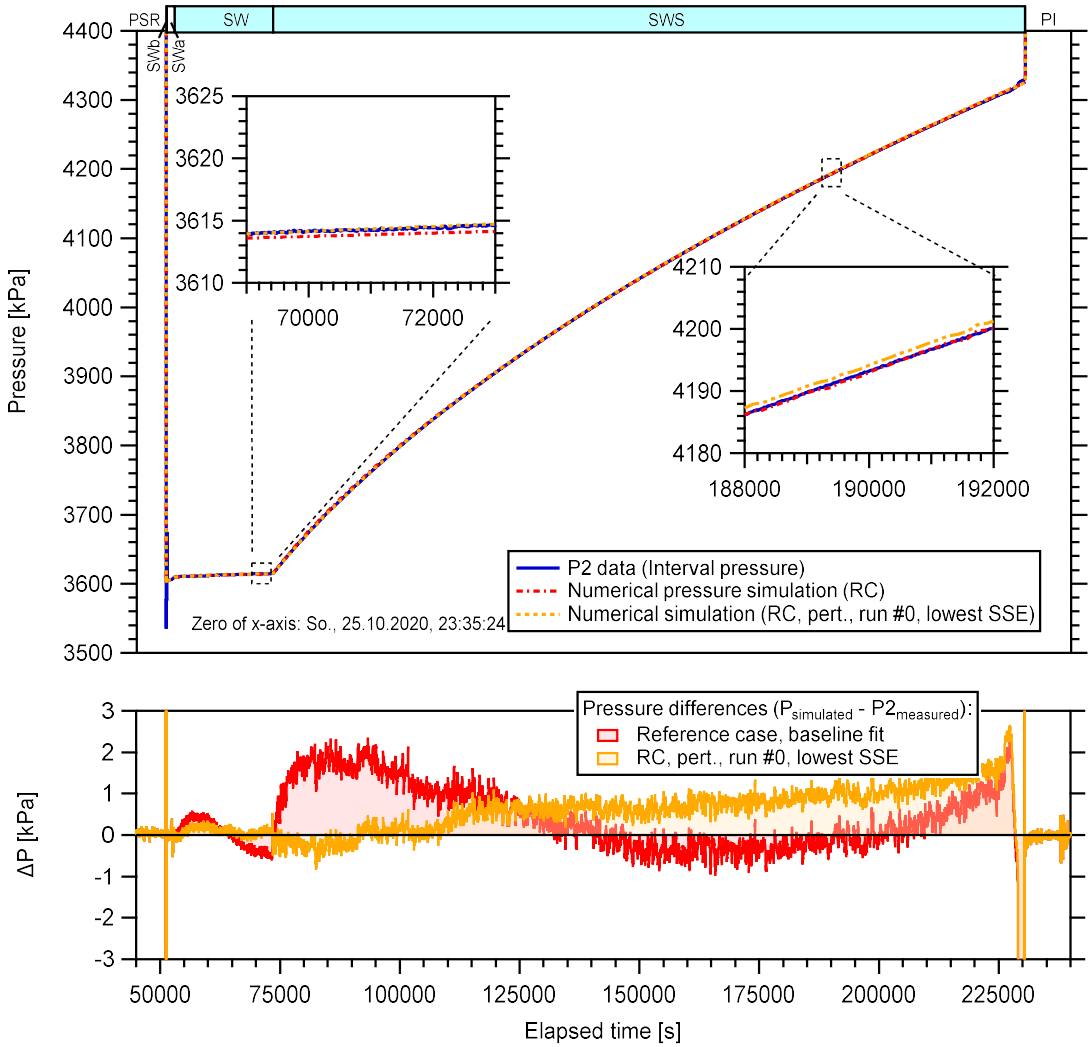

Fig. B-9: Hydraulic test BOZ2-1-OPA4: Comparison of the simulations based on the initial parameter optimisation and the simulation using the parameter sets associated with the lowest SSE (run#0) from the perturbation results

SWa and SWb as part of SW was excluded from the analysis due to its irregular behaviour.

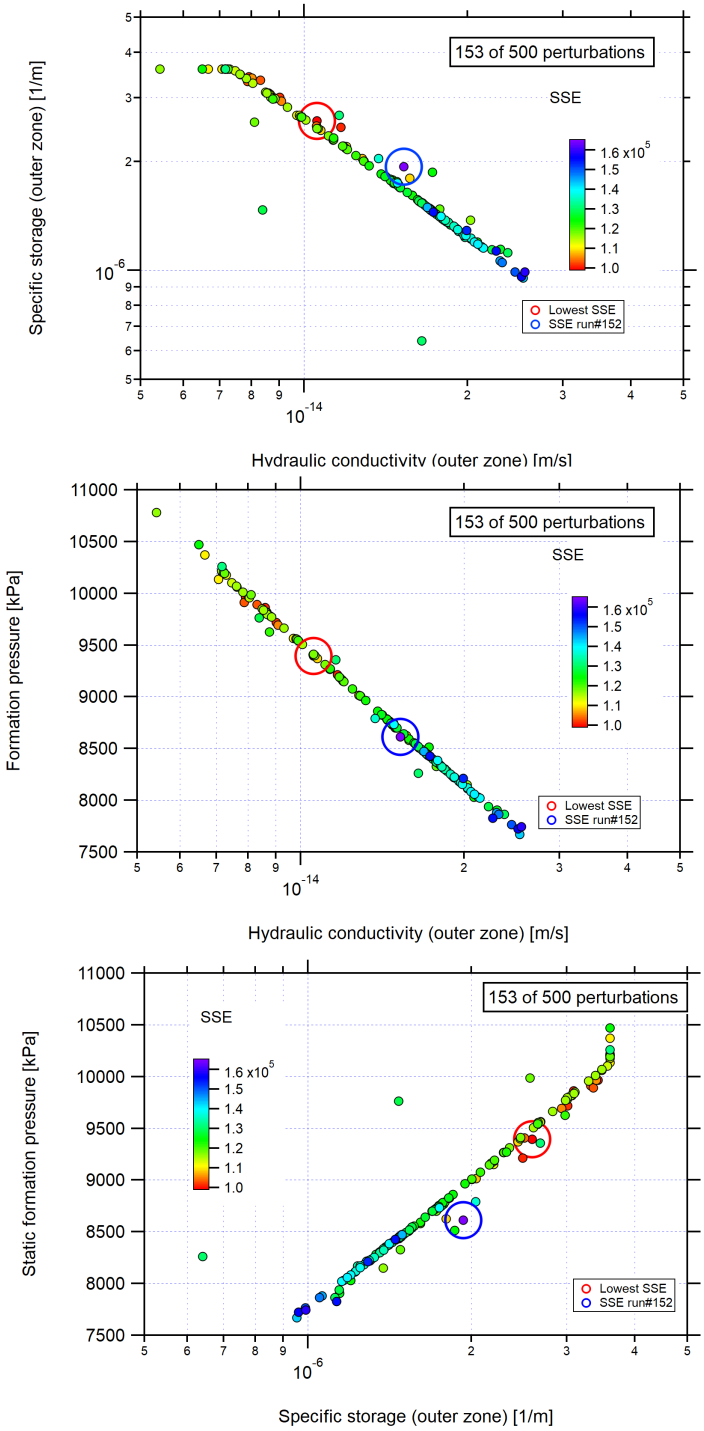

Fig. B-10: Hydraulic test BOZ2-1-OPA4: Scatter plots and associated SSE values for the optimised formation parameters given by the perturbation analysis showing K_{out} versus S_{Sout} (top), K_{out} versus P_f (middle) and S_{Sout} versus P_f (bottom)

The red and the blue circle in each figure indicate the parameters from run#0 (associated with the lowest SSE value) and from run#152 (upper limit of the uncertainty range estimation), respectively

153 / 500 results with an objective function / sum of squared errors (SSE) value less than 164'474.

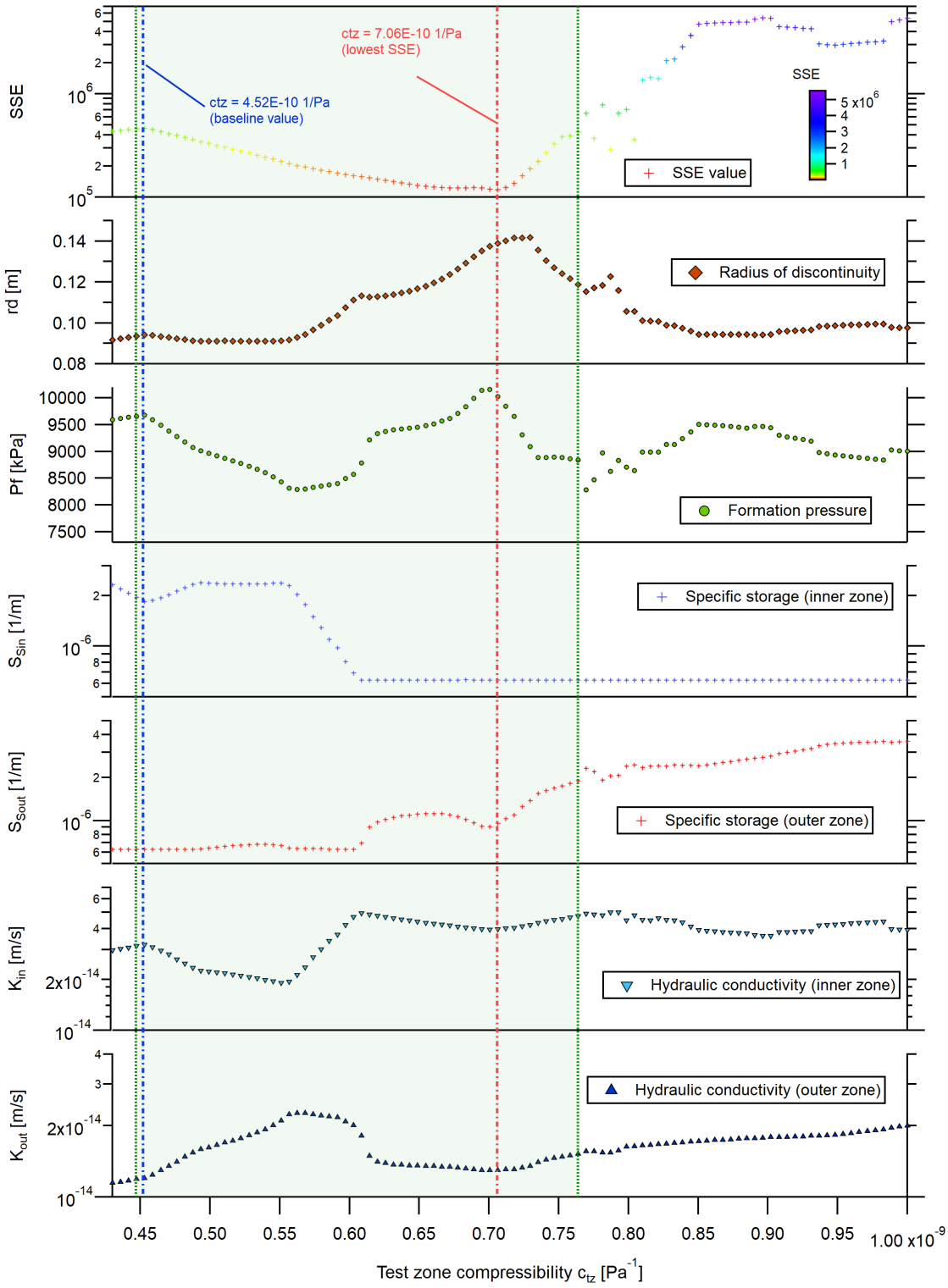

Fig. B-11: Hydraulic test BOZ2-1-OPA4: Parameter sets for the sampling analysis of test zone compressibility

The SSE value is given for each simulation (top graph in figure). The blue dot-dashed line indicates the value used in the initial parameter optimisation; the red dot-dashed line indicates the value associated with the lowest SSE. The green dotted lines indicate the upper and lower limit of the resulting uncertainty range.

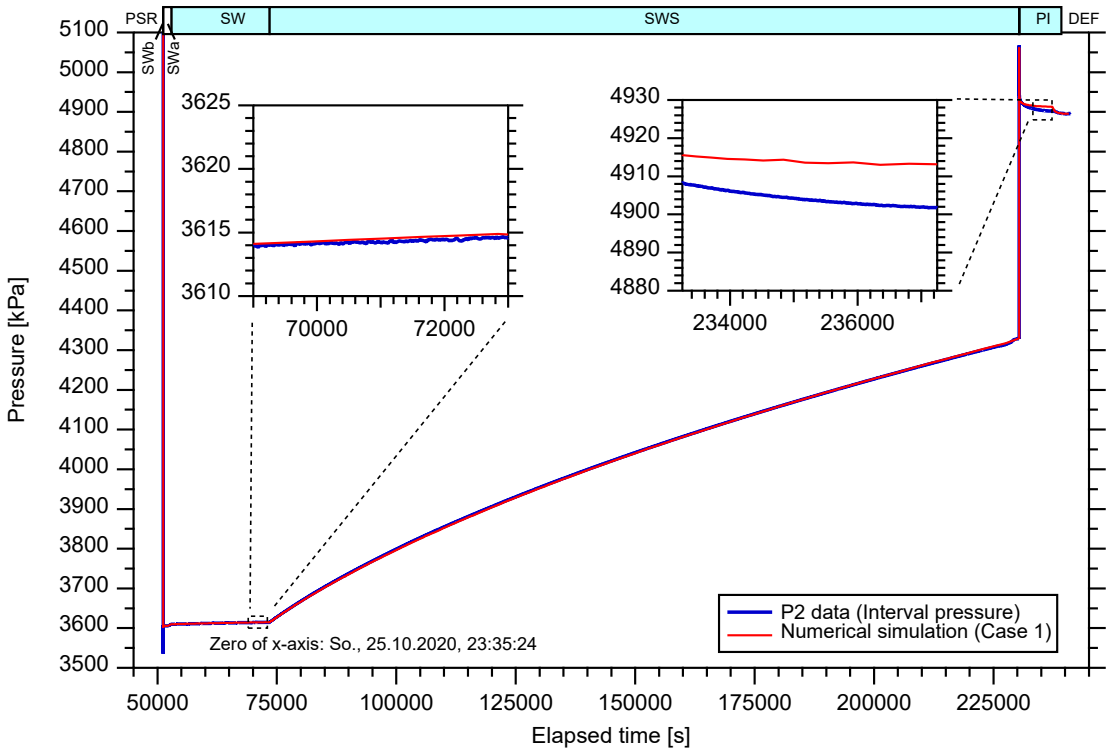

Fig. B-12: Hydraulic test BOZ2-1-OPA4: Cartesian pressure measurement with numerical cartesian fits of the SW-SWS-PI sequence (Case 1) using a radial-composite (skin)

SWa and SWb as part of SW was excluded from the analysis due to its irregular behaviour.

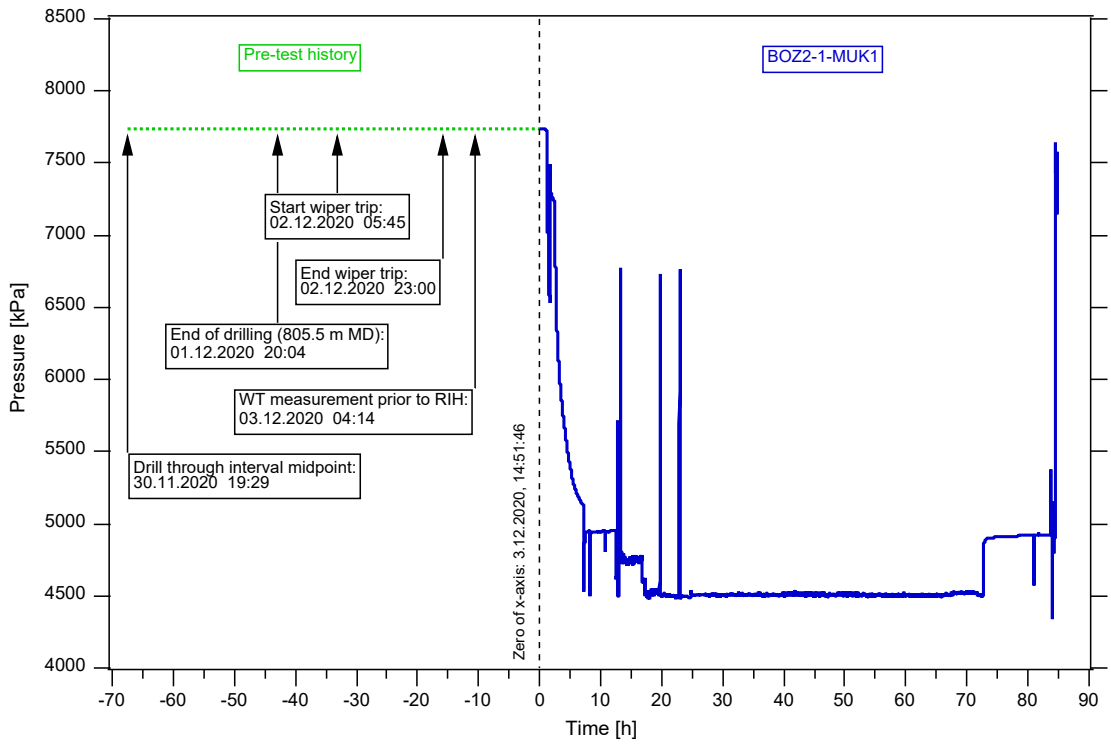

Fig. B-13: Hydraulic test BOZ2-1-MUK1: Entire record of the borehole pressure history used in the analysis

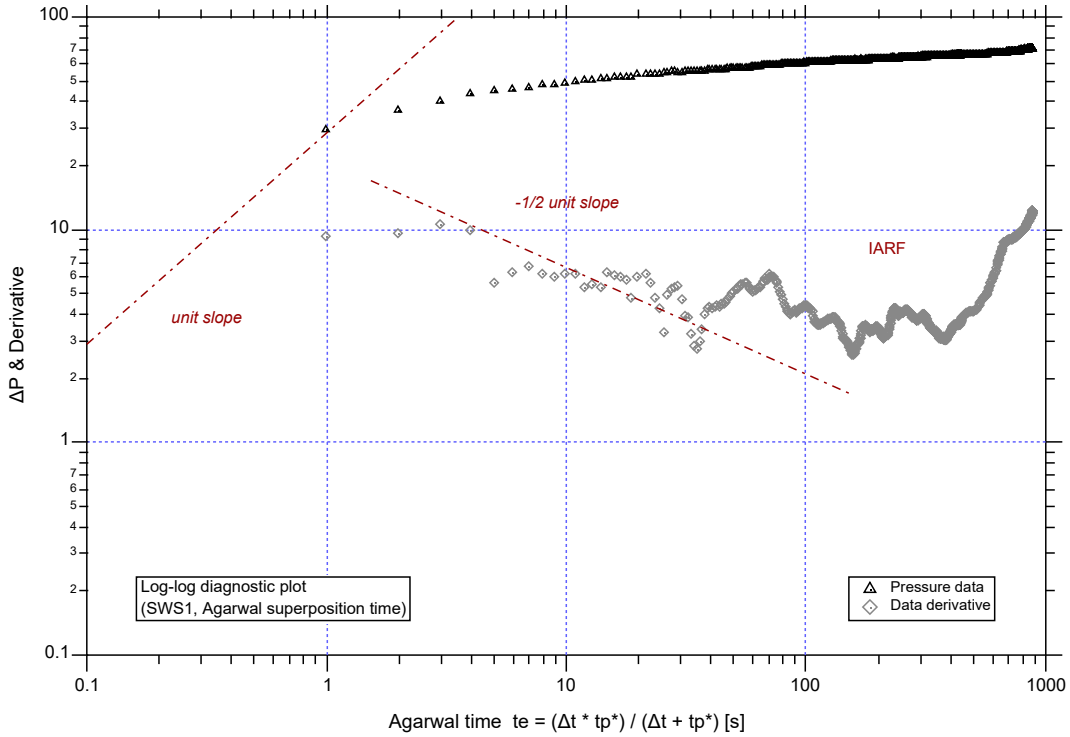

Fig. B-14: Hydraulic test BOZ2-1-MUK1: Log-log diagnostic plot of the SWS2 phase using Agarwal time

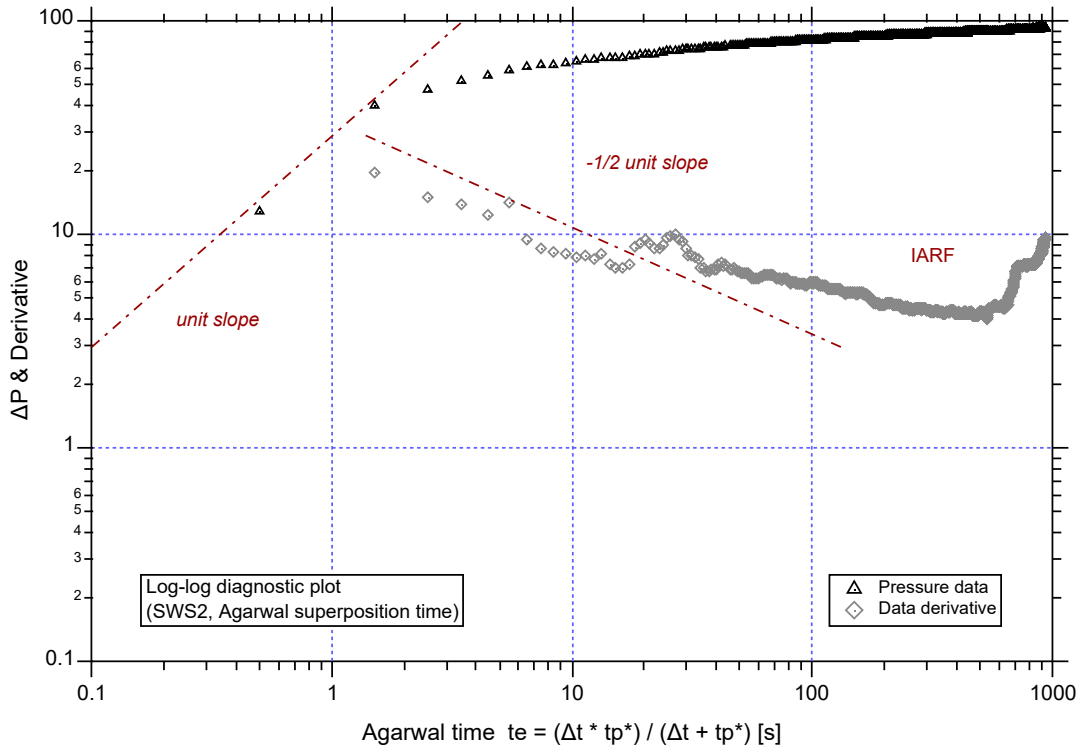

Fig. B-15: Hydraulic test BOZ2-1-MUK1: Log-log diagnostic plot of the SWS2 phase using Agarwal time

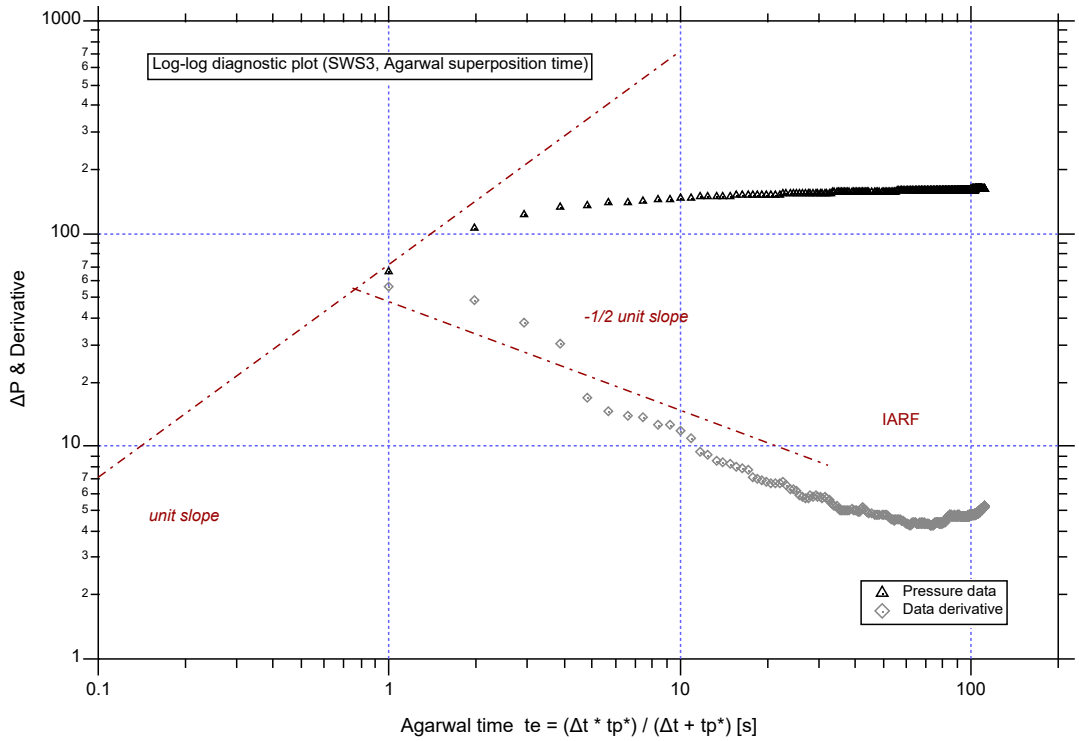

Fig. B-16: Hydraulic test BOZ2-1-MUK1: Log-log diagnostic plot of the SWS3 phase using Agarwal time

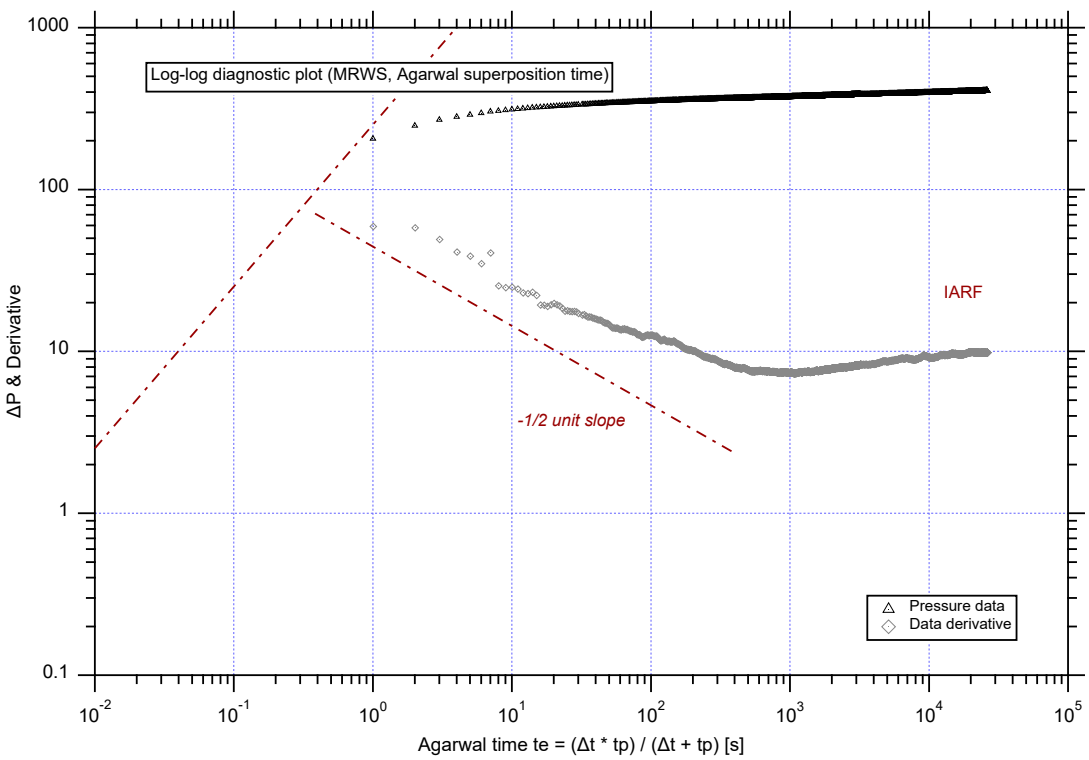

Fig. B-17: Hydraulic test BOZ2-1-MUK1: Log-log diagnostic plot of the MRWS phase using Agarwal time

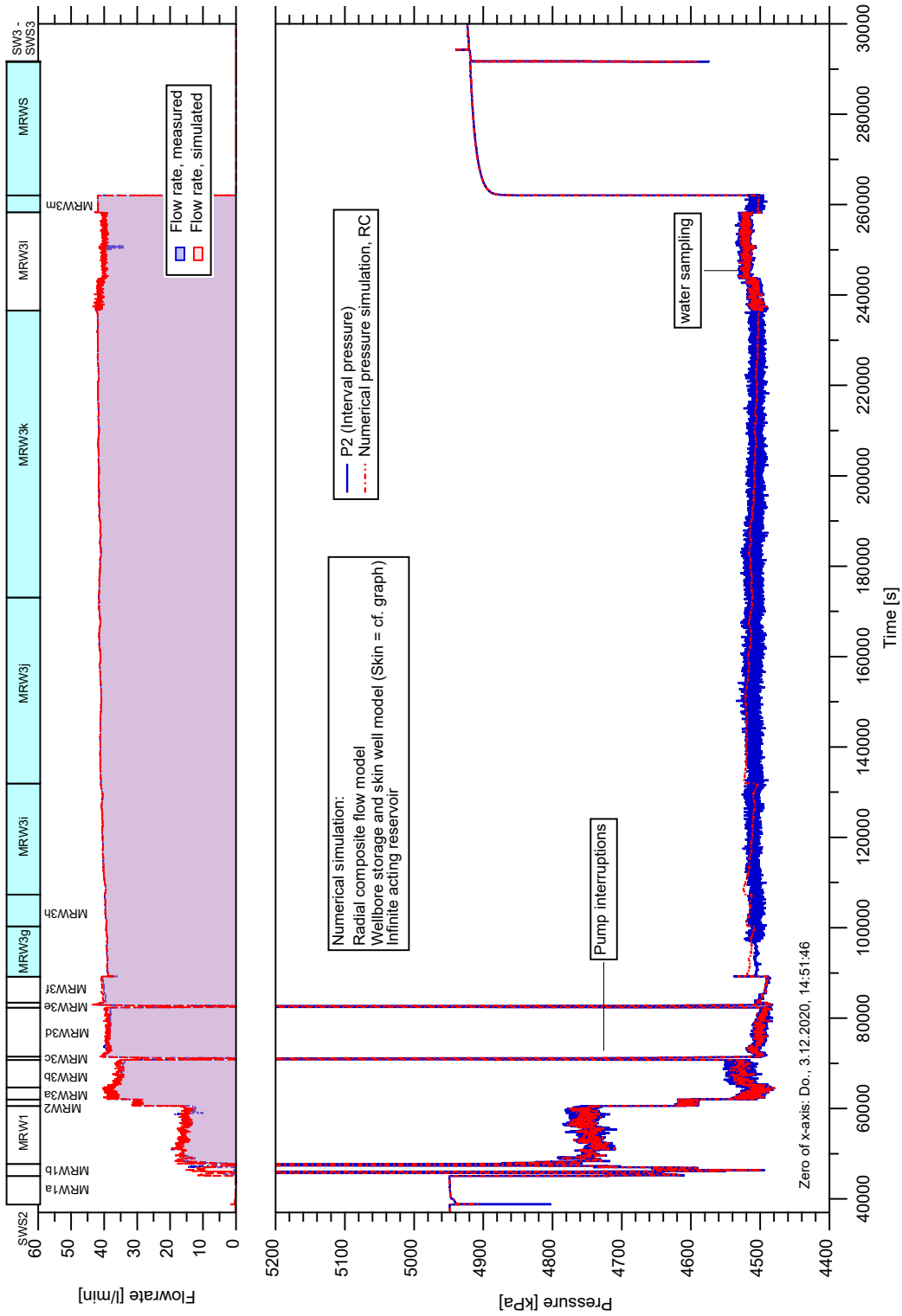

Fig. B-18: Hydraulic test BOZ2-1-MUK1: Cartesian plot of measured and simulated rates and pressure values for the simulation based on a parameter optimisation of MRW3-MRWS

Simulated phases are highlighted in light blue.

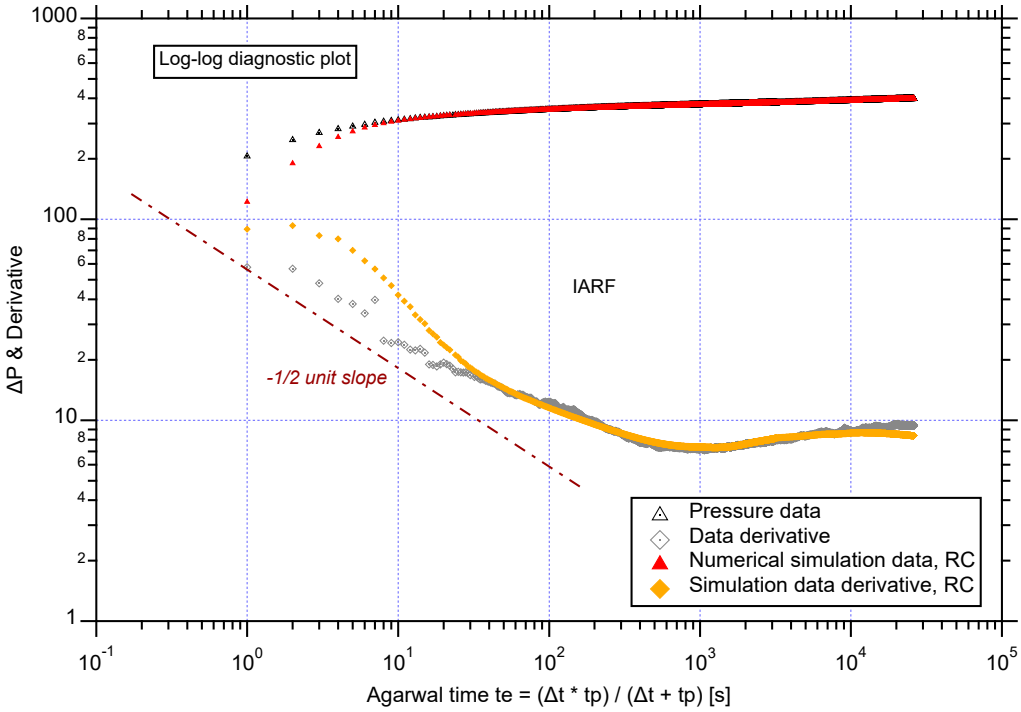

Fig. B-19: Hydraulic test BOZ2-1-MUK1: Detailed view of the simulations based on a parameter optimisation of MRW3-MRWS shown in a log-log plot of the MRWS phase (no superposition plot) using Agarwal time

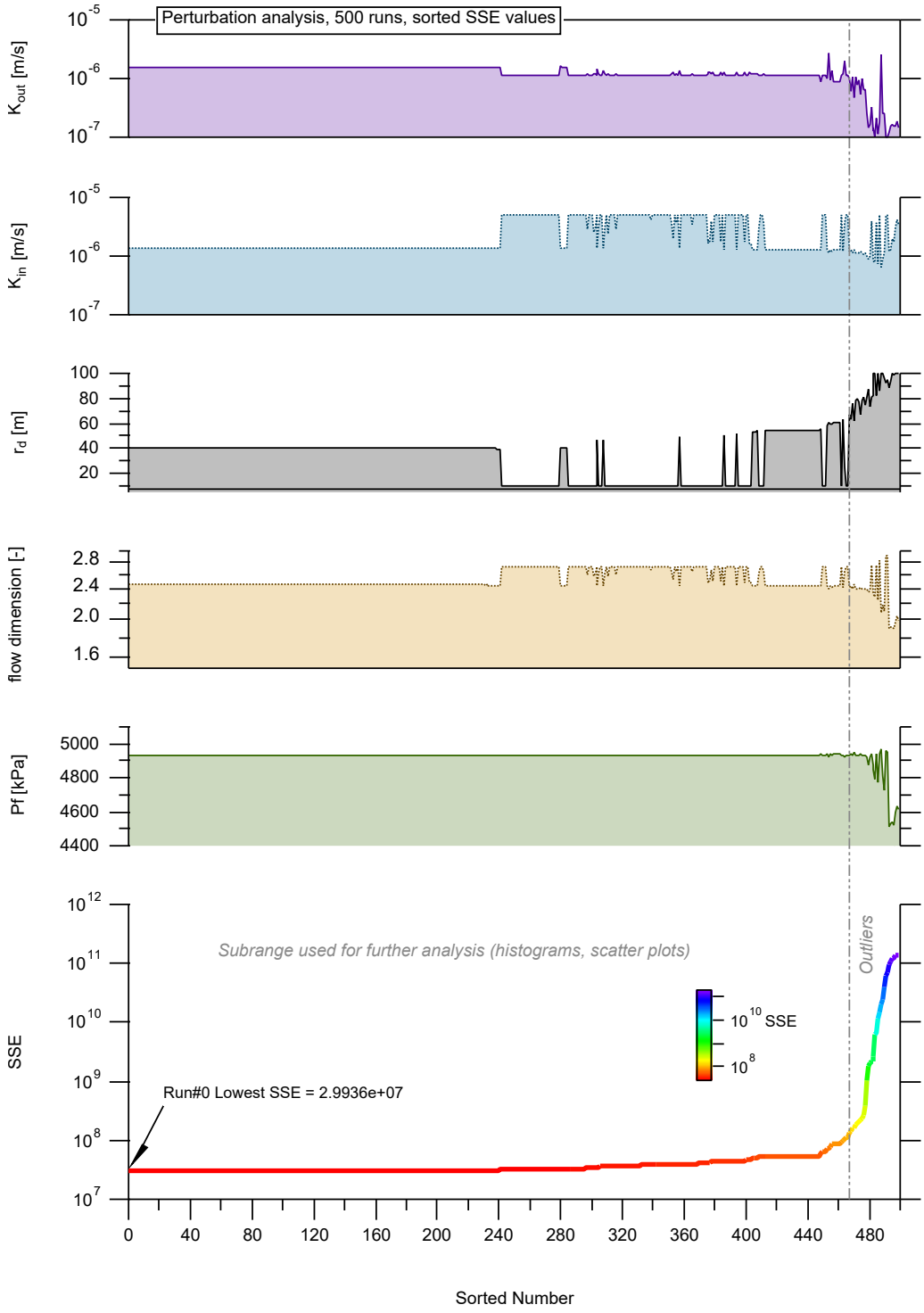

Fig. B-20: Hydraulic test BOZ2-1-MUK1: Optimised parameter sets of the perturbation analysis plotted versus sorted SSE run numbers (in the lowest plot, the SSE values are plotted against sorted run number)

The grey dot-dashed line indicates the selection of the subrange used for the estimation of the parameter uncertainty ranges.

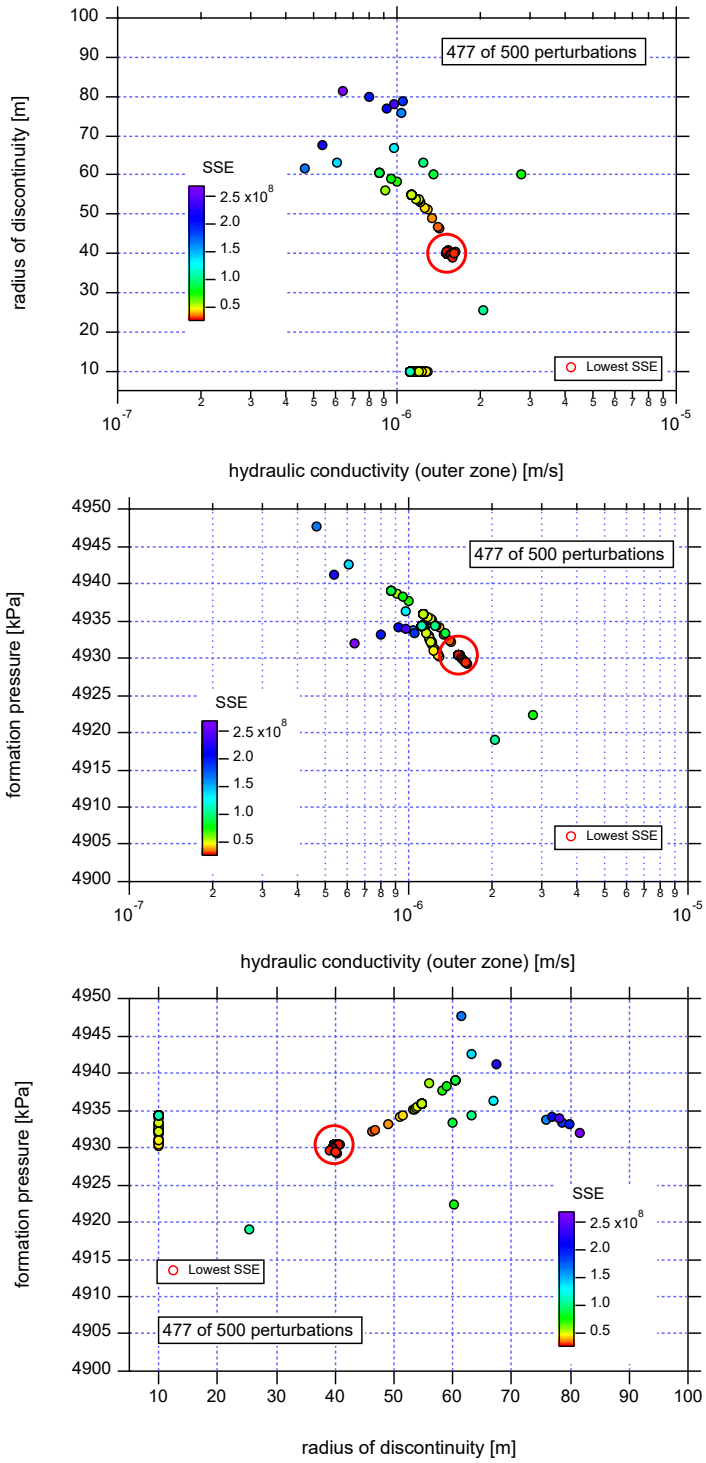

Fig. B-21: Hydraulic test BOZ2-1-MUK1: Scatter plots and associated SSE values of the optimised formation parameters from the perturbation analysis showing r_d versus K_{out} (top), K_{out} versus P_f (middle) and r_d versus P_f (bottom plot)

The red circle in each graph indicates the parameters from run#0 (associated with the lowest SSE value).

477 / 500 results with an objective function / sum of squared errors (SSE) value less than 2.63×10^8.

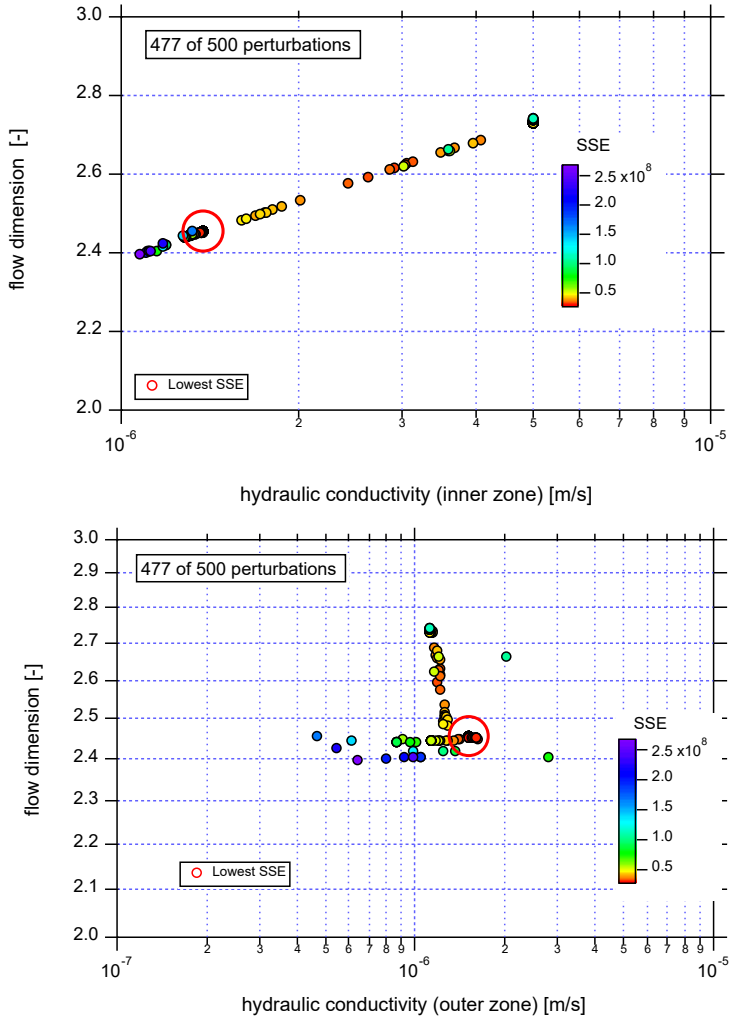

Fig. B-22: Hydraulic test BOZ2-1-MUK1: Scatter plots and associated SSE values of the optimised formation parameters from the perturbation analysis showing flow dimension of the inner zone versus K_{in} (top), flow dimension of the inner zone versus K_{out} (bottom plot)

The red circle in each graph indicates the parameters from run#0 (associated with the lowest SSE value).

477 / 500 results with an objective function / sum of squared errors (SSE) value less than 2.63×10^8.

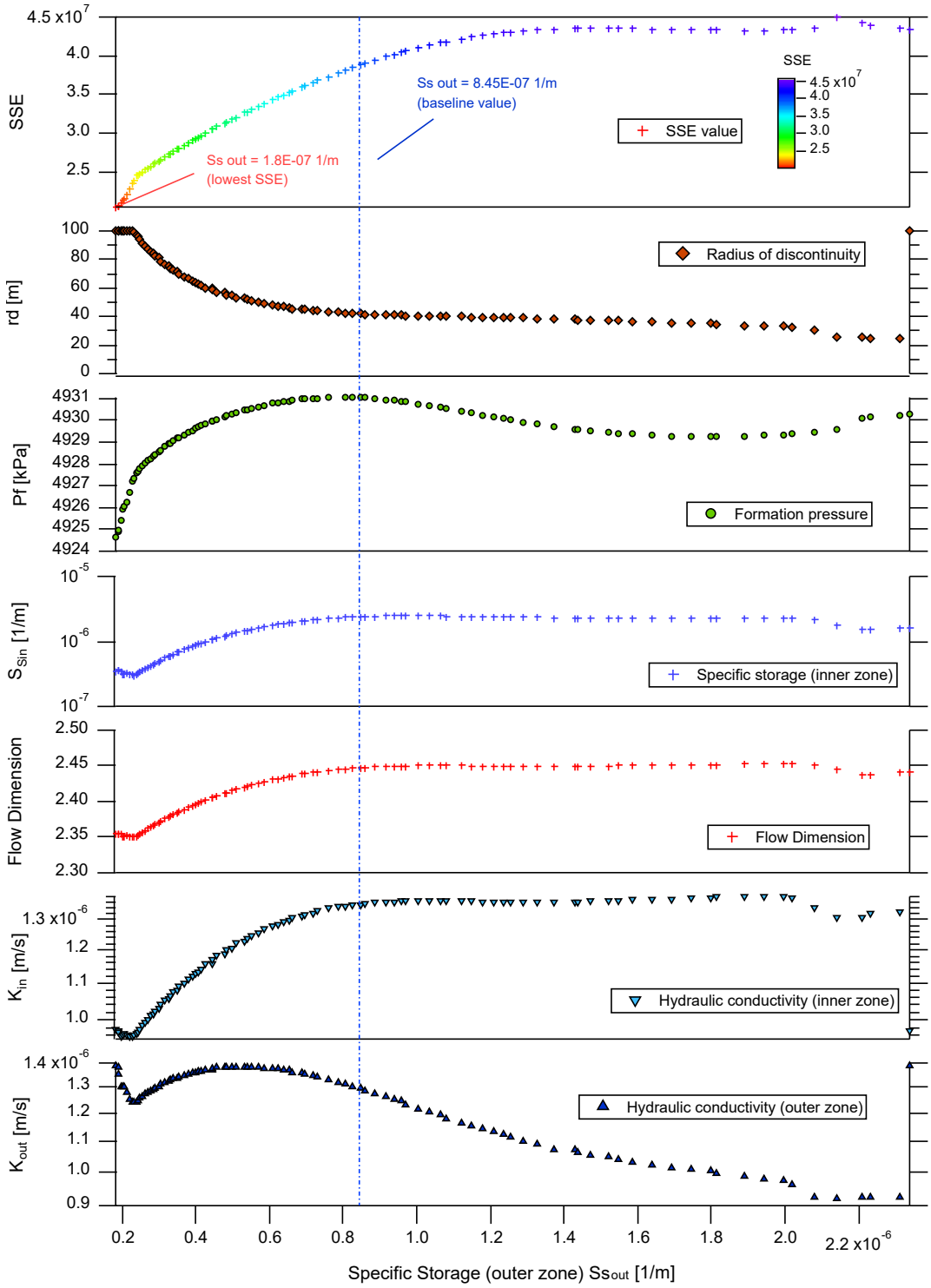

Fig. B-23: Hydraulic test BOZ2-1-MUK1: Parameter sets of the sampling analysis of the formation specific storage

The SSE value is given for each simulation (top plot in figure). The vertical blue dash-dot line indicates the theoretical value used in all other simulations.

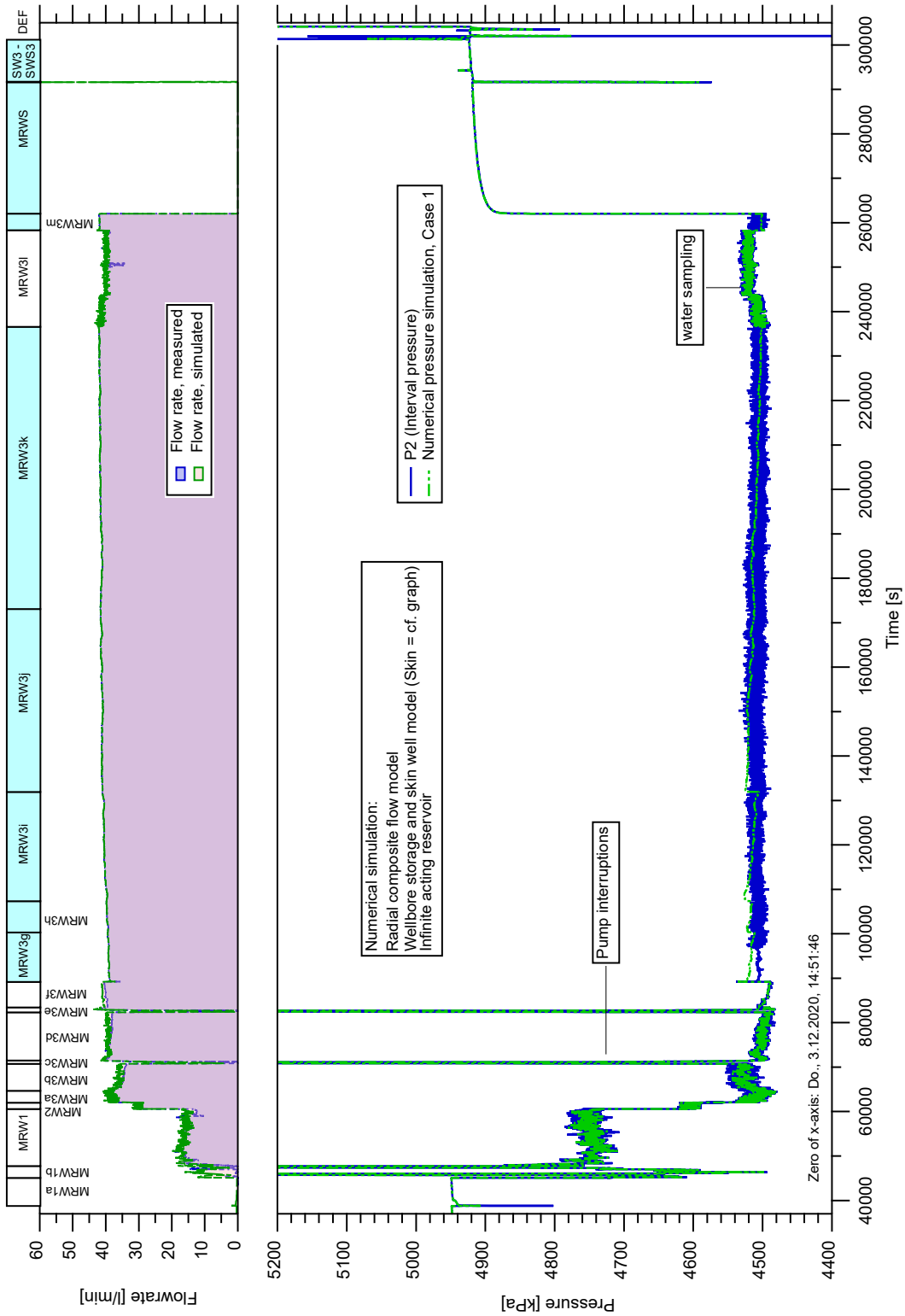

Fig. B-24: Hydraulic test BOZ2-1-MUK1: Cartesian plot of measured and simulated rates and pressure values for the simulation based on a parameter optimisation of MRW3-MRWS-SW3-SWS3

Simulated phases are highlighted in light blue.